NASA Tech Briefs

Official Publication of
National Aeronautics and
Space Administration
Volume 14 Number 8

Transferring Technology to
American Industry
and Government
August 1990

Virtual Reality: Computers Shape Worlds of Illusion

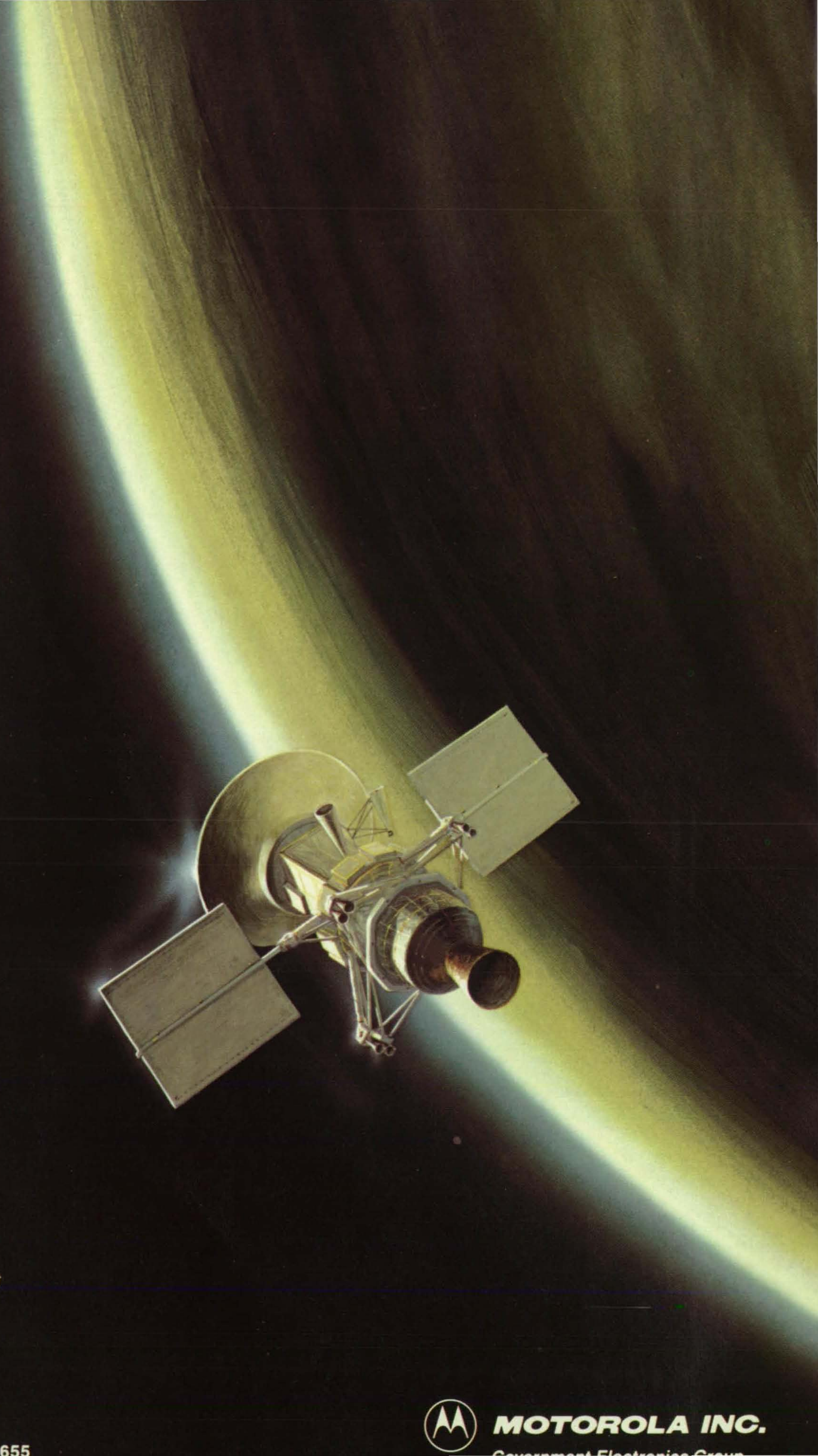

WILL YOUR SCOPE DRAW A BLANK WHEN YOU NEED IT MOST?

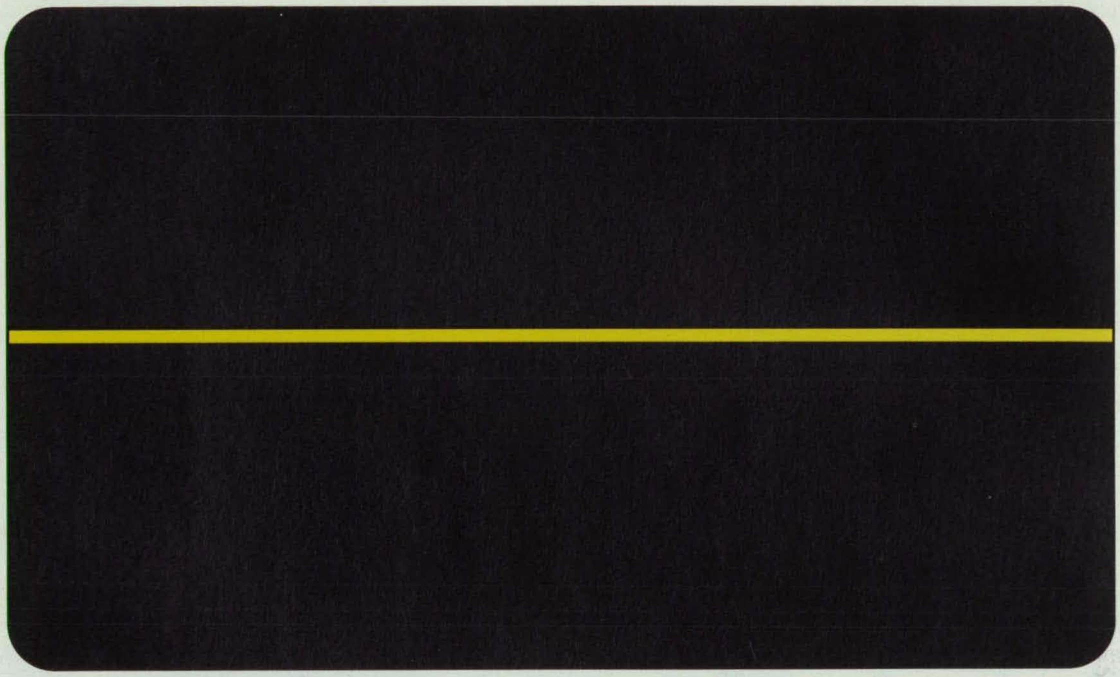

Once it's gone, it's gone.

Nothing can bring back a rare event when your memory isn't long enough. Not complex triggering. Not an extended bandwidth. Nothing.

That's why *only* the high precision Nicolet 400 is designed with expandable 64K-256K memory *per channel.* (Five to 10 times longer than the nearest competition.) As well as an optional 44MB external removable hard disk, also only from Nicolet.

Seven different 400 models and over 200 configurations make it simple to pick the right number of channels, speed and resolution for your needs. Including a memory that *is* long enough.

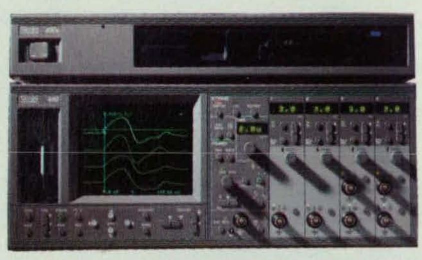

Each 400 features a built-in MS-DOS disk drive. A LEARN mode to help automate test sequences. And FFT and averaging for complete waveform processing. You can even add a dual timebase, or powerful *Nicolet-Windows* PC software for instant remote control.

So don't be caught short. Send for details on the Nicolet 400 today, or call 1-800-356-3090.

Nicolet

INSTRUMENTS OF DISCOVERY

Nicolet Test Instruments Division

5225 Verona Road, Madison, WI 53711-4495
608/273-5008 or 800/356-3090

Circle Reader Action No. 696

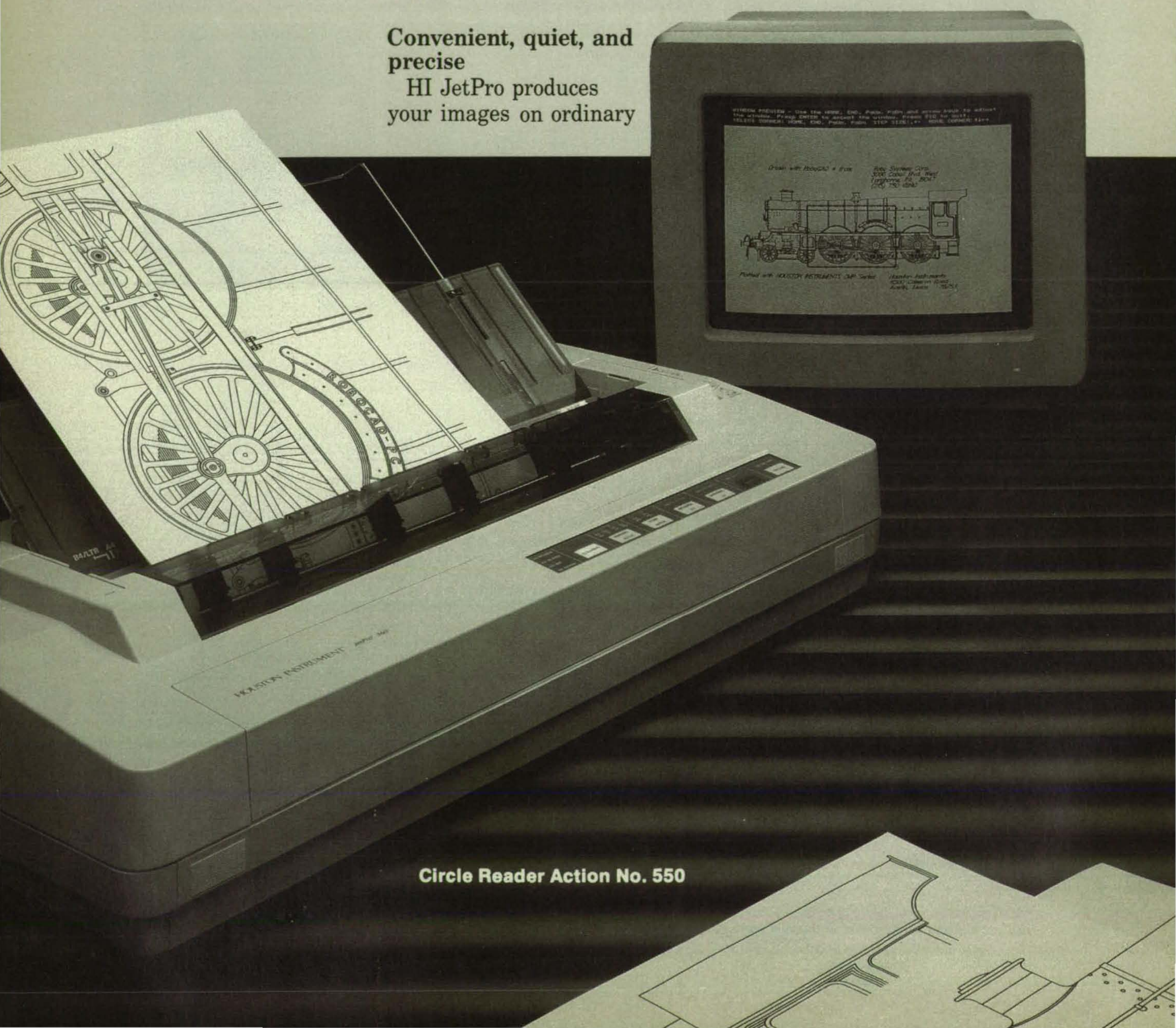

NASA Tech Briefs

Transferring Technology to
American Industry and Government

August 1990
Volume 14 Number 8

Photo courtesy Ames Research Center

A helmet-mounted display system at NASA's Ames Research Center provides a pilot with a broad range of visual data for flight simulation. No matter how the pilot turns his or her head—sideways, rearward, up, or down—the display shows the image the pilot would see in a real situation. ***Turn to page 30.***

SPECIAL FEATURE

TECHNICAL SECTION

DEPARTMENTS

On The Cover: A computer-generated view of Mars' surface using the Virtual Workstation, a head-mounted system that combines three-dimensional graphics and sound to immerse the user in a "virtual reality." The NASA invention has paved the way for a variety of commercial applications of virtual reality technology. ***See page 10.***
(Photo coutesy Ames Research Center)

Photo courtesy VPL Research Inc.

Researchers have developed a sensor-lined glove (page 10) that enables the wearer to control computer images with simple hand movements.

NASA Tech Briefs, ISSN 0145-319X, USPS 750-070, copyright © 1990 in U.S., is published monthly by Associated Business Publications Co., Ltd., 41 E. 42nd St., New York, NY 10017-5391. The copyrighted information does not include the individual tech briefs which are supplied by NASA. Editorial, sales, production and circulation offices at 41 East 42nd Street, New York, NY 10017-5391. Subscription for non-qualified subscribers in the U.S. , Panama Canal Zone, and Puerto Rico, $75.00 for 1 year; $125.00 for 2 years; $200.00 for 3 years. Single copies $10.00. Remit by check, draft, postal or express orders. Other remittances at sender's risk. Address all communications for subscriptions or circulation to NASA Tech Briefs, 41 East 42nd Street, New York, NY 10017-5391. Second-class postage paid at New York, NY and additional mailing offices.

POSTMASTER: please send address changes to NASA Tech Briefs, 41 E. 42nd Street, Suite 921, New York, NY 10017-5391.

NASA Tech Briefs

Official Publication of
National Aeronautics and
Space Administration

ABP BPA

NASA Tech Briefs:

Published by .... **Associated Business Publications**
Editor-in-Chief/Publisher .... **Bill Schnirring**
Associate Publisher .... **Frank Nothaft**
Editor .... **Joseph T. Pramberger**
Managing Editor .... **R. J. Laer**
Assistant Editor .... **Theresa M. Detko**
Technical Advisor .... **Dr. Robert E. Waterman**
Production Manager .... **Rita Nothaft**
Traffic Manager .... **James E. Cobb**
Circulation Manager .... **Cheryl Golden**
Telecommunications Specialist .... **Evelyn Mars**
Reader Service Manager .... **Sylvia Valentin**

Briefs & Supporting Literature:
Provided to National Aeronautics and Space Administration by **International Computers & Telecommunications, Inc.,** NY, NY with assistance from **Logical Technical Services,** NY, NY
Technical/Managing Editor .... **Ted Selinsky**
Art Director .... **Luis Martinez**
Administrator .... **Elizabeth Texeira**
Chief Copy Editor .... **Lorne Bullen**
Staff Writers/Editors .... **Dr. James Boyd, Dr. Larry Grunberger, Dr. Theron Cole, Jordan Randjelovich, George Watson, Oden Browne**
Graphics .... **Vernald Gillman, Charles Sammartano**
Editorial & Production .... **Bill Little, Ivonne Valdes, Frank Ponce, Susan Finelli**

NASA:
NASA Tech Briefs are provided by the National Aeronautics and Space Administration, Technology Utilization Division, Washington, DC:
Administrator .... **Richard H. Truly**
Assistant Administrator for Commercial Programs ..... **James T. Rose**
Deputy Assistant Administrator (Programs) .... **Henry J. Clarks**
Acting Director TU Division (Publications Manager) .... **Leonard A. Ault**
Manager, Technology Utilization Office, NASA Scientific and Technology Information Facility .... **Walter M. Heiland**

Associated Business Publications
41 East 42nd Street, Suite 921, New York, NY 10017-5391
(212) 490-3999 FAX (212) 986-7864
President .... **Bill Schnirring**
Executive Vice President .... **Frank Nothaft**
Vice President .... **Domenic A. Mucchetti**
Operations Manager .... **Rita Nothaft**
Controller .... **Felecia Lahey**

Advertising:
New York Office: (212) 490-3999 FAX (212) 986-7864
Director of Advertising Sales .... **Domenic A. Mucchetti**
Account Executive (NY, NJ) .... **Brian Clerkin** at (201) 285-0880
Account Executive (VA, DC, MD, DE, WV) .... **John D. Floyd** at (215) 399-3265
Account Executive .... **Debby Crane** at (201) 967-9838
Account Executive (Midwest) .... **Paul Lesher, CBC** at (708) 501-4140
Account Executive (Northwest) .... **Bill Hague** at (206) 858-7575
Regional Sales Manager (South-Central) .... **Douglas Shaller** at (212) 490-3999
Account Executives (Eastern MA, NH, ME, RI) .... **Paul Gillespie** at (508) 429-8907; **Bill Doucette** at (508) 429-9861
Account Executives (Western MA, CT, VT) .... **George Watts** or **David Haggett** at (413) 253-9881
Account Executives (Southeast) .... **Newton Collinson** or **Jonathan Kiger** or **Lawrence Mischik** at (404) 939-8391
Account Executives (Calif., AZ, NV, NM) ....
for Area Codes 818/213/805 —**Robert D'Alexander**
for Area Codes 408/415/916/209 —**Elizabeth Cooper**
and for Area Codes 619/714 —**Karen Mock** at (213) 372-2744

NTBM-Research Center
Account Supervisor .... **Lourdes Del Valle**

In college, you would have killed for MathCAD. So why aren't you calculating with it now?

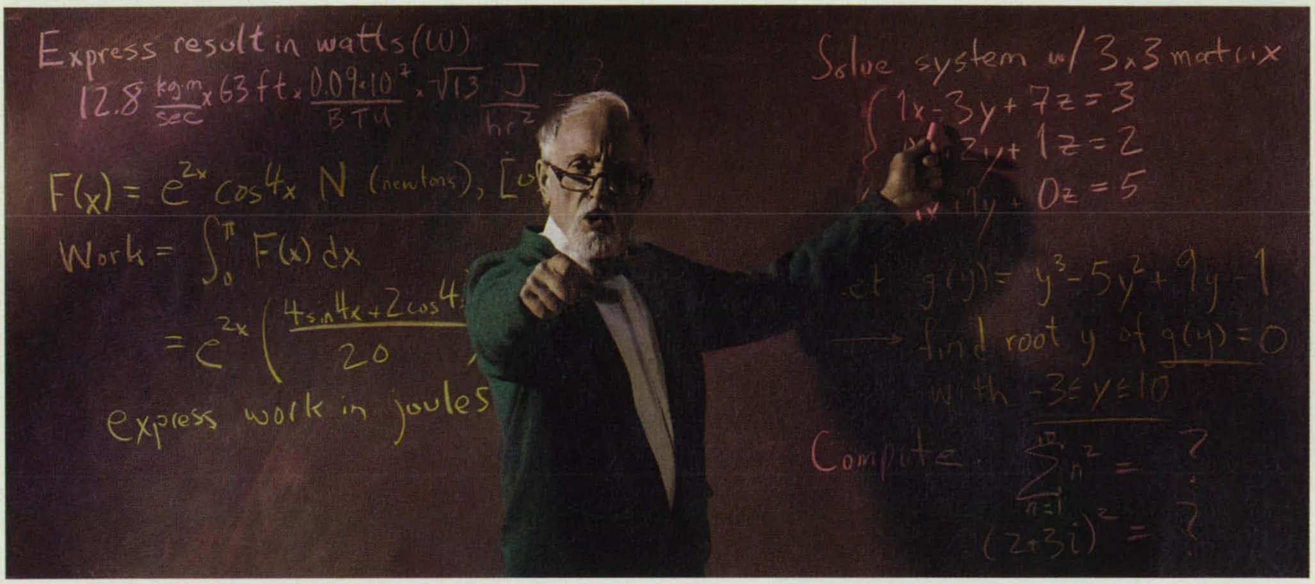

100,000 engineers and scientists already let MathCAD do their calculations for them.

Now that college is far behind you, perhaps it's time you graduated from spreadsheets, calculators and programming.

Because in today's working world of engineering and science, there's no time for anything less than MathCAD. The software that lets you perform engineering and scientific calculations in a way that's faster, more natural, and less error-prone than any calculator, spreadsheet, or program you could write yourself.

Thanks to MathCAD's live document interface,™ you can enter equations anywhere on the screen, add text to support your work, and graph the results.

PC MAGAZINE EDITOR'S CHOICE
March 14, 1989 issue.
Best of '88
Best of '87

It also comes complete with over 120 commonly used functions built right in. Perfect for creating complex equations and formulas, as well as exponentials, differentials, cubic splines, FFTs and matrices.

You get three-dimensional plotting, vivid graphing, and the ability to import HPGL files from most popular CAD programs, including AutoCAD.®

Done calculating? MathCAD prints *all* your analyses in presentation-quality documents, even on PostScript® compatible printers.

All of which has made MathCAD far and away the best-selling math software in the world. In fact, it's used by over 100,000 engineers and scientists—just like you.

There's MathCAD for the PC. MathCAD for the Mac, written to take full advantage of the Macintosh® interface. And a Unix® version that utilizes the speed and unlimited memory of your Unix workstation.

We also have Applications Packs for Advanced Math, Statistics, Mechanical, Chemical, and Electrical Engineering. Each is a collection of adaptable mathematical models, designed to let you start solving your real world problems right away.

For a free MathCAD demo disk, or upgrade information, dial 1-800-MATHCAD (in MA, 617-577-1017). Or see your software dealer.

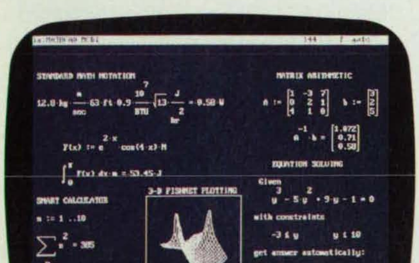

MathCAD 2.5 includes 3-D plotting, HPGL sketch import, and PostScript output.

Available for IBM® compatibles, Macintosh computers, and Unix workstations.

TM and ® signify manufacturer's trademark or registered trademark, respectively.

1-800-MATHCAD

MathCAD®

MathSoft, Inc., 201 Broadway, Cambridge, MA 02139

22

U.K.: Adept Scientific 0462-480055; France: ISECEGOS 1-46092768; Germany: Softline 07802-4036; Japan: CRC 03-665-9762; Finland: Zenex Oy 90-692-7677; Italy: Channel 02-4229441. *PSE*

Mission Accomplished

Computerized Reality Comes Of Age

Rapidly-Advancing Technology Could Revolutionize The Way Humans Interact With Computers

You are an astronaut exploring a vast canyon on the surface of Mars. With a wave of your hand, you begin to fly over the terrain and out into the depths of space. Flick your wrist and suddenly you are transformed into a single molecule speeding through the human circulatory system.

Welcome to the brave new world of virtual reality (VR) , where you can be anything and anywhere you want to be—given the right software program. To enter this artificial environment, you don a pair of goggles containing two liquid crystal displays (LCDs)—one to cover each eye—which serve as viewing screens. Optics mounted on the LCDs present wide-angle stereoscopic color images of the real world or imaginary ones generated by a computer linked to the display via cable. A sensor on the goggles tracks head position and orientation, allowing the computer to shift the image in correlation with your head movements. Headphones provide three-dimensional audio, enhancing the illusion of being inside the display.

NASA and the Department of Defense developed the first VR systems for specialized applications such as flight simulation. Now the technology is moving from the research laboratories into the private sector, with uses ranging from computer-aided design and communications to education and entertainment. "We're just beginning to scratch the surface in terms of commercial development," said NASA scientist Dr. Michael McGreevy, who designed the Virtual Workstation *(NTB Vol. 12, Num. 7)*, considered the first practical VR system.

One of the leading purveyors of virtual reality products is VPL Research Inc. of Redwood City, CA. With NASA's assistance, VPL developed the DataGlove , a sensor-lined lycra glove that converts hand gestures and positions into computer-readable form, enabling the wearer to interact with simulated environments and control the action. "It lets you pick up and handle objects in the virtual world as if they are real," said

The DataGlove allows a computer user to handle onscreen images as if they are real three-dimensional objects. Sensors lining the glove communicate hand movements to a graphics computer.
Photo courtesy VPL Research Inc.

Ann Lasko, director of product design at VPL. "If you hold your hand in front of your face you see a virtual version of your hand. You can wiggle your virtual fingers."

Tested extensively as part of the Virtual Workstation, the DataGlove incorporates fiber optic sensors that measure flexion and extension of the fingers, and a Polhemus magnetic tracking device that determines the hand's position and orientation. A microprocessor-based control unit transmits data from the glove to the host computer.

In addition to its role as an interface for VR systems, the DataGlove can be used to control conventional computer screens, replacing mice and joysticks. "It provides a natural, intuitive way to interact with your computer," said Ms. Lasko. Mattel Inc. has introduced a plastic glove based on VPL's technology as an accessory for Nintendo video games. The "Power Glove" allows players to directly manipulate onscreen graphics. "You can use hand motions to throw a ball or battle a villian," she explained.

The VPL glove also offers applications in telerobotics and biomedicine. New York University researchers use the device to control a dexterous robot hand, while Greenleaf Medical Systems of Palo Alto, CA, employs the glove in a system that measures how much the different joints of the human hand can bend, enabling doctors to accurately determine hand impairment. Greenleaf recently hooked up a speech synthesizer to the DataGlove to demonstrate the capability for turning hand gestures into audible words. They hope to develop a low-cost system that would translate sign language into speech.

VPL has incorporated DataGlove principles into a suit that covers the entire human frame. This "DataSuit" permits full-body participation in virtual reality. Presently, the suit's main use is to lend realistic motion to characters in computer-generated special effects. "An actor wears the suit, and every body movement can be fed into the computer," said Ms. Lasko.

Photo courtesy VPL Research Inc.

An EyePhone wearer sees a 3D image of his hand while the same image is displayed on the monitor.

Playing a game of "virtual" racquetball

Photo courtesy Autodesk Inc.

Shared Realities

The company recently introduced a system called Reality Built for Two, or RB2, that enables multiple users to share a virtual space and interact with one another. The forms and behaviors of RB2's virtual worlds are specified graphically, so that non-programmers can design them. "You decide what you want your virtual body to look like," said Ms. Lasko. "The experience is like being at a costume party except that the external environment can also be changed."

RB2's primary user input devices are the DataGlove and a head-tracking Polhemus sensor attached to the 3D goggles, or EyePhone. The design and control workstation is a Mac II running a solid modeling application called RB2 Swivel and a real-time animation control package known as Body Electric. Position and orientation data are translated by Body Electric into graphics commands for the rendering software, Isaac, which runs on Silicon Graphics IRIS POWERSeries workstations. In order to maintain high frame rates, one IRIS is used for each eye. The configuration utilizes Ethernet and NTSC cables.

VPL is now laying the groundwork for a project called RealityNet which will connect the company with RB2 users at the University of North Carolina, MIT, and the Washington Technology Center in Seattle by way of modems and ordinary telephone lines. It could pave the way for a variety of multi-user applications of VR systems. In coming years, engineers separated by thousands of miles may share a virtual workspace where they can collaborate on the design of aircraft or automobile components; they would be able to rotate a part or change its size and shape using simple hand gestures such as pointing or waving. Similarly, a group of medical students may perform surgery on a virtual patient in a computer-generated operating room.

Virtual Audio

RB2 incorporates a three-dimensional sound reproduction system originally developed for the Virtual Workstation by Dr. Elizabeth Wenzel of NASA's Ames Research Center and Scott Foster of Crystal River Engineering (CRE) Inc., a California-based start-up company. Called the Convolvotron, it is a digital signal processing (DSP) system that enables the listener, using standard headphones, to locate in space up to four independent and simultaneous sound sources. At the heart of the Convolvotron is its exceptional processing capacity—128 parallel multiply/accumulate/shift processors make the system more than 20 times faster than conventional DSPs.

The Convolvotron's utility extends beyond virtual reality to fields such as hearing research, telecommunications, and architectural acoustics, according to Mr. Foster, whose company markets the system nationwide. Current customers include MIT, which is using the system as part of an effort to develop binaural hearing aids, and Bellcore, which is studying ways to improve teleconferencing systems.

CRE has developed a single-source system called the Microtron for basic audio research, and an advanced prototype system with four times the Convolvotron's throughput. This system is capable of over one billion multiply-accumulate operations per second. Under contract to NASA, the company is designing a workstation-level software package for the Convolvotron that will allow researchers to quickly devise and run experiments involving human subjects.

VR On A PC

Current head-mounted VR systems are too expensive for widespread use; they rely on customized graphics workstations and can cost over $200,000 each. Autodesk Inc., a major supplier of computer-aided design software, is developing a PC-based virtual reality software package called Cyberspace that should dramatically slash the cost of creating artificial worlds. Expected on the market next year, Cyberspace will be a generic program adaptable to almost any type of graphics or design work.

"Our goal is to produce a simulation kernel that will be small and fast and run under a variety of operating systems," said Chris Allis, public relations director for the Cyberspace project. "We'll license it to third-party developers who will then build customized applications."

Bringing Mars Down To Earth

Meanwhile, NASA is refining its pioneering VR machine for advanced applications such as space telerobotics and virtual solar system exploration. Dr. McGreevy's team is developing a flight-qualifiable system for possible use on space station Freedom. Astronauts aboard the orbiting facility may eventually use the Virtual Workstation to guide robots repairing satellites in space. The astronaut would see what the robot sees and, by wearing a glove embedded with force reflectors, would feel the tightness of the robot's grip on a tool or spacecraft part.

Another project looks to bring the planets and moons virtually down to Earth by recreating interactive digital models from pictorial data. "Using personal simulators, we could all participate in the exploration of the planets," said Dr. McGreevy. "It would democratize space exploration." ❑

For further information about the technologies described in this article, contact:

Laurance Milov
Technology Utilization Officer
Ames Research Center
Mail Code 223-3
Moffett Field, CA 94035

Ann Lasko
VPL Research Inc.
656 Bair Island Road
Suite 304
Redwood City, CA 94063

Scott Foster
Crystal River Engineering Inc.
12350 Wards Ferry Road
Groveland, CA 95321

Chris Allis
Autodesk Inc.
2320 Marinship Way
Sausalito, CA 94965

THERE'S ONLY ONE THING TO SAY ABOUT INFORMATION SECURITY.

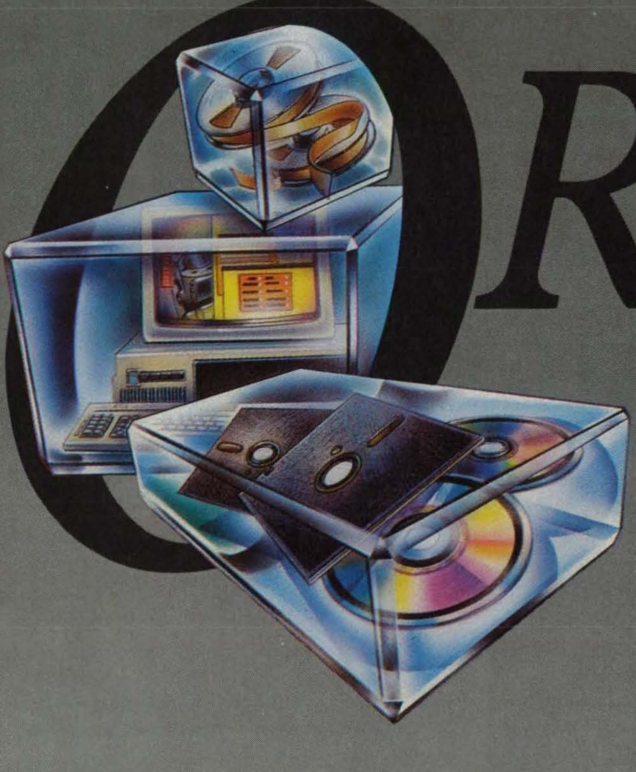

ORACLE

The term "state-of-the-art database security" can be written more concisely:

Oracle.

That's because Oracle's commitment to providing leading edge information security solutions to numerous federal agencies and military branches is well established and growing.

Already, Oracle's relational DBMS software provides high-level data integrity and security on everything from micros and minis to workstations and mainframes.

Add Oracle's reputation for exceptional quality, service and support and you'll arrive at a winning combination for high-security software.

To learn more about how Oracle can help you manage information with security and integrity, register for an Oracle seminar, or call **1-800-345-DBMS, ext. 6764** for a free brochure.

Incidentally, there's one more thing to say about information security: Authorized ADP Schedule Price List Contract No. GS00K 88 AGS 5937.

ORACLE®

FEDERAL DIVISION

Compatibility. Portability. Connectability. Capability.

Oracle Federal Division
3 Bethesda Metro Center, Suite 1400
Bethesda, MD 20814

Circle Reader Action No. 494

New Product Ideas

New Product Ideas are just a few of the many innovations described in this issue of *NASA Tech Briefs* and having promising commercial applications. Each is discussed further on the referenced page in the appropriate section in this issue. If you are interested in developing a product from these or other NASA innovations, you can receive further technical information by requesting the TSP referenced at the end of the full-length article or by writing the Technology Utilization Office of the sponsoring NASA center (see page 16). NASA's patent-licensing program to encourage commercial development is described on page 16.

Implantable Electrode for Critical Locations

An implantable electrode is expected to hold itself in place until body tissue grows around it and retains it. Used for delivering electrical stimuli to muscles that have become inactive through accident or disease, the electrode can help paraplegics and others to exercise voluntary control over arms and legs.
(See page 74)

Flow-Control Unit for Nitrogen and Hydrogen Gases

A gas-flow-control unit replaces a system that had nine separately serviced components. Reliable performance was demonstrated in 30 days of cyclic testing, which included 2,244 operating cycles and tank-filling sequences.
(See page 54)

Liquid-Air Breathing Apparatus

An emergency liquid-air breathing apparatus can supply air for 60 minutes or more. The pack is worn on the user's back and weighs approximately 28 lb (12.7 kg) when full.
(See page 74)

Additives Lower Dielectric Constants of Polyimides

A new process incorporates diamic acid additives to lower the dielectric constants of aromatic condensation polyimide films and coatings. Dielectric constants as low as 2.43 reached by this process make polyimides more attractive for electronic applications.
(See page 49)

Polyimidazoles via Aromatic Nucleophilic Displacement

Ten different polyimidazoles were synthesized by aromatic nucleophilic displacement, from the reactions of bisphenolimidazoles with activated difluoro compounds. These polyimidazoles have good mechanical properties suitable for use as films, moldings, and adhesives.
(See page 48)

Monolithic Optoelectronic Integrated Circuit

A monolithic optoelectronic integrated circuit is a compact unit that converts a serial input light signal from an optical fiber at data rates of up to 1 Gb/s into 16 parallel electrical output signals. In comparison with similar demultiplexers made with hybrid or discrete components, this unit has about one-fifth the size, one-tenth the power consumption, and two-fifths the weight and can be integrated monolithically with other GaAs devices.
(See page 25)

Last Year, This Is How They Won The IBM Supercomputing Competition.

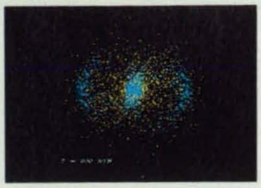

1st Place: Gas dynamics and star formation in merging galaxies. Kevin M. Olson, University of Massachusetts.

1st Place: 3-D reconstruction of cochlea structure. Carl S. Brown and Alan C. Nelson, University of Washington.

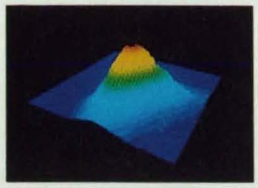

1st Place: Stretching and bending of material surfaces in turbulence. Stephen B. Pope and Sharath Girimaji, Cornell University; Pui-Kuen Yeung, Pennsylvania State University.

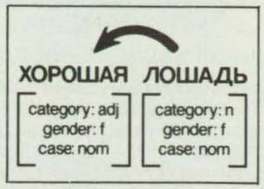

1st Place: A dependency parser for variable word order languages. Michael A. Covington, University of Georgia.

This Year, This Is How You Can.

For information and an entry form, write to:

Supercomputing Competition Administrator
IBM Corporation
36 Mill Plain Road, Suite 404
Danbury, CT 06811

Name____________________

Affiliation____________________

Address____________________

City__________ State_____ Zip_____

Phone__________ FAX__________

NTB

Call For Papers

Last year, the response was overwhelming. So this year, the IBM Supercomputing Competition, with a new division, returns.

Created to discover, acknowledge and reward gifted American and Canadian scientists and engineers, this prestigious competition honors those whose papers describe innovative approaches to large-scale analysis and modeling.

Each paper must describe work using an IBM 3090™ Supercomputer and/or the paper must describe distributed or cooperative processing in which IBM technical workstations are linked to IBM mainframes.

The papers will be judged in five divisions: Physical Sciences and Mathematics; Engineering; Life and Health Sciences; Social Sciences, Humanities and the Arts; and Computer Sciences—Distributed and Cooperative Processing (new division). Each division will receive a first, second and third prize of $25,000, $15,000 and $10,000, respectively. Also, a "PROCEEDINGS" of selected papers will be published.

Contestants must register an abstract of their paper by October 16, 1990. Those who have registered their abstracts must forward their papers by January 15, 1991.

To select winners, IBM will retain a panel of independent authorities in each division. Winners will be announced by March 30, 1991.

For more information, contact your IBM marketing representative or call the IBM Supercomputing Competition Administrator at (203) 794-1355, FAX: (203) 792-7507 in the U.S.; (416) 758-4136 in Canada.

IBM®

HOW YOU CAN BENEFIT FROM NASA's TECHNOLOGY UTILIZATION SERVICES

If you're a regular reader of TECH BRIEFS, then you're already making use of one of the low- and no-cost services provided by NASA's Technology Utilization (TU) Network. But a TECH BRIEFS subscription represents only a fraction of the technical information and applications/engineering services offered by the TU Network as a whole. In fact, when all of the components of NASA's Technology Utilization Network are considered, TECH BRIEFS represents the proverbial tip of the iceberg.

We've outlined below NASA's TU Network—named the participants, described their services, and listed the individuals you can contact for more information relating to your specific needs. We encourage you to make use of the information, access, and applications services offered by NASA's Technology Utilization Network.

How You Can Utilize **NASA's Industrial Applications Centers**—A nationwide network offering a broad range of technical services, including computerized access to over 100 million documents worldwide.

You can contact NASA's network of Industrial Applications Centers (IACs) for assistance in solving a specific technical problem or meeting your information needs. The "user friendly" IACs are staffed by technology transfer experts who provide computerized information retrieval from one of the world's largest banks of technical data. Nearly 500 computerized data bases, ranging from NASA's own data base to Chemical Abstracts and INSPEC, are accessible through the ten IACs located throughout the nation. The IACs also offer technical consultation services and/or linkage with other experts in the field. You can obtain more information about these services by calling or writing the nearest IAC. User fees are charged for IAC information services.

Aerospace Research Applications Center (ARAC)
Indianapolis Center for Advanced Research
611 N. Capitol Avenue
Indianapolis, IN 46204
Dr. F. Timothy Janis, Director
(317) 262-5036

Central Industrial Applications Center/NASA (CIAC)
Rural Enterprises, Inc.
P.O. Box 1335
Durant, OK 74702
Dr. Dickie Deel, Director
(405) 924-5094
(800) 658-2823 (toll-free US)

Science and Technology Research Center (STRC)
Post Office Box 12235
Research Triangle Park, NC 27709-2235
H.L. (Lynn) Reese, Director
(919) 549-0671

NASA Industrial Applications Ctr. 823 William Pitt Union
University of Pittsburgh
Pittsburgh, PA 15260
Robert G. Konecny, Acting Director
(412) 648-7000

Southern Technology Applications Center (STAC)
Box 24
Progress Ctr., One Progress Blvd.
Alachua, FL 32615
J. Ronald Thornton, Director
(904) 462-3913
(800) 354-4832 (FL only)
(800) 225-0308 (toll-free US)

NASA/UK Technology Applications Program
University of Kentucky
109 Kinkead Hall
Lexington, KY 40506-0057
William R. Strong, Director
(606) 257-6322

NERAC, Inc.
One Technology Drive
Tolland, CT 06084
Dr. Daniel U. Wilde, President
(203) 872-7000

Technology Application Center (TAC)
University of New Mexico
Albuquerque, NM 87131
Dr. Stanley A. Morain, Director
(505) 277-3622

NASA Industrial Applications Center
University of Southern California Research Annex
3716 South Hope Street
Los Angeles, CA 90007-4344
Robert Stark, Director
(213) 743-6132
(800) 642-2872 (CA only)
(800) 872-7477 (toll-free US)

NASA/SU Industrial Applications Center
Southern University Department of Computer Science
P.O. Box 9737
Baton Rouge, LA 70813-9737
Dr. John Hubbell, Director
(504) 771-6272
(504) 771-4950

If you represent a public sector organization with a particular need, you can contact NASA's Application Team for technology matching and problem solving assistance. Staffed by professional engineers from a variety of disciplines, the Application Team works with public sector organizations to identify and solve critical problems with existing NASA technology. **Technology Application Team, Research Triangle Institute, P. O. Box 12194, Research Triangle Park, NC 27709. *Doris Rouse, Director,* (919) 541-6980**

How You Can Access Technology Transfer Services At NASA Field Centers: **Technology Utilization Officers & Patent Counsels**—Each NASA Field Center has a Technology Utilization Officer (TUO) and a Patent Counsel to facilitate technology transfer between NASA and the private sector.

If you need further information about new technologies presented in *NASA Tech Briefs,* request the Technical Support Package (TSP). If a TSP is not available, you can contact the Technology Utilization Officer at the NASA Field Center that sponsored the research. He can arrange for assistance in applying the technology by putting you in touch with the people who developed it. If you want information about the patent status of a technology or are interested in licensing a NASA invention, contact the Patent Counsel at the NASA Field Center that sponsored the research. Refer to the NASA reference number at the end of the Tech Brief.

Ames Research Ctr.
Technology Utilization Officer: Laurance Milov
Mail Code 223-3
Moffett Field, CA 94035
(415) 604-4044
Patent Counsel: Darrell G. Brekke
Mail Code 200-11
Moffett Field, CA 94035
(415) 604-5104

Lewis Research Center
Technology Utilization Officer: Anthony F. Ratajczak
Mail Stop 7-3
21000 Brookpark Road
Cleveland, OH 44135
(216) 433-2225
Patent Counsel: Gene E. Shook
Mail Code LE-LAW
21000 Brookpark Road
Cleveland, OH 44135
(216) 433-5753

John C. Stennis Space Center
Technology Utilization Officer: Richard A. Galle (acting)
Code HA-32
Stennis Space Center, MS 39529
(601) 688-1929

John F. Kennedy Space Center
Technology Utilization Officer: Thomas M. Hammond
Mail Stop PT-PMO-A
Kennedy Space Center, FL 32899
(407) 867-3017
Patent Counsel: James O. Harrell
Mail Code PT-PAT
Kennedy Space Center, FL 32899
(407) 867-2544

Langley Research Ctr.
Technology Utilization Officer: John Samos
Mail Stop 139A
Hampton, VA 23665
(804) 864-2484
Patent Counsel: George F. Helfrich
Mail Code 279
Hampton, VA 23665
(804) 864-3523

Goddard Space Flight Center
Technology Utilization Officer: Donald S. Friedman
Mail Code 702.1
Greenbelt, MD 20771
(301) 286-6242
Patent Counsel: R. Dennis Marchant
Mail Code 204
Greenbelt, MD 20771
(301) 286-7351

Jet Propulsion Lab.
NASA Resident Office
Technology Utilization Officer: Gordon S. Chapman
Mail Stop 180-801
4800 Oak Grove Drive
Pasadena, CA 91109
(818) 354-4849
Patent Counsel: Paul F. McCaul
Mail Code 180-801
4800 Oak Grove Drive
Pasadena, CA 91109
(818) 354-2734
Technology Utilization Mgr. for JPL: Dr. Norman L. Chalfin
Mail Stop 156-211
4800 Oak Grove Drive
Pasadena, CA 91109
(818) 354-2240

George C. Marshall Space Flight Center
Technology Utilization Officer: Ismail Akbay
Code AT01
Marshall Space Flight Center,
AL 35812
(205) 544-2223
Fax (205) 544-3151
Patent Counsel: Bill Sheehan
Mail Code CC01
Marshall Space Flight Center,
AL 35812
(205) 544-0021

Lyndon B. Johnson Space Center
Technology Utilization Officer: Dean C. Glenn
Mail Code IC-4
Houston, TX 77058
(713) 483-3809
Patent Counsel: Edward K. Fein
Mail Code AL3
Houston, TX 77058
(713) 483-4871

NASA Headquarters
Technology Utilization Officer: Leonard A. Ault
Code CU
Washington, DC 20546
(202) 453-8377
Assistant General Counsel for Patent Matters: Robert F. Kempf, Code GP
Washington, DC 20546
(202) 453-2424

A Shortcut To Software: **COSMIC®**—For software developed with NASA funding, contact COSMIC, NASA's Computer Software Management and Information Center. New and updated programs are announced in the Computer Programs section. COSMIC publishes an annual software catalog. For more information call or write: **COSMIC®** 382 East Broad Street, Athens, GA 30602 *John A. Gibson, Dir.,* (404) 542-3265

If You Have a Question. . . **NASA Scientific & Technical Information Facility** can answer questions about NASA's Technology Utilization Network and its services and documents. The STI staff supplies documents and provides referrals. Call, write or use the feedback card in this issue to contact: **NASA Scientific and Technical Information Facility,** Technology Utilization Office, P.O. Box 8757, Baltimore, MD 21240-0757. *Walter M. Heiland, Manager,* (301) 859-5300, Ext. 242, 243

Automatic Range Changer for SWR Meter

A commercial unit is modified for antenna-pattern measurements.

NASA's Jet Propulsion Laboratory, Pasadena, California

The addition of an automatic range-changing circuit converts the Hewlett-Packard 415E standing-wave-ratio (SWR) meter into a radio-frequency detector suitable for computer-controlled measurements of radiation patterns of antennas. This modification gives the SWR meter an effective dynamic range of at least 40 dB.

The circuit (see figure) includes two digital lines that communicate one of four range settings to the controlling computer and one digital line to inhibit the transfer of data when a range is being changed. The cost of the components is less than $150.00 (1988 prices), and the circuit can be installed without any permanent change to the SWR meter. The additional capability provided by the auto-range circuit makes the SWR meter an ideal instrument for use in applications involving computer-controlled monitoring of power when large changes in signal level are expected.

When the automatic range-changing circuit is engaged, the modified SWR meter accomplishes all changing of ranges internally, independently of any external controller. In most applications, a computer will be used to log data, and data are transferred through the recorder output lines of the SWR meter with appropriate buffering. The input signal power is derived from the analog meter circuitry, which, although it displays only 10 dB, actually has a range of 13 dB. These extra 3 dB are used as headroom during a range-changing operation. The analog-to-digital conversion is not performed in the SWR meter and must be effected by the controller. The selection of range is displayed on light-emitting diodes,

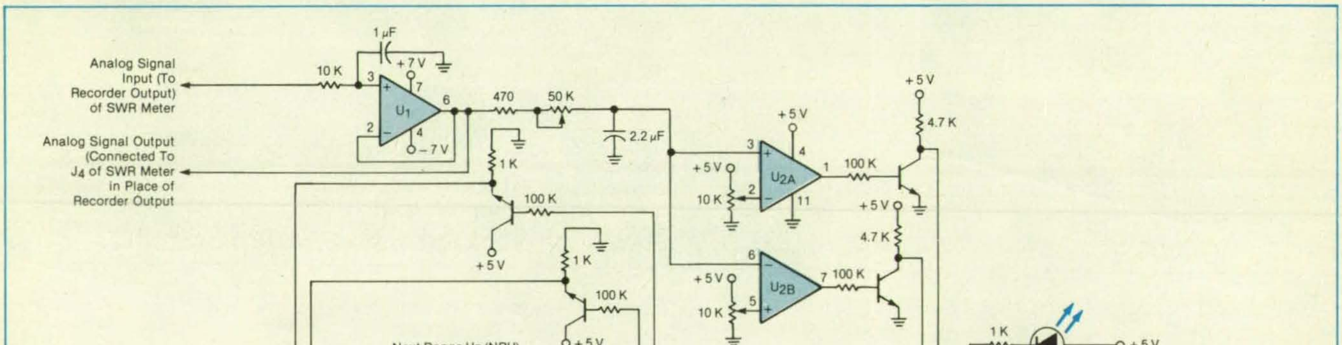

The **Automatic Range-Changing Circuit** is installed in the HP415E SWR meter. The five output lines are shown on the left. Connections to the circuit board of the SWR meter are shown on the right.

which have been added around the input attenuator dial of the SWR meter.

The modified SWR meter is being used in an automated antenna-pattern-measuring facility at NASA's Jet Propulsion Laboratory. Upon incorporation of the modified SWR meter into this system, the speed of measurement was increased by a factor of 10 over that of a sophisticated spectrum analyzer equipped with general-purpose-interface-bus readout, and the dynamic range was extended by more than 20 dB over that of a lock-in amplifier, the range of which cannot be changed without allowing extensive time for autophasing.

This work was done by Robert J. Dengler and Peter H. Siegel of Caltech for **NASA's Jet Propulsion Laboratory**. *For further information, Circle 128 on the TSP Request Card.*

NPO-17822

Self-Aligned Guard Rings for Schottky-Barrier Diodes

The active area would be increased.

NASA's Jet Propulsion Laboratory, Pasadena, California

A proposed self-aligned guard ring would increase the active area of a Schottky-barrier infrared detector. The self-alignment concept was developed for silicide Schottky-barrier diodes in which platinum silicide or iridium silicide Schottky-contacts provide cutoff wavelengths of about 6 or 10 μm, respectively.

Silicide diodes have been built into focal plane arrays of 512 by 512 elements for infrared imaging. Usually, each diode element must be surrounded and overlapped by an n-type guard ring to disperse electric-field lines at the edge of the silicide layer in order to suppress the leakage current.

Self-alignment eliminates the need for much of the overlap between the guard ring and the silicide contact. Ordinarily, an overlap of 2 μm is necessary to allow for misalignment of the ring mask and lateral diffusion and straggling of dopant ions during the fabrication of the guard rings. In a diode of 30 by 48 μm, for example, the overlap reduces the effective area by about 20 percent. Inasmuch as the overlap area is not sensitive to infrared, the result is a significant loss of output.

To begin the fabrication of a self-aligned array of diodes, a layer of silicon dioxide doped with phosphorus would be deposited on a silicon substrate. This layer would be etched to form a grid defining the elements of the array (see figure). The phosphorus in the grid would be diffused into the silicon to form a grid of n-type guard rings. Thus, self-alignment would make fabrication simpler by eliminating the masking step for diffusion of the n-type guard ring. Finally, the desired metal would be deposited on the exposed silicon surface, and the silicide layer would be formed by annealing. The only overlap of a guard ring with the silicide layer of a cell would be that caused by sideways diffusion of the phosphorus, which can be kept quite low by adjusting the time and temperature of the diffusion process.

This work was done by True-Lon Lin of Caltech for **NASA's Jet Propulsion Laboratory**. *For further information, Circle 138 on the TSP Request Card.*

This invention is owned by NASA, and a patent application has been filed. Inquiries concerning nonexclusive or exclusive license for its commercial development should be addressed to the Patent Counsel, NASA Resident Office-JPL [see page 16]. Refer to NPO-17734.

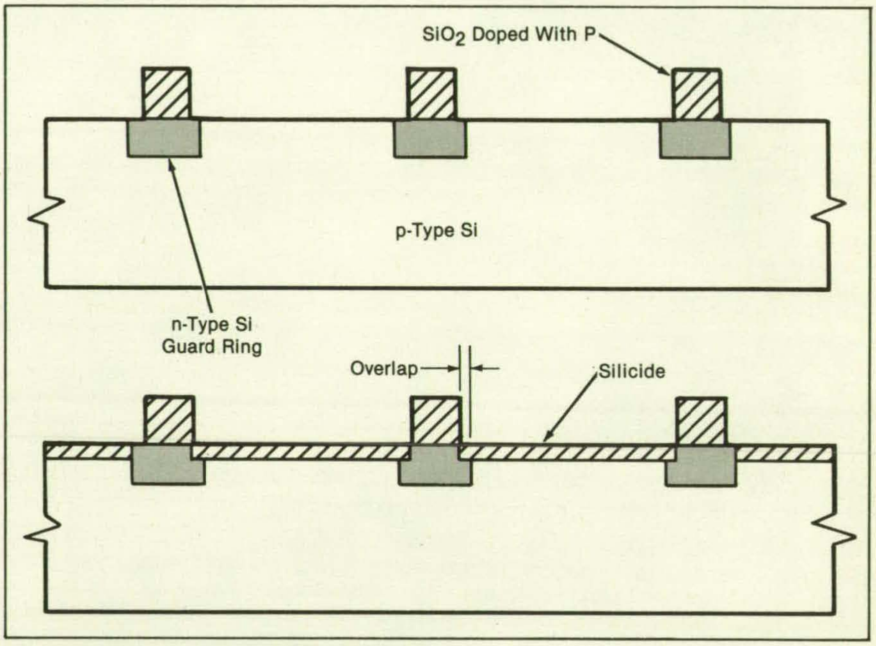

A **Grid of Silicon Dioxide Doped With Phosphorus** would be etched on a silicon wafer, and phosphorus from the grid would diffuse into the substrate (top), creating n-type guard rings. Silicide layers would be formed in the open areas of the grid (bottom). The overlap of the guard rings and the silicide layers would be small.

Starting Circuit for Erasable Programmable Logic Device

The voltage regulator is bypassed to supply the starting current.

NASA's Jet Propulsion Laboratory, Pasadena, California

A starting or "pullup" circuit supplies the large inrush of current required by an erasable programmable logic device (EPLD) while it is being turned on. The starting circuit operates only during such intervals of high demand for current and has little effect at any other time.

An EPLD is an integrated circuit in which cells erasable by ultraviolet radiation are used to configure elements that perform logical functions. Typically, an EPLD is intended to operate from a regulated 5-Vdc power supply, drawing about 3 mA when at full power with a slow (100 kHz) clock. This low power is an advantage where power must be supplied by a battery.

Because of certain voltage-dependent design features in the portion of the EPLD circuitry that affects the current drawn in the operating mode, the EPLD draws a relatively high current when the supply voltage, V_{CC}, is first turned on. This current rises to a peak of about 40 mA as V_{CC} rises to 3 V. As V_{CC} goes higher, the current abruptly drops to the full operating level. If V_{CC} subsequently falls below 2.5 V, the device abruptly returns to the high-current mode (see Figure 1).

The 40-mA peak starting current is more than can be supplied by a typical voltage regulator designed for operation with low-power circuitry. Therefore, if no provision were made to bypass the voltage regulator during startup, the EPLD would continue to draw the maximum current that the regulator could supply, and V_{CC} could not be made to reach or exceed 3 V.

The starting circuit (see Figure 2) performs the needed bypass, acting as a current-dependent shunt that connects the battery or other source of power more

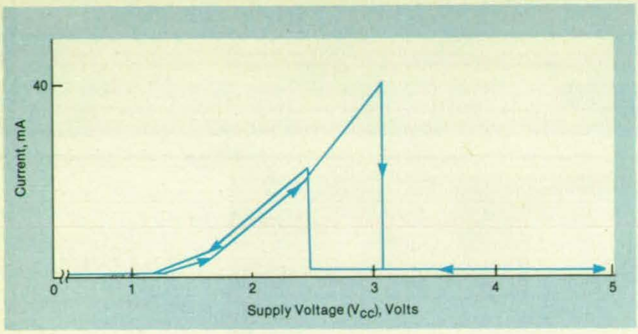

Figure 1. The **Current vs Supply Voltage** of a typical EPLD includes a partly hysteretic high-current, low-voltage regime.

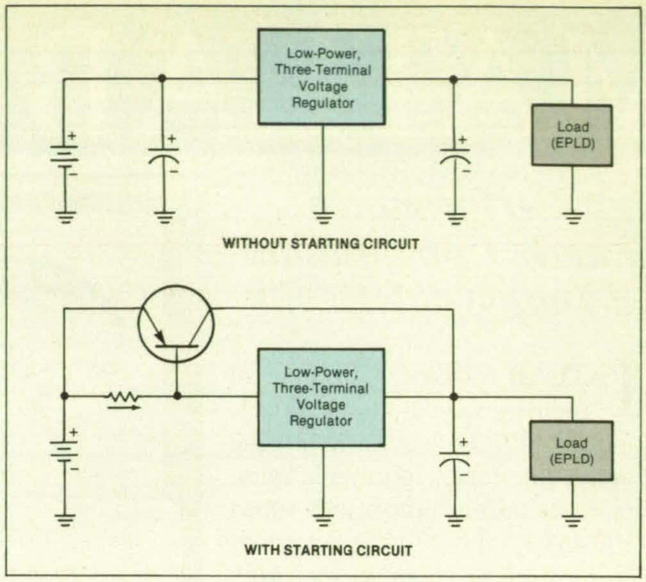

Figure 2. The **Starting Circuit** shunts current around the voltage regulator during the initial rise in V_{cc} to pull the EPLD out of the low-voltage, high-current regime.

nearly directly to the EPLD. The resistor in the starting circuit is chosen so that the voltage across it is 0.6 V when the current through it (which nearly equals the load current) is 80 percent of the maximum rated current of the voltage regulator. As long as the current is less than this value, the transistor remains turned off and effectively out of the circuit. When the current exceeds this value, the transistor turns on, diverting current around the voltage regulator.

It is also noteworthy that the input capacitor of the regulator is removed when the starting circuit is installed. This is done to protect the transistor. The battery can supply a large current, but not as much as can a capacitor during a momentary surge. Thus, the deletion of the capacitor reduces the probability of damage to the transistor in the event of a short circuit in or across the load.

This work was done by Steven W. Cole of Caltech for **NASA's Jet Propulsion Laboratory**. *For further information, Circle 141 on the TSP Request Card.*
NPO-17827

Multi-Pinned-Phase Charge-Coupled Device

A new technology reduces dark-current generation in charge-coupled devices.

NASA's Jet Propulsion Laboratory, Pasadena, California

A new technique, called multi-pinned-phase (MPP) technology allows a charge-coupled device (CCD) to operate totally inverted during both integration and readout while maintaining other performance characteristics. For CCD imagers there are three main sources of dark current: (1) thermal generation and diffusion in the neutral bulk, (2) thermal generation in the depletion region, and (3) thermal generation due to surface states at the Si/SiO_2 interface. Of these sources, the contribution from the surface states is the dominant factor for multiphase CCD's. Dark-current generation at this interface depends on two factors: (1) the density of interface states, and (2) the density of free carriers (holes or electrons) that populate the interface.

Electrons that thermally "hop" from the valence band to an interface state (sometimes referred to as a midband state) and to the conduction band produce a dark-current electron–hole pair. The presence of free carriers will fill the interface states, inhibiting the hopping conduction process and in turn substantially reducing dark current to the bulk dark level.

Conventional CCD operation depletes the signal channel and interface of free carriers, maximizing dark-current generation. Under depleted conditions, dark current is determined by the quality of the Si/SiO_2 interface or the density of midband states, which varies widely among CCD manufacturers.

Channel inversion is easily promoted for a CCD by biasing the array clocks sufficiently negative to invert the n-buried channel and "pin" the surface potential beneath each phase to substrate potential (hence the name multi-pinned-phase). Biasing the array clocks in this manner causes holes from the p^+ channel stops to migrate and populate the Si/SiO_2 interface, eliminating surface dark-current generation. Unfortunately when conventional CCD's are inverted, the full well capacity of the sensor is destroyed because the potential wells within a pixel all assume the same level. This condition results in severe blooming up and down the signal-carrying channel because there is no preferential potential well for charge to collect. To circumvent this difficulty, in MPP CCD technology, a weak implant is employed beneath one or more phases during the fabrication of the sensor. The extra dopant creates a potential difference between phases, allowing charge to accumulate in collecting sites when biased into inversion (see Figure 1).

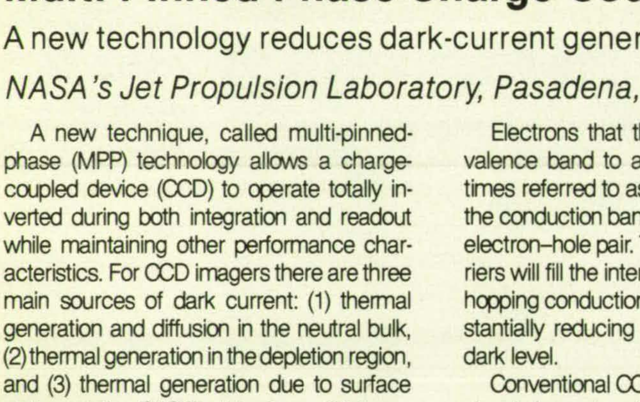

Figure 1. The **MPP-CCD** is made with positive doping (in this case, boron) implants that define barrier phases. When all phases are biased together into inversion, dark current is reduced, and the potential of the charge-collecting wells is the difference between the potentials of the barrier and collection phases.

Other advantages of the MPP CCD include complete elimination of residual image effects during integration and readout, low pixel nonuniformity, and an increase in quantum efficiency in the near infrared because higher operating temperatures can be used. Also, MPP CCD's are more tolerant to ionizing radiation environments. For example, Figure 2 shows dark levels measured under inverted and noninverted conditions before and after the sensor was exposed to 20 kilorads of Co-60 (a source of 1.2-MeV gamma rays). The difference in dark-rate generation

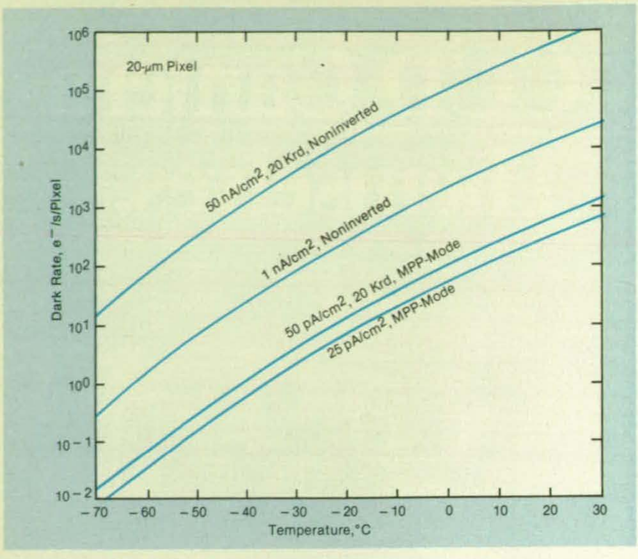

Figure 2. **Dark-Current Generation** as a function of temperature of a Ford MPP-CCD. The dark current is more than three orders of magnitude greater for the noninverted condition than for the inverted state after the sensor was subjected to 20 kilorads of Co-60 radiation. The finite dark-current increase for MPP-operation (a factor of 2) is due to radiation damage in the bulk.

after radiation is over three orders of magnitude between the two operating modes, demonstrating the power of MPP operation in a radiation environment.

This work was done by James R. Janesick of Caltech for **NASA's Jet Propulsion Laboratory**. *For further information, Circle 115 on the TSP Request Card.*

In accordance with Public Law 96-517, the contractor has elected to retain title to this invention. Inquiries concerning rights for its commercial use should be addressed to

Edward Ansell
Director of Patents and Licensing
Mail Stop 305-6
California Institute of Technology
1201 East California Boulevard
Pasadena, CA 91125

Refer to NPO-17462, volume and number of this NASA Tech Briefs *issue, and the page number.*

Imaging Antenna Structure for Submillimeter Wavelengths

Integrated-circuit technology is applied to obtain a two-dimensional array.

NASA's Jet Propulsion Laboratory, Pasadena, California

An integrated-circuit antenna structure contains a two-dimensional array of antennas and antenna reflectors. When operating in the receiving mode, each antenna acts as part of the detector for one picture element in a millimeter- or submillimeter-wavelength imaging radar system (see Figure 1). A millimeter-wave imaging system can be used to view objects through fog, smoke, or smog with resolution intermediate between that of microwave and visible-light imaging systems.

Each element of the array includes a reflecting pyramidal horn and a dipole antenna suspended on a membrane in the horn (see Figure 2). The pyramidal holes for the horns are made by anisotropic etching along the <111> crystal planes of the front and back silicon substrates. The reflecting surfaces are made by depositing gold or other suitable metal on the sides of the pyramidal holes.

The membrane is a layer of silicon nitride or other suitable material that is transparent at the millimeter or submillimeter wavelength of interest. About 1 μm thick, it is made by depositing the membrane material on the back side of the front silicon substrate before etching the horns. Portions of the membrane layer between the pyramidal cavities and around the edges of the front substrate are etched away to make room for detecting and processing electronic circuitry.

The antennas are either mounted or fabricated lithographically on the back side of the membrane. Thus, the antennas can radiate as though they were suspended in free space within the horns, unencumbered by auxiliary supporting structures. Electrical contact to the antennas and processing electronics is made via bonding pads around the edge of the back side of the front substrate. After fabrication of the antennas, circuitry, and reflecting pyramidal surfaces, the front and back substrates are fastened together by conventional means such as epoxy.

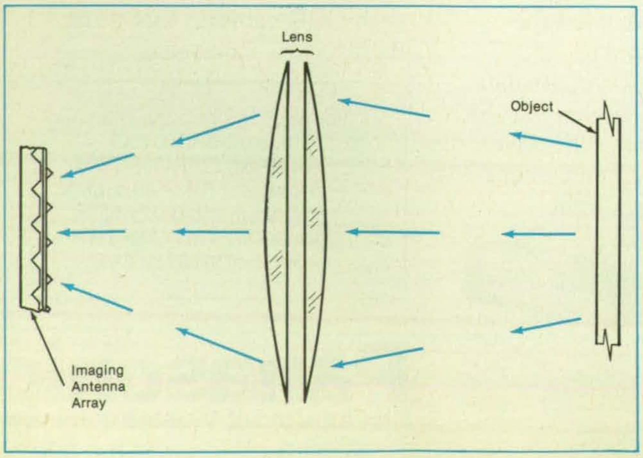

Figure 1. The **Antenna Structure** is placed in the focal plane of a millimeter-or submillimeter-wave imaging system. The antennas and associated circuitry in the structure are the detectors for the picture elements of the imaging system.

The new integrated-circuit design is a relatively inexpensive way to provide the large number of small antenna elements required for imaging, all mounted rigidly in a way that does not degrade operation. The reflectors increase the efficiency of

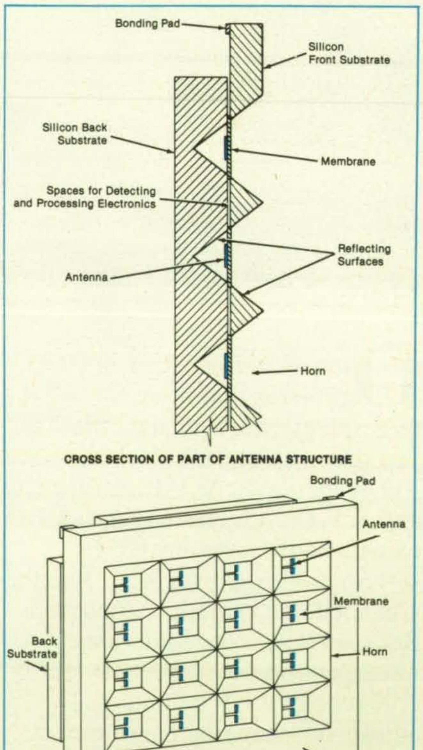

Figure 2. The **Antenna Elements, Supports, and Reflectors** are made by integrated-circuit techniques. The structures are fabricated on the front and back substrates separately. The substrates are then joined.

collection of incident radiation, making it unnecessary to increase the density of antenna elements for this purpose. (Placing the antenna elements too close to each other could result in undesirable electromagnetic coupling between elements and limit the space available for interconnections and other circuitry.)

This work was done by G. Rebeiz and D. Rutledge of Caltech for **NASA's Jet Propulsion Laboratory**. *For further information, Circle 119 on the TSP Request Card.*

In accordance with Public Law 96-517, the contractor has elected to retain title to this invention. Inquiries concerning rights for its commercial use should be addressed to

Edward Ansell
Director of Patents and Licensing
Mail Stop 305-6
California Institute of Technology
1201 East California Boulevard
Pasadena, CA 91125

Refer to NPO-17799, volume and number of this NASA Tech Briefs *issue, and the page number.*

Monolithic Optoelectronic Integrated Circuit

Input data at rates up to 1 Gb/s are demultiplexed to 16 outputs.

Lewis Research Center, Cleveland, Ohio

A monolithic optoelectronic integrated circuit (OEIC) receives a single digitally modulated input light signal via an optical fiber and converts it into a 16-channel electrical output signal. The OEIC (see figure) is potentially useful in any system in which digital data must be transmitted serially at high rates, then decoded into and used in parallel format at the destination. Examples of applications include the transmission and decoding of control signals to phase shifters in phased-array antennas and also the communication of data between computers and peripheral equipment in local-area networks.

All of the electronic functions of the OEIC are performed by components that are monolithically integrated on a GaAs substrate. The input optical fiber, which has a core of 50 μm in diameter, is mounted in a ceramic V-groove block. The end of the fiber is beveled to couple the signal into a photodetector, which converts the input optical signal into an electrical signal of identical format. This signal is fed to a three-stage amplifier.

The input signal is in the form of sequential 16-bit words. The amplified input signal is fed to a 1:16 demultiplexer (decoder), which assigns parts of the stream of data to each of the 16 parallel output channels according to a code contained in the input signal.

The OEIC contains a total of 2,000 transistors. It is sealed in a package 0.5 in. (12.7 mm) wide and 1 in. (25.4 mm) long. It consumes 150 mW of power. In comparison with similar demultiplexers made by assembling hybrid or discrete components, this unit has about one-fifth the size, one-tenth the power consumption, and two-fifths the weight. In addition, the new unit can be integrated monolithically with other GaAs devices.

This work was done by Kul B. Bhasin of **Lewis Research Center** *and Wayne Walters, Jerry Gustafsen, and Mark Bendett of Honeywell, Inc. No further documentation is available.*
LEW-14922

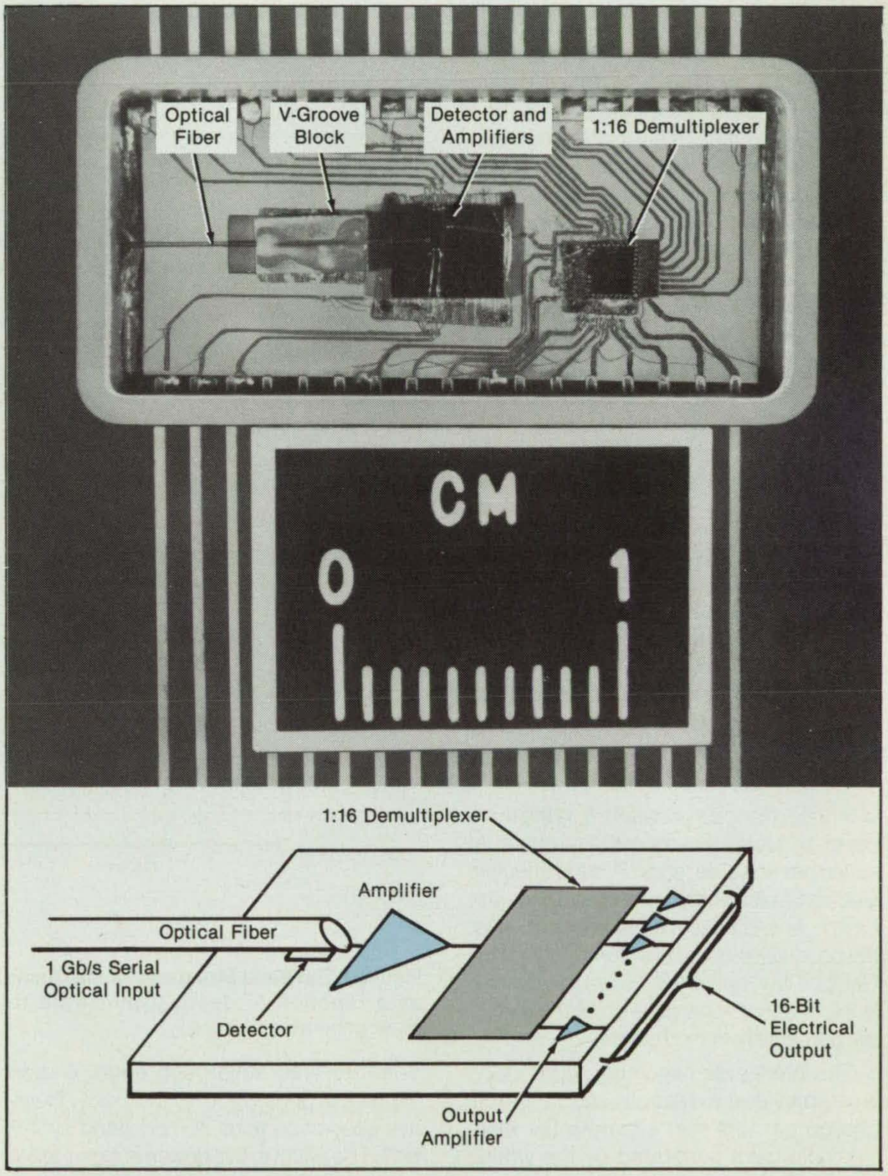

The **Monolithic Optoelectronic Integrated Circuit** is a compact unit that converts a serial input light signal from an optical fiber into 16 parallel electrical output signals.

Improved Photovoltaic-Driven Quantum Light Modulator

Additional features would increase sensitivity and utility.

NASA's Jet Propulsion Laboratory, Pasadena, California

Modifications are proposed to improve the device described in "Photovoltaic-Driven Multiple-Quantum-Well Modulator" (NPO-16914) and "Strain-Layer-Superlattice Light Modulator" (NPO-16915), *NASA Tech Briefs*, Vol. 13, No. 5, pages 42 and 51. The modified device is a photovoltaic-driven multiple-quantum-well light modulator similar to the one described previously, but with added features to increase its sensitivity and its utility as a spatial light modulator.

As shown in Figure 1, antireflection coating is applied to the front surface, and a reflective metal layer, to the back surface. These layers provide for two passes of the read signal (the signal to be modulated), thus doubling the effective modulation depth. Alternatively, the device could be fabricated into an etalon structure for multiple passes of the read signal and a further increase in the modulation depth. Also, as shown in Figure 1, grooves could be etched to divide the device into an array of picture elements. Each element could be made in the desired size (e.g., 10 μm square) for use in a large-array spatial light modulator.

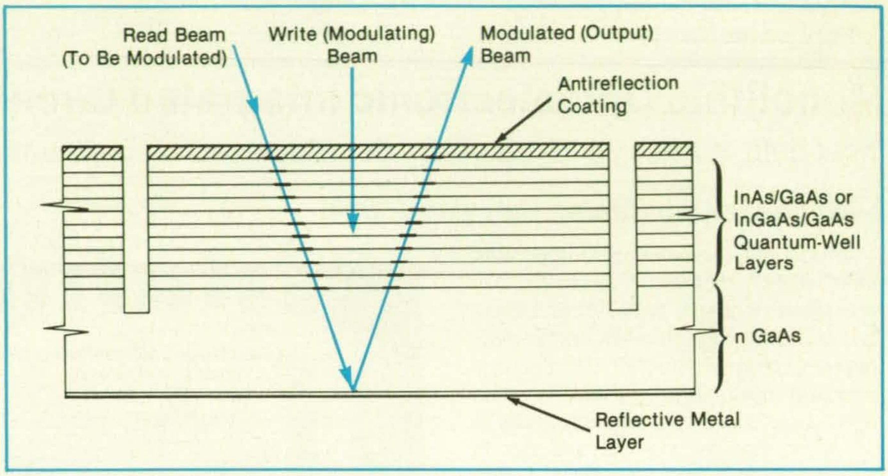

Figure 1. The **Improved Photovoltaic-Driven Multiple-Quantum-Well Light Modulator** resembles prior devices of this general type but includes an active region that uses quantum state filling and a more optimum structure.

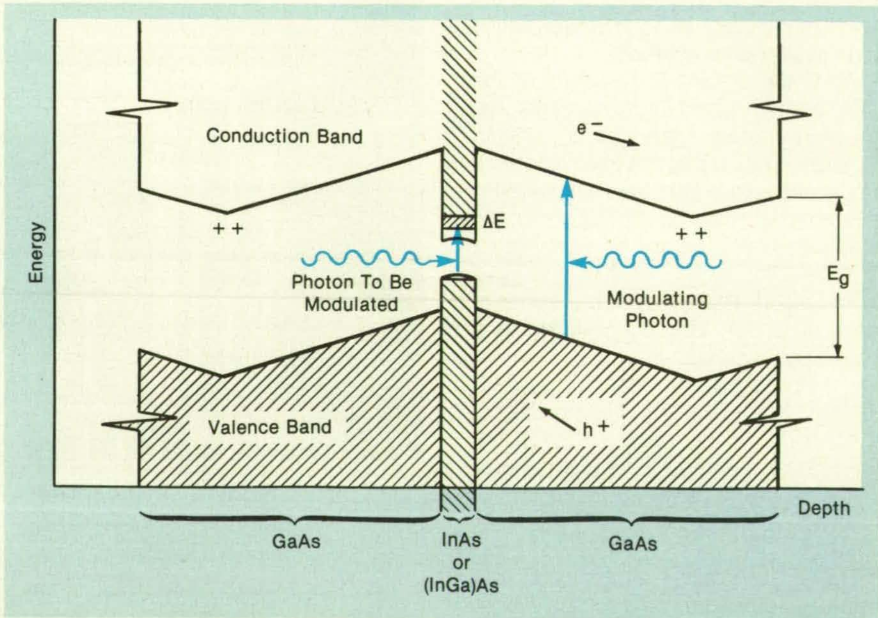

Figure 2. The **Band Structures of the Quantum Wells and Barriers** are shown schematically as a function of depth to illustrate the principle of quantum state filing due to photogenerated carriers.

The modified device exploits the quantum well equivalant of the Moss–Burnstein shift, denoted by ΔE in Figure 2. This is a shift in the energy of the quantum-well absorption edge caused by the filling of two-dimensional quantum states in the multiple quantum wells, and which results in high modulation sensitivity in the quantum wells. This shift is given by

$$\Delta E = h^2 n_s / \pi m^*$$

where h is Planck's constant, n_s is the number of occupied two-dimensional quantum states per unit area, and m^* is the effective electron mass in the InAs or InGaAs. The term n_s is related to the electric field, F_s, at the boundaries of the quantum well through Gauss's law; namely, $F_s = en_s/\varepsilon$, where e is the electrical charge and ε is the electrical permittivity of the material.

The interleaved negatively-doped GaAs layers provide the electrons and the space-charge barriers that separate the electron/hole pairs generated by the writing (modulating) light beam of photon energy greater than the semiconductor energy-band gap (E_g) of GaAs for strong absorption (or greater than the quantum well absorption edge for weaker absorption). The photo holes drift to the quantum wells and recombine there with electrons, thereby depleting n_s by an amount Δn_s that depends on the flux of photons. In turn, Δn_s causes a change in ΔE, thus shifting the quantum-well absorption edge. A read signal with photon energy just below the initial absorption edge is modulated by this shift. The effect in this device is expected to be about 10 times as large as in the AlGaAs/GaAs multiple-quantum-well structures that operate according to the quantum-confined Stark effect previously described.

This work was done by Joseph Maserjian of Caltech for **NASA's Jet Propulsion Laboratory**. *For further information, Circle 133 on the TSP Request Card.*

In accordance with Public Law 96-517, the contractor has elected to retain title to this invention. Inquiries concerning rights for its commercial use should be addressed to

Edward Ansell
Director of Patents and Licensing
Mail Stop 305-6
California Institute of Technology
1201 East California Boulevard
Pasadena, CA 91125

Refer to NPO-17357, volume and number of this NASA Tech Briefs *issue, and the page number.*

Test Processor for PCM Telemetry

The user can display telemetric data in a variety of formats.

Goddard Space Flight Center, Greenbelt, Maryland

The TDPlus system is a data-processing subsystem designed for use in testing pulse-code-modulation (PCM) telemetry equipment. It can accommodate a variety of PCM formats (e.g., different bit rates) and modes of display.

The TDPlus system (see figure) includes a custom-built set of four circuit cards that plug into any personal computer compatible with the Industry Standard Architecture (ISA) bus. Its extensive operating-system software provides for "pop-down windows" to enable the user to edit, examine, and display telemetry data in various forms, including binary, hexadecimal, decimal, and engineering units; bar charts; and elapsed-time and XY formats. This software is written in 'C', is very user-friendly, and enables anyone who has basic knowledge of telemetry to use the system without an instruction manual.

The TDPlus system can handle words of any size from 4 to 16 bits, and up to 8,192 words in a major frame. The maximum data rate is now 3.3 Mbits per second, and a new prototype board to handle 5.5 Mbits per second has been built.

The TDPlus system contains 32 digital-to-analog converters (DAC's), two 16-bit parallel output ports, a cathode-ray-tube (CRT) display, a keyboard, a floppy-disk drive, and the software to generate, edit, and record PCM telemetry data. Optionally, a PCM bit synchronizer, a PCM simulator, a real time display, and a printer can be included to make the TDPlus a stand-alone PCM decommutator and data-reduction system.

The memory and input/output (I/O) of the TDPlus are allocated such that there is no conflict with existing memory and I/O of standard ISA personal computers. The TDPlus system has its own bus in addition to the computer bus. This bus enables the distribution of incoming data to the set of TDPlus circuit cards.

The frame-synchronizing card is the first card in the TDPlus system. It uses very-large-scale-integration (VLSI) and erasable programmable logic devices (EPLD's) to generate all synchronization signals (i.e., bit clock, frame clock, and subframe clock). It also provides the addresses for the parallel telemetry (TM) data matrix located on the card described next.

The TM-memory/parallel-port card has two major functions: it writes all incoming data to a dual-port, eight-kiloword random-access-memory (RAM) section and provides tagged data to be sent to either of the two 16-bit parallel ports or 32 digital-to-analog converters. If the data are designated for display, access to them is gained by the computer through the dual-port RAM. If the incoming data are tagged to be sent to either of the parallel ports, they are picked from the stream of incoming data and sent to the selected port in real time for further reduction by the user. If the incoming data are tagged to be sent to one of the 32 DAC's, the data, along with the selected DAC address, is sent to the card described next.

The DAC-controller card decodes the DAC addresses for tagged TM data and computer-generated calibration points. These selected data are sent to the DAC card (described below) to be converted into an analog signal. The DAC's can have either 8-bit or 12-bit resolution.

The DAC card contains 32 voltage-mode digital-to-analog converters with output-buffer amplifiers to provide drive to external recording devices. Several types of DAC's are compatible with the DAC controller. These range from a unipolar output to a selectable bipolar output. All DAC's are monotonic and use no external trim. All output amplifiers are internally compensated to provide stable operation over a wide range of loads.

This work was done by David Massey and Brian Corbin of **Goddard Space Flight Center**. *For further information, Circle 104 on the TSP Request Card.* *GSC-13291*

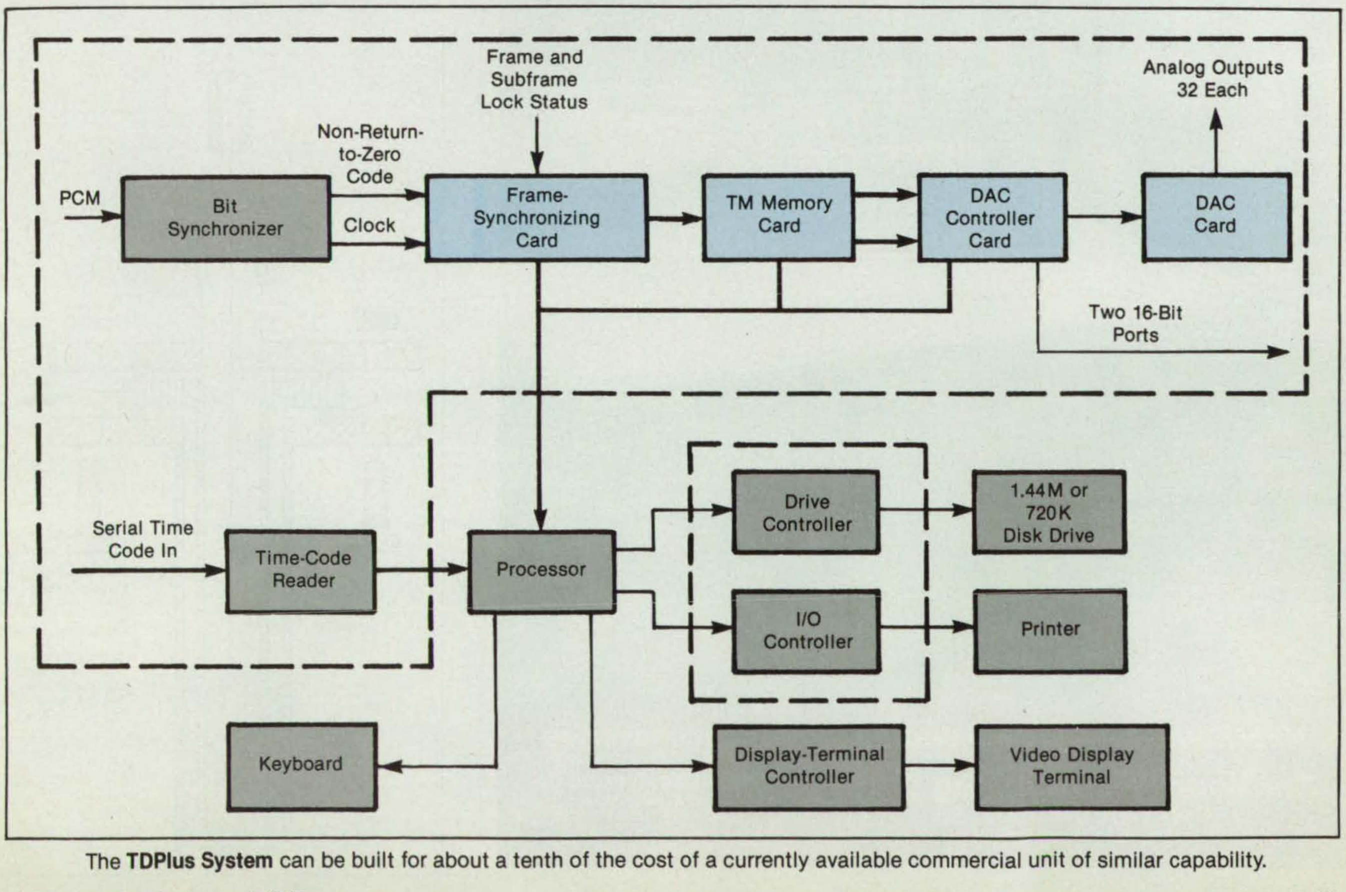

The **TDPlus System** can be built for about a tenth of the cost of a currently available commercial unit of similar capability.

Copper Chloride Cathode for Liquid-Sodium Cell

Energy density is higher than that of previous liquid-sodium cells.

NASA's Jet Propulsion Laboratory, Pasadena, California

A rechargeable liquid-sodium cell with a copper chloride cathode offers a substantial increase in energy density over cells made with other cathode materials. The unit has a theoretical maximum energy density of 1135 W•h/kg, whereas the best previously available cathodes — ferrous chloride and nickel chloride — were limited to energy densities of 1000 to 1070 W•h/kg.

The cell generates electricity by the electrochemical reaction of molten sodium and solid copper chloride immersed in a molten electrolyte, sodium tetrachloroaluminate ($NaAlCl_4$), at a temperature of ⩾200 °C. A wall of solid electrolyte, β'' alumina, separates the anode from the cathode (see figure). The cathode consists of porous sintered nickel impregnated with copper chloride, or of a directly sintered copper chloride cathode in the discharged state.

Copper chloride provides a higher energy density by virtue of its large cell potential ~2.85 V; i.e., 0.25 V higher than that of nickel chloride and 0.5 V higher than that of ferrous chloride. Moreover, the conductivity of the copper chloride electrode increases as the discharge proceeds, because metallic copper collects in it. Thus, the battery can be discharged at higher power densities.

This work was done by Ratnakumar V. Bugga, Salvador DiStefano, Ganesan Nagasubramanian and Clyde P. Bankston of Caltech for **NASA's Jet Propulsion Laboratory**. *For further information, Circle 118 on the TSP Request Card.*

This invention is owned by NASA, and a patent application has been filed. Inquiries concerning nonexclusive or exclusive license for its commercial development should be addressed to the Patent Counsel, NASA's Resident Office-JPL [see page 16]. Refer to NPO-17640.

The **Wall of the Alumina Tube** separates the molten electrolyte from the molten sodium anode. The copper chloride cathode is embedded in the pores of a sintered nickel cylinder or directly sintered.

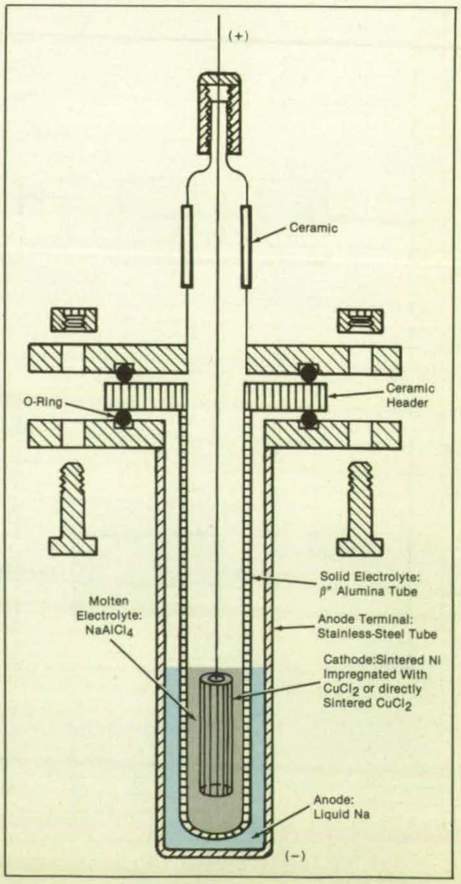

Electro-optical Probing of Terahertz Integrated Circuits

Measurements are made without touching micron-sized circuit structures.

Lewis Research Center, Cleveland, Ohio

An electro-optical probe has been developed to perform noncontact, nondestructive, and relatively noninvasive measurements of electric fields over a broad spectrum at millimeter and shorter wavelengths in integrated circuits. The probe is manipulated with conventional integrated-circuit-wafer-probing equipment and is operated without any special preparation of the integrated circuits.

The tip of the probe is a small electro-optical crystal that serves as a proximity electric-field sensor. Typically, it is used to measure the fringing or guided electric field between, say, two parallel conductor lines to determine the signal potential between them. The tip is brought close to (but not touching) the conductors (see figure) so that the fringing field can induce changes in the index of refraction of the electro-optical material. These changes modulate a pulsed laser beam reflected from the tip. The modulation, proportional to the electric field, is displayed on a sampling oscilloscope. The temporal resolution of this technique is determined by the duration of the pulses (typically, 80 fs), which act as the sampling-gate signals for the oscilloscope.

The electro-optical material of the tip is chosen according to the orientation of the electric field to be measured. For a field transverse to the probing laser beam (parallel to the surface of the integrated circuit in the figure), the required electro-optical material is lithium tantalate; for a field along the laser beam (perpendicular to the surface in the figure), the required material is potassium dihydrogen phosphate. Because a transverse field is ordinarily measured when the axis of the probe is aimed between two parallel conductors, it is usually necessary in this case to use a mirror coat on the tip to reflect the laser beam. Because a longitudinal field is ordinarily measured when the axis of the probe is aimed at a conductor, the beam can be reflected from the conductor, and a mirror coat is not needed.

The transverse version of the probe typically gives a measurement of voltage only over a small range of positions between two conductors. The longitudinal version, on the other hand, can sense the electric field over a range of positions across a conductor and, therefore, gives a measure of signal voltage more quickly and accurately. The longitudinal version gives a more accurate measure of a broadband signal voltage.

This work was done by K. B. Bhasin and R. Romanofsky of **Lewis Research Center**; *J. F. Whitaker, J. A. Valdmanis, and G. Mourou of the University of Michigan; and T. A. Jackson of the University of Rochester. Further information may be found in NASA TM-101990 [N89-21142], "External Electro-optic Probing of Millimeter-Wave Integrated Circuits."*

Copies may be purchased [prepayment required] from the National Technical Information Service, Springfield, Virginia 22161, Telephone No. (703) 487-4650. Rush orders may be placed for an extra fee by calling (800) 336-4700.

LEW-14956

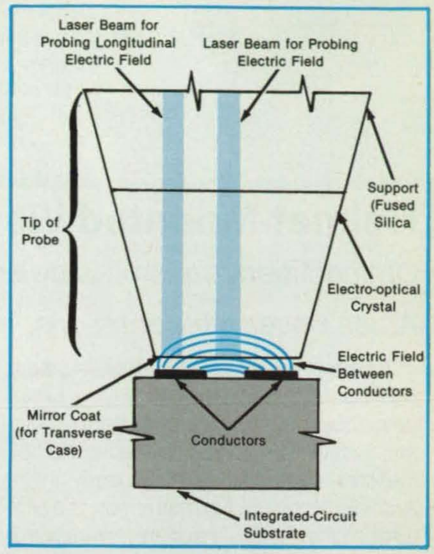

The **Electric Field To Be Measured** changes the index of refraction of the electro-optical crystal, thereby modulating the probing laser beam.

Books and Reports

These reports, studies, handbooks are available from NASA as Technical Support Packages (TSP's) when a Request Card number is cited; otherwise they are available from the National Technical Information Service.

Failures of CMOS Circuits Irradiated at Low Rates

Experiments confirm previous findings that low dose rates decrease failure doses.

A report describes experiments on the irradiation of SGS 4007 complementary metal oxide/semiconductor (CMOS) integrated inverter circuits by ^{60}Co and ^{137}Cs radioactive sources. The purpose of the experiments was to supplement previous observations that the minimum radiation doses at which failure occurred in more-complicated CMOS parts were lower at lower dose rates. The underlying physical cause of this premature-failure phenomenon remains unknown, but the data accumulated in these experiments may be useful in future studies directed toward identification of the cause. The SGS 4007 circuit was considered appropriate for such an investigation because it is constructed simply and all of the sources, gates, and drains of its transistors are readily accessible; consequently, it lends itself readily to the acquisition and interpretation of data.

The specimens were 25 ordinary commercial (that is, not "radiation-hardened") SGS 4007 circuits. Typical operating voltages were applied, and the drain-to-source current, I_{gs}, as a function of the drain-to-source voltage, V_{gs}, was measured on each of the six transistors in each specimen. Seventeen specimens were irradiated to failure: four by ^{60}Co at a dose rate of 20 rad(Si)/s, four by ^{60}Co at 0.50 rad(Si)/s, three by ^{60}Co at 0.14 rad(Si)/s, three by ^{137}Cs at 0.21 rad(Si)/s, and three at 0.010 rad(Si)/s. Malfunctions in the experimental apparatus prevented the collection of data on the remaining eight specimens. A specimen was deemed to fail when the average I_{gs} or the average threshold V_{gs} of the transistors in that specimen exceeded the level specified by the manufacturer or by the laboratory.

The investigators conclude that the measurements taken in these experiments confirm the previous observations of premature failure at low dose rates. The investigators describe a method, reported in a previous article in *NASA Tech Briefs*, for using the measurements to determine approximately the dose rate at which an integrated circuit can be expected to fail first, without having to test the device to failure. To recapitulate briefly, this method involves plotting a current or other parameter that increases with dose versus the dose rate. The plot should indicate clearly the dose rate at which the device is most sensitive to radiation and will fail first. The report concludes with some suggestions for designs that would reduce the vulnerability of CMOS integrated circuits to premature failure and with recommendations for more studies of premature failure at low and intermediate dose rates.

This work was done by Charles A. Goben and William E. Price of Caltech for **NASA's Jet Propulsion Laboratory**. *To obtain a copy of the report, "Premature Failure at Low Dose Rates in SGS 4007 CMOS Devices," Circle 84 on the TSP Request Card.*

NPO-17867

Electronic Systems

Helmet-Mounted Visual Display for Flight Simulation

Optical fibers transmit wide-angle images in response to motions of the head.

Ames Research Center, Moffett Field, California

A helmet-mounted visual display system (see figure) provides a pilot with a broad range of visual information for flight simulation. Unlike earlier visual systems, the helmet-mounted display offers a nearly unlimited field of regard. No matter how the pilot turns his/her head — sideways, rearward, up, or down — the display shows the image that the pilot would see in a real situation. In this respect, it is superior to cathode-ray-tube "window" displays, and even to dome projection displays. Moreover, the image is bright and undistorted.

Two "pancake" lenses are mounted on a lightweight helmet. A cable of optical fibers carries images to each lens. "Light-valve" projectors deliver the computer-generated binocular images to the cables.

Four overhead infrared cameras track the motion of the pilot's head by monitoring a ring of light-emitting diodes on the helmet. A sensor on the rear of the helmet measures the rate of acceleration. With the video and rate data, the host computer can calculate and anticipate the position of the head and direct the display computer to generate the appropriate binocular images, in real time.

The pilot sees two overlapping displays — one for each eye — and a high-resolution inset field in the overlap (middle) region for heads-up-display symbology. The pilot can see cockpit displays and controls through the optics. A software model of the aircraft structure in the display computer prevents the pilot from seeing through the simulated aircraft structure.

A helmet is custom-fitted for each pilot so that it rests securely and comfortably on the head, and the optics are aligned. During the fitting of a helmet, precise measurements of the pilot's interpupillary distance, eye relief, and anomalies of the positions of the eye are made. Then, during the assembly of the helmet, the mounting fixtures for optics are set for the pilot. These adjustments ensure that the exit pupils of the optics coincide with the pilot's pupils as soon as the optics are placed on the helmet, so that there is no need for time-consuming adjustments.

Because the optical elements of the display are costly, they are not permanently mounted in a helmet. Instead, the helmets are designed so that the optics can be quickly inserted at the beginning of a simulation session and just as quickly removed for use by another pilot.

This work was done by Anthony M. Cook of **Ames Research Center**. *For further information, Circle 32 on the TSP Request Card.*

Inquiries concerning rights for the commercial use of this invention should be addressed to the Patent Counsel, Ames Research Center [see page 16]. Refer to ARC-12160.

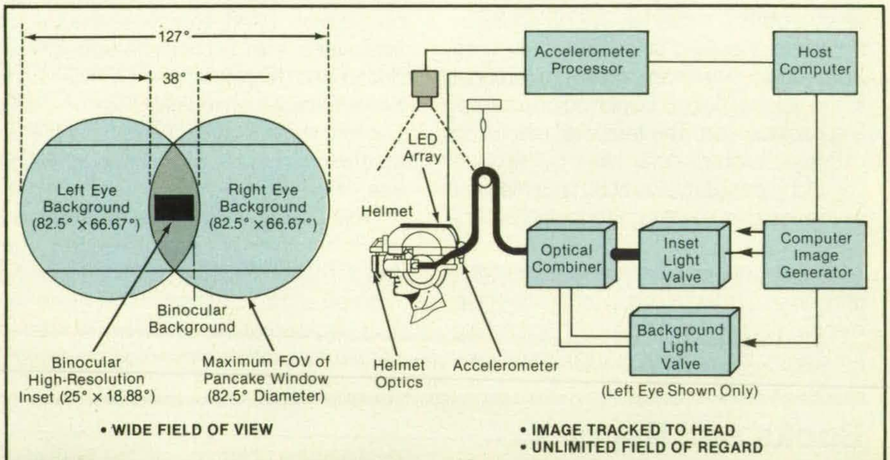

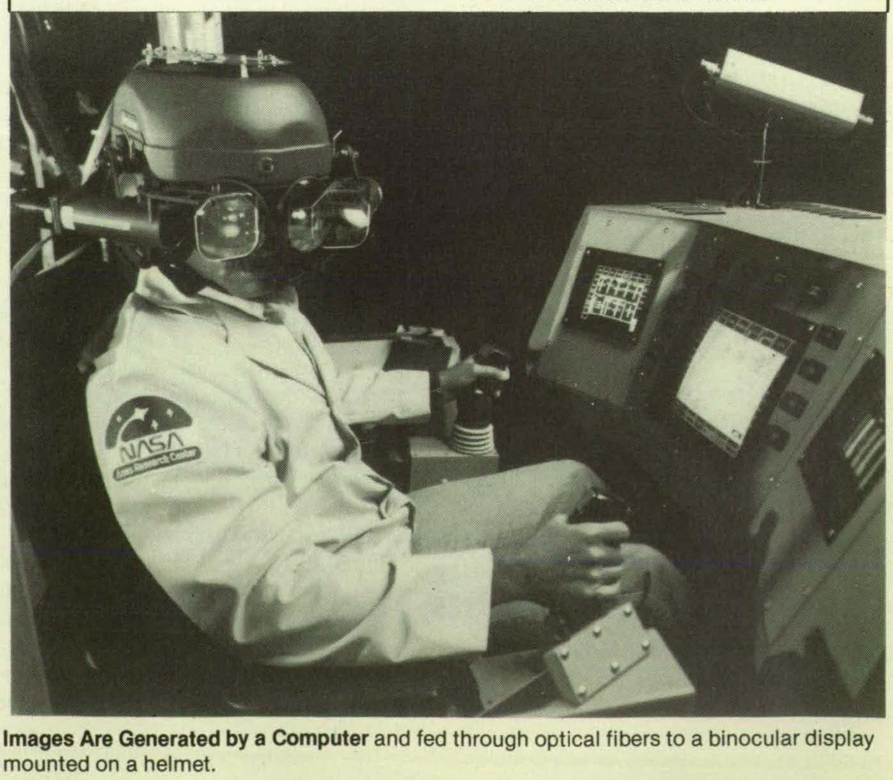

Images Are Generated by a Computer and fed through optical fibers to a binocular display mounted on a helmet.

Compensating for Doppler Shift in Laser Instrumentation

The frequency of a tunable diode laser is adjusted to oppose the shift.

Goddard Space Flight Center, Greenbelt, Maryland

An electronic tuning system continually adjusts the frequency of a tunable diode laser to compensate for the Doppler shift caused by the motion of a transmitter or receiver that contains the laser. The Doppler-shift-compensating system is intended primarily for use in the transmitter or receiver of a laser remote-sensing or communication system to keep the frequency of the received signal within the frequency range of a narrow-band-pass filter. By use of the narrow-band filter (instead of the wide-band filter that would be required in the absence of Doppler compensation), the signal-to-noise ratio of the laser system can be increased. Thus, a less-powerful transmitter might be usable.

The system (see figure) includes two current-modulated tunable diode lasers, the first of which provides an unshifted reference frequency f_1, and the second of which puts out the Doppler-compensated signal at frequency f_2. The frequency of the reference laser is dithered at an acoustic frequency f_A about the steady or slowly varying value f_1. The dither is detected in a photoacoustic gas cell, which is part of a first feedback loop that adjusts the direct current supplied to the laser to keep f_1 at the frequency of an atomic- or molecular-energy-level transition of the gas in the cell.

Parts of the outputs of both tunable diode lasers are sent to a photodetector, which acts as a mixer in putting out a signal that contains the beat frequency $|f_1 - f_2|$. At the same time, a computer calculates the expected Doppler shift f_D from data on the trajectory of the laser platform and the direction of aim of the laser beam. The computer commands a radio-frequency synthesizer to put out a signal at a frequency of $|f_D| + f_I$, where f_I is an intermediate radio frequency. The $|f_1 - f_2|$ and $|f_D| + f_1$ signals are fed to a radio-frequency mixer, the output of which is low-pass filtered to yield the component that has the frequency $f_I + |f_D| - |f_1 - f_2|$. This signal is fed to a frequency discriminator tuned to f_I, and the output of the discriminator is fed to the inverting or noninverting input of a differential amplifier, depending on the arithmetical sign of the computed Doppler shift. The output of the differential amplifier is fed to another differential amplifier, which adjusts the dc supply of the shifted laser. This completes a second feedback loop that continually strives to keep the output frequency of the shifted laser at $f_2 = f_1 + f_D$.

This work was done by Geary K. Schwemmer of **Goddard Space Flight Center**. *For further information, Circle 78 on the TSP Request Card.*

This invention is owned by NASA, and a patent application has been filed. Inquiries concerning nonexclusive or exclusive license for its commercial development should be addressed to the Patent Counsel, Goddard Space Flight Center [see page 16]. Refer to GSC-13194.

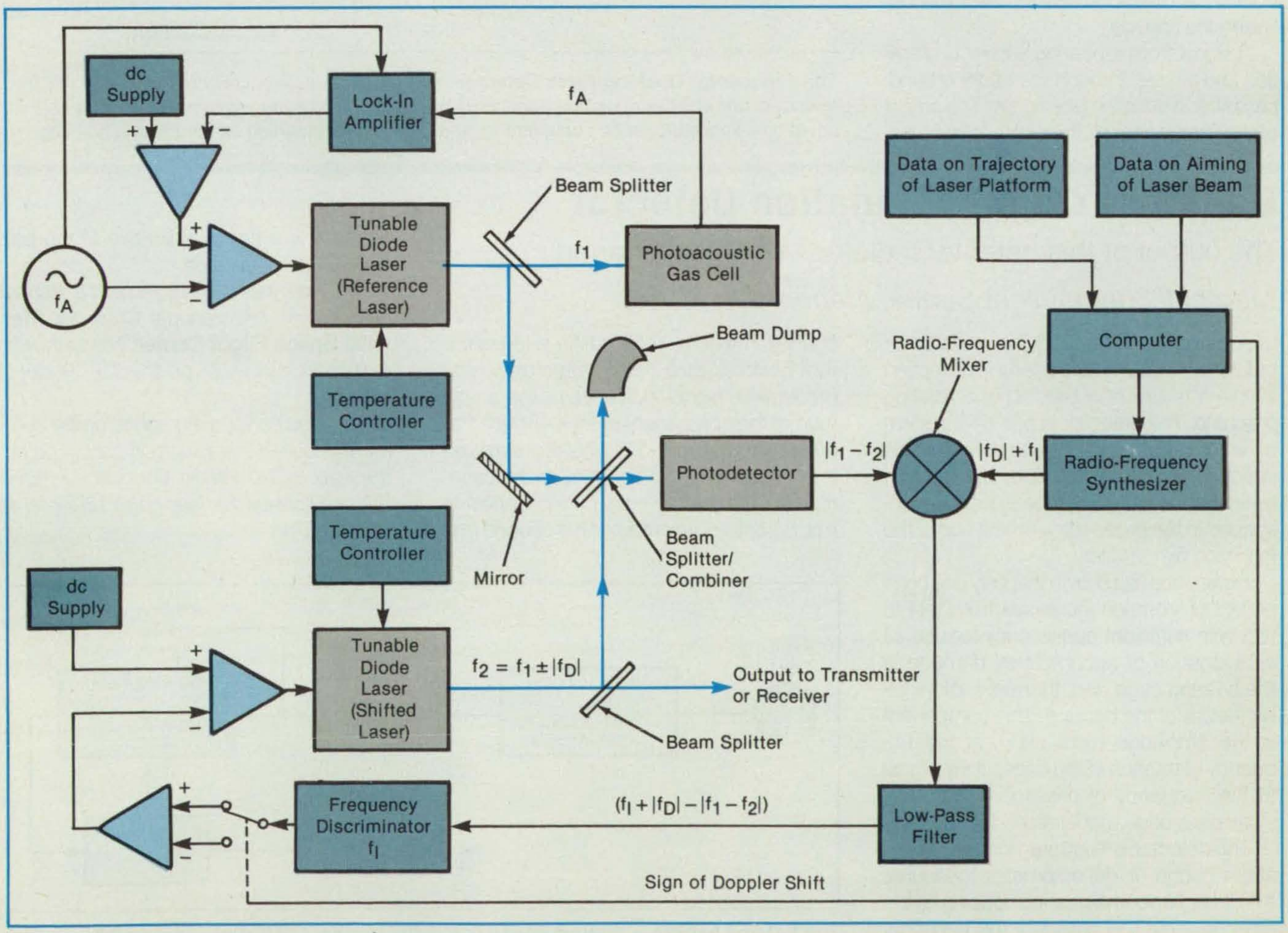

The **Electronic Tuning System** continually strives to maintain the output frequency f_2 at a value shifted above or below the reference frequency f_1 by an amount that compensates for the computed Doppler shift f_D.

Frequency-Tracking-Error Detector

A circuit compares the average periods of two signals.

Marshall Space Flight Center, Alabama

A frequency-tracking-error detector compares the average period of the output signal from a band-pass tracking filter with the average period of the signal of frequency 100 f_o that controls the center frequency f_o of the tracking filter. The frequency-tracking-error detector is part of a system of electronic equipment used to measure vibrations in bearings in rotating machinery.

In this system, measurements of the speed of rotation of a shaft and estimates of the ratio between the speed of rotation of a bearing cage and the speed of rotation of the shaft that turns in the bearing are used to set f_o at a harmonic of the frequency of rotation of the bearing cage. The frequency-tracking-error detector is needed because the ratio between the speeds is not constant, and yet it is necessary to keep the frequency-tracking error as close to zero as possible to maximize the accuracy and reliability of measurements. The output of the frequency-tracking error detector is used as an error signal to tune f_o manually or automatically to the desired bearing-cage harmonic. In effect, it gives a continous measurement of the ratio between the speeds.

A signal from a bearing sensor is amplified and passed through the tracking band-pass filter in question (see figure). The output of the filter is passed through a zero-crossing detector. The output of the zero-crossing detector is passed through a delay logic circuit that recognizes a zero crossing only when it appears to be stable during at least 16 cycles of 100 f_o. Two counters measure 100 cycles of 100 f_o for every 8 filter-output cycles. The result is stored in a register and converted to a dc signal that can be used as an error or control signal.

A value of 800 in the register indicates zero tracking error; a greater or lesser value indicates that the tracking-control frequency 100 f_o is too high or too low, respectively. The deviation from 800 can be used to correct 100 f_o and the estimate of the ratio between the speeds.

This work was done by Richard L. Randall of Rockwell International Corp. for **Marshall Space Flight Center**. *For further information, Circle 75 on the TSP Request Card.*

MFS-29538

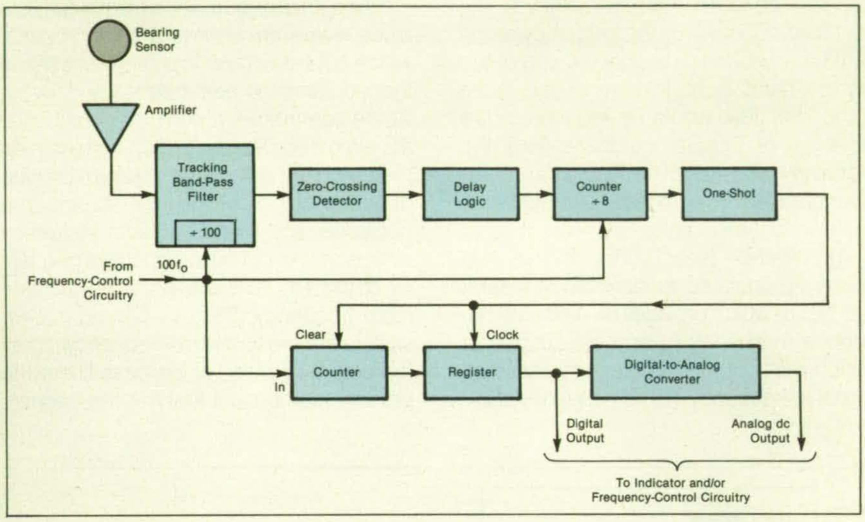

The **Frequency-Tracking-Error Detector** measures the difference between f_o and the frequency of one of the periodic components in the output of the bearing sensor. The bearing sensor could be an accelerometer, strain gauge, or deflectometer mounted on the bearing housing.

Ball-Pass Cage-Modulation Detector

The output of this detector indicates wear in a bearing.

Marshall Space Flight Center, Alabama

A ball-pass cage-modulation detector puts out a signal that is useful in detecting incipient failure of a bearing in a rotating machine. The detector is part of a system of electronic equipment that measures various components of vibrations in such bearings. Other parts of the system are described in the preceeding article and in the following two articles.

Experience has shown that only one component of vibration increases from test to test with sufficient consistency for use as an indication of accumulated damage in the bearing cage and, therefore, of incipient failure of the bearing. This component is the amplitude modulation, at the frequency of rotation of the cage, of the signal at the frequency of passage of the balls ("ball-pass cage modulation" for short).

The detector is illustrated in the figure. A strain gauge or deflectometer measures the deflection of the bearing housing as the balls pass by. The output of this sensor is fed to the ball-pass tracking filter, which is a band-pass filter tuned to the ball-pass frequency. The output of this filter is fed to the root-mean-square (rms) detector, which produces a signal indicative of the amplitude of the component at the ball-pass frequency. The amplitude signal is processed through a tracking filter tuned to the cage-rotation frequency, then through another rms detector. The output of the second rms detector is a signal indicative of the ball-pass cage modulation.

This work was done by Richard L. Randall of Rockwell International Corp. for **Marshall Space Flight Center**. *For further information, Circle 72 on the TSP Request Card.*

Inquiries concerning rights for the commercial use of this invention should be addressed to the Patent Counsel, Marshall Space Flight Center [see page 16]. Refer to MFS-29539.

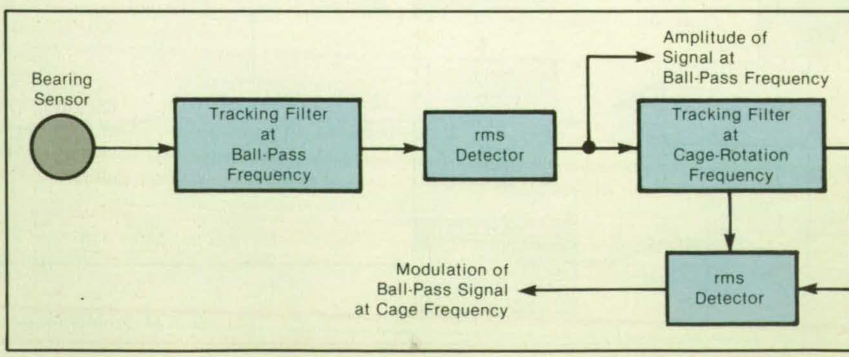

The **Bearing Sensor** — a strain gauge or a deflectometer on the bearing housing — measures the deflections of the housing as the balls pass by. The output of the sensor is filtered to extract the ball-pass cage modulation, which is indicative of wear in the bearing.

Shaft-Rotation Detector

Rotation is deduced from a subtle component of vibration.

Marshall Space Flight Center, Alabama

A signal-processing subsystem generates a signal indicative of the rotation of a shaft from the output of an accelerometer mounted on the housing of the bearing that supports the shaft. The output of the subsystem is a binary signal at the frequency of rotation of the shaft. The subsystem is part of an assembly of electronic equipment that measures vibrations in rotating machinery. Some of the other equipment is described in the two preceding articles and the following article. The other equipment uses the binary shaft-speed signal as a phase and frequency reference in the analysis of other vibration signals.

The accelerometer is mounted in such a way as to be sensitive to vibrations of the shaft perpendicular to its axis. The output of the accelerometer includes noise and components of vibration at frequencies higher than the rotational frequency of the shaft. The shaft-rotation-detector subsystem extracts the fundamental-frequency component of the vibration of the shaft (which is presumed to be synchronized with the rotation of the shaft) by acting as a tracking low-pass filter, the cutoff frequency of which is determined iteratively by the measurement itself.

As shown in the figure, the output of the accelerometer is processed through a zero-crossing detector into a delay logic circuit, which recognizes a zero crossing only when it appears to be stable for the equivalent of 1/16 of the current measured period. For this purpose, the period is the period of the binary output of the delay logic circuit, as measured by a counter. The measured period, divided by 16, is loaded into a preset counter to generate the required delay. The binary output of the delay logic circuit is taken to be the shaft-rotation reference signal.

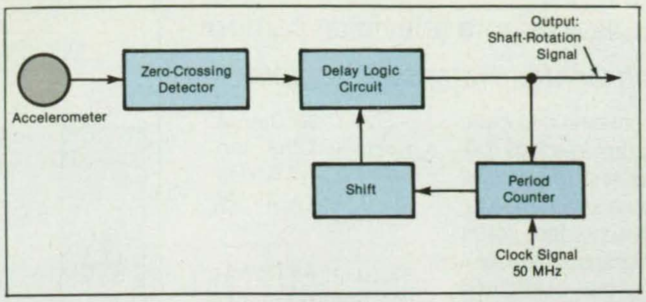

The **Shaft-Rotation Detector** finds a fundamental-frequency component of lateral vibration of a rotating shaft in the output of an accelerometer mounted on the housing of a bearing that supports the shaft. It measures the period of this component, which is assumed to be synchronized with the rotation.

The basic measurement performed by the subsystem — the period corresponding to the rotation of the shaft — is made with a precision of 28 bits. To suppress random errors yet still be able to track changes in speed, the measurements of the 16 most recent periods are averaged exponentially.

The shaft-rotation-detector subsystem detects the shaft-rotation component of the noisy accelerometer signal over the range of frequencies from 0.3 to 500 Hz (18 to 30,000 rpm). The dynamic range of the subsystem greatly exceeds those of analog and phase-locked-loop filter circuits. Its precision, response time, frequency range, and resolution can all be extended, inasmuch as they are all determined by parameters of the digital circuits within it.

This work was done by Richard L. Randall of Rockwell International Corp. for **Marshall Space Flight Center.** *For further information, Circle 73 on the TSP Request Card.*

Inquiries concerning rights for the commercial use of this invention should be addressed to the Patent Counsel, Marshall Space Flight Center [see page 16]. Refer to MFS-29540.

Frequency Synthesizer for Tracking Filter

Frequency is updated every 2 μs.

Marshall Space Flight Center, Alabama

A digital frequency-synthesizing subsystem generates trains of pulses, free of jitter, for use as frequency-control signals in tracking filters. The frequency synthesizer is part of an assembly of electronic equipment used to measure vibrations in bearings in rotating machinery. The three preceding articles describe some of the other equipment. The frequency synthesizer was designed to meet the requirements for tracking the narrow-band cage-rotation and ball-pass components of vibrations, as discussed in the first two articles, "Frequency-Tracking Error Detector" (MFS-29538) and "Ball-Pass Cage-Modulation Detector" (MFS-29539).

The digital frequency synthesizer uses binary logarithm and antilogarithm lookup tables in programmable read-only memories (PROM's) to compute filter-control frequencies from 20-bit binary measurements of the period of rotation (T), the ratio between the speed of rotation of the cage and the speed of rotation of the shaft (CSR), and the number of balls (N) in the bearing to be analyzed. The synthesizer (see figure) includes a preset counter, the output of which is the control signal for the ball-pass filter. The input to this preset counter is updated every 2 μs: thus, the synthesizer responds almost immediately, effectively eliminating the relatively long response time (lock-in time) and phase jitter like those encountered in conventional phase-lock-loop frequency synthesizers.

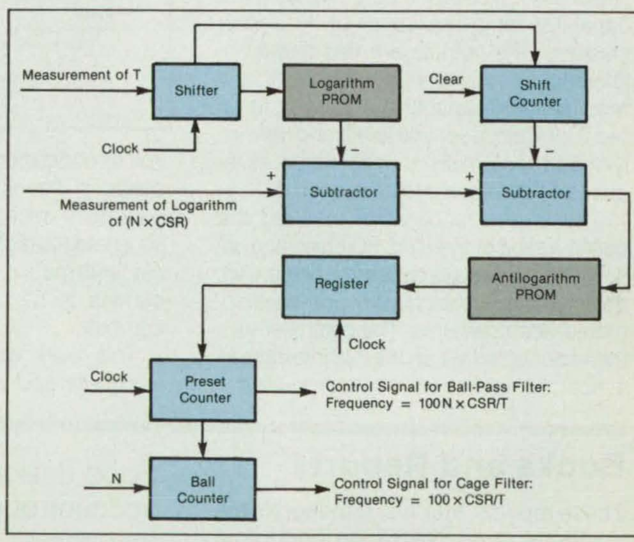

The **Digital Frequency Synthesizer** responds rapidly, computing and generating filter-control signals from input measurements.

The digital frequency synthesizer can put out precise filter-control signals at frequencies over a range of 1500 to 1. The update rate, the precision of the output frequency, and the dynamic range are limited only by the selected clock frequencies and by the number of bits used to process the input variables. These features can, therefore, be changed by design to meet the requirements of different systems.

This work was done by Richard L. Randall of Rockwell International Corp. for **Marshall Space Flight Center.** *For further information, Circle 76 on the TSP Request Card.* *MFS-29541*

General-Purpose Serial Interface for Remote Control

A computer controls a remote television camera.

Langley Research Center, Hampton, Virginia

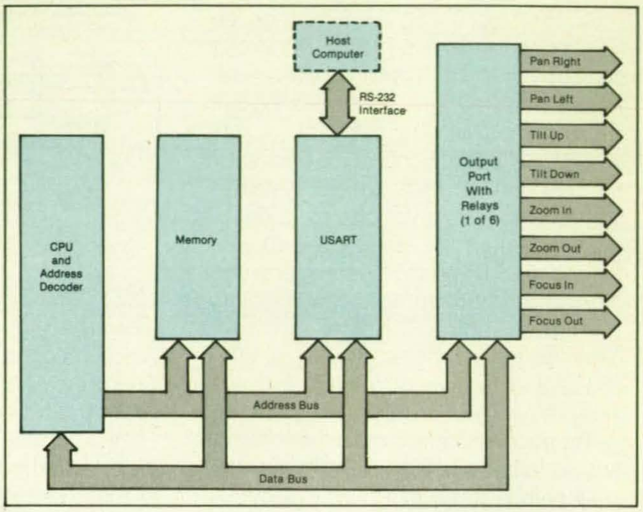

Figure 1. **Six Output Ports** control the opening and closing of as many as 48 switches.

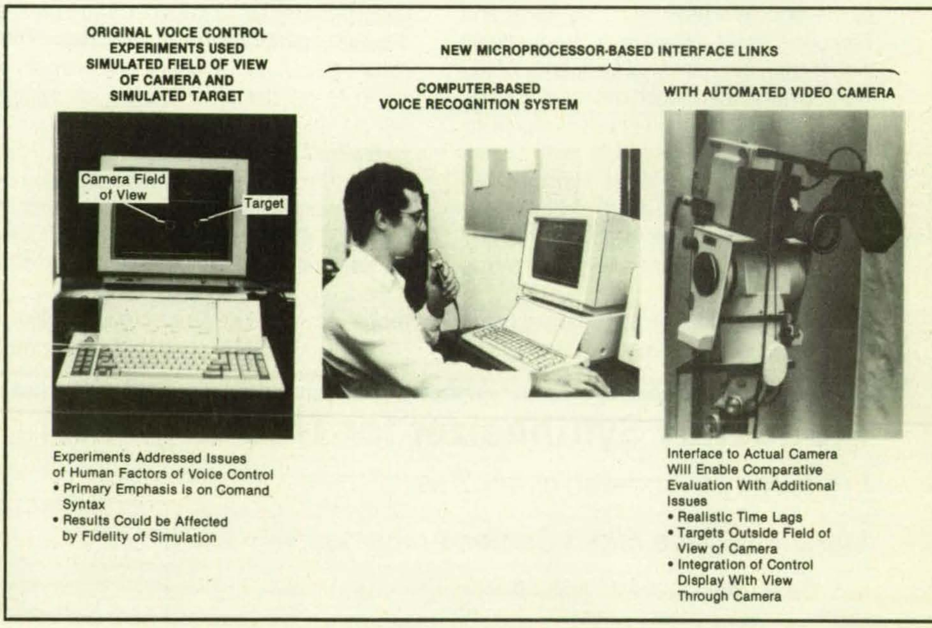

Figure 2. An **Operator Controls a Remote Television Camera** by speaking commands, in a system that includes the general-purpose controller.

A general-purpose controller has been developed to serve as an interface between a host computer and the pan/tilt/zoom/focus functions on a series of automated video cameras. The interface port is based on an 8251 programmable communications-interface circuit configured for tristated outputs, and it connects the controller system to any host computer with an RS-232 input/output (I/O) port. The controller accepts byte-coded data from the host, compares them with prestored codes in read-only memory (ROM), and closes or opens the appropriate switches.

The system comprises a central processing unit (CPU), a universal synchronous or asynchronous receiver and transmitter (USART), and the output ports (Figure 1). The CPU and interface port carry out the decoding and transfer of data between the host computer and the output ports. The CPU is based on an 8085 8-bit microprocessor with a bidirectional data bus.

The memory system consists of 16K of ROM with a simple address-decoding mechanism for memory mapping the I/O subsystem. This addressing mechanism consists of an 8205 1-of-8 binary decoder that generates eight chip-enable signals corresponding to eight preset memory addresses. Six of the chip-enable signals select an 8212 8-bit I/O port, providing the capability for a maximum of 48 switch closures. The outputs are tied to dual-in-line-packaged single-pole, double-throw reed relays to enable the user to strap them for various voltage levels and normally closed or normally open operation, as required by the device to be operated.

The original application required the configuration of the 8212 I/O chips and associated reed relays to control the pan, tilt, zoom, and focus functions of up to six automated video cameras. The controller was then connected via an RS-232 interface to a host computer, which incorporated a voice-recognition system to enable the control of the remote video cameras by the operator's voice (Figure 2). The addition of an analog-to-digital converter would enable information on the position of the camera to be relayed back to the host computer.

This work was done by Anthony M. Busquets and Lawrence E. Gupton of **Langley Research Center.** *No further documentation is available.*

Inquiries concerning rights for the commercial use of this invention should be addressed to the Patent Counsel, Langley Research Center [see page 16]. Refer to LAR-13739.

Books and Reports

These reports, studies, handbooks are available from NASA as Technical Support Packages (TSP's) when a Request Card number is cited; otherwise they are available from the National Technical Information Service.

Human Factors in the Design of Video Displays

Good designs will take account of perceptual tendencies and conceptual biases in observers.

A report presents an overview of the evolving knowledge of the interactions between video displays and human observers. It discusses the relative advantages and disadvantages of static and dynamic displays, with attention to the human factors that combine with the characteristics of the video-display medium to affect the observer's percepts.

No longer limited to static alphanumerical presentations, video displays can now also present a wide variety of graphical information in static or dynamic modes. While designers exploit the increased capabilities of such displays, they must also take account of the limitations of video displays (e.g., the reduction of three-dimensional representations to two-dimensional projections) and the perceptual and conceptual biases of the observer.

The static video image of a trapezoid provides a simple example of the problems that arise in interpreting static displays. Should the observer regard the image as representative of a trapezoid or of a rectangle tilted out of the plane of the display? Unless the observer is given additional information — for example, a rule or convention for the projection of geometric shapes, there is no way to resolve the ambiguity.

In general, static displays can be understood only through the implementation of conventions. Few of these conventions are explicitly known or understood. Further, some draw on operators' intuitive mental models, which are known to manifest conceptual errors. Even trained operators resort to less formal modes of reasoning in problem-solving situations. This leads to the introduction of erroneous models and logic.

The introduction of motion into displays can eliminate some of the operator's conceptual biases by directly providing dynamic information. In the case of the trapezoidal image, for example, the ambiguity as to shape can be resolved by projecting the gradually changing image as the shape is rotated about some axis. However, in general, such reduced dynamic displays still lack much of the spatial and other information available in actual events. Thus, the operator is still forced to make assumptions to resolve ambiguities. Caution must be taken to ensure that the operator's perception matches the information the designer intends to convey. Further, the designer must appreciate the inherent tendencies of perceptual organization for the perception of motion and the particular organizational issues associated with periodically updated displays.

The display technologies currently available and undergoing development vastly improve the capability to transfer information between operator and machine. The challenge now is to appreciate operators' context-specific biases to enhance the likelihood that what is transferred is information, not misinformation.

This work was done by Mary K. Kaiser of **Ames Research Center** *and Dennis R. Proffitt of the University of Virginia. Further information may be found in NASA TM-89430 [N87-20747], "Human-Display Interactions: Context-Specific Biases."*

Copies may be purchased [prepayment required] from the National Technical Information Service, Springfield, Virginia 22161, Telephone No. (703) 487-4650. Rush orders may be placed for an extra fee by calling (800) 336-4700.
ARC-11847

Estimability and Regulability of Linear Systems

These properties provide criteria for reductions of errors and cost functions in control systems.

A report presents two new properties of systems characterized by linear state space models (e.g., dynamical systems and associated control systems): estimability and regulability. These properties are useful in the design of optimal controllers and estimators.

The benefit of using observation or feedback signals in estimating the states or the regulation of dynamical systems is normally manifested by the reduction of certain cost functions with respect to the values taken by those functions when no such signals are used. The new properties yield reductions in the mean-square errors in the estimates of the states and in the quadratic cost functions in state-feedback control. Estimability and regulability are different from observability and controllability, which were introduced by Kalman and are widely recognized as key structural properties in linear estimation and control.

A stochastic linear system is said to be estimable if, in estimating its state from its output, the posterior error covariance matrix is strictly smaller than the prior state covariance matrix. This condition is equivalent to the condition that no direction in the state space at any time is orthogonal to all the past observations. It is also shown to be equivalent to the reachability of a certain pair of matrices, related to the covariance function of the observations process. The notion of estimability is independent of that of observability in the sense that one does not imply the other.

When a system is not estimable, the corresponding Kalman filter can be reduced to a lower-order estimator of the state process. A linear-state-space system driven by white noise is shown to be a minimal-order realization of its output process if and only if it is observable and estimable. These results apply to time-variant and time-invariant linear systems in discrete and continuous time. In the stationary case, the estimability condition leads directly to conditions for minimality of the Kalman filter.

A linear system is said to be regulable if, for any nonzero initial condition, the quadratic cost in applying optimal control is strictly smaller than the cost when no control is applied. This means that when a system is not regulable, the feedback signal may be eliminated for some nonzero initial condition without increasing the cost. Necessary and sufficient conditions for regulability are obtained for time-variant and time-invariant systems. The regulability condition is the same as the condition for the complete dependence of the regulation problem, which in turn has been shown previously to be equivalent to the irreducibility of the optimal linear quadratic regulator.

It is shown that the estimability condition and the regulability condition, which involve the Lyapunov equation and the time-reversed Lyapunov equation, respectively, are similar, modulo time reversal. Such similarity, which has also been shown to exist between the Riccati equations associated with the estimation and the regulation problems, has been termed "duality" in the literature. The duality between the estimability and the regulability properties is then shown to be consistent with the one between the Lyapunov and the Riccati equations corresponding to the estimation and the regulation problems. Next, by use of this duality, the regulability condition is obtained from the estimability condition.

This work was done by Yoram Baram of **Ames Research Center** *and Thomas Kailath of Stanford University. To obtain a copy of the report, "Estimability and Regulability of Linear Systems," Circle 158 on the TSP Request Card.*
ARC-12173


• Tap Into The Latest NASA Technology
• Meet Top Government/Industry R&D Experts
• Find Innovative Ideas For New Products
TECHNOLOGY 2000
the first national conference and exhibition
of NASA's technology for transfer
Washington DC Hilton Hotel
November 27-28, 1990

NASA Invites You To The High-Tech Event Of 1990

Where Industry Can:

- access technology from NASA and its contractors
- meet industry/government tech transfer experts
- find new partners for R&D ventures
- discover what's in the pipeline from current NASA projects
- explore future applications of space-related research
- share the experiences of current spinoff companies

A Gold Mine Of Technology Awaits You

High-tech innovation—from the revolutionary to the incremental, from the million dollar idea to the .05% reduction in cost—is what **TECHNOLOGY 2000** is all about. Join NASA and NASA Tech Briefs magazine as they launch the first annual conference and exposition of NASA technology and technology transfer.

In two jam-packed days, government and industry trailblazers will bring you up to speed on the latest innovations in computer technology, communications, electronics, materials science, and other key areas—with a focus on potential commercial applications.

Between and after these sessions, you will visit the idea-stocked exhibit area and meet experts from all nine NASA field centers as well as many of the top companies around the country. You will have ample opportunity to talk with these leaders, to develop contacts with potential R&D partners, and to learn what's directly ahead in a variety of high-tech fields.

Thousands of firms have picked up NASA's ideas and run with them, creating new products and processes. Others have used space-based technology to hone their internal operations or improve their manufacturing systems. You too can benefit from this wealth of government-sponsored research. Join NASA, its leading contractors and spinoff companies at **TECHNOLOGY 2000**, November 27-28, 1990.

Explore The Leading Edge

The **TECHNOLOGY 2000** program will feature more than 90 presentations by top NASA researchers and industry leaders. Key symposia topics include:

Artificial Intelligence

- Electronic Neural Network Technology
- CLIPS: A Tool For Developing Expert Systems
- Intelligent Computer-Aided Training
- COMPASS: The Computer-Aided Scheduling System
- The Evolution Of Intelligent Information Management

Communications

- Fiber Optic Local Area Networks
- The Hyperswitch Communication Network
- Advances In Mobile Satellite And Personal Communications
- Developments In Coding Theory For Near-Error-Free Communications
- Multichannel Demultiplexer/Demodulator Technologies For Future Communications Systems

Computer Science

- Exploring Virtual Reality: The Virtual Environment Display System
- Three-Dimensional Perspective Visualization
- Digital Optical Computing
- Hypercube Technology
- Applications Of Fuzzy Logic

Electronics

- Superconducting Microwave Electronics
- Microwave Integrated Circuits
- New CCD Technologies
- The ERBE Optical Disk Archival System
- Power-By-Wire And Fly-By-Light Technology

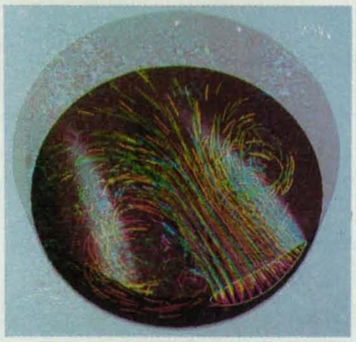

Learn how space-based computer techniques are aiding medical researchers.

Life Sciences

- The Temperature Pill, The Programmable Implantable Medication System, Functional Electrical Stimulation, and Other Biomedical Breakthroughs
- Computer-Aided Design Of Artificial Hearts
- Space-Based Cytometry
- The Ultrasonic Burn Depth Monitor
- Advances In Biogenerative Life Support Systems

Explore new developments in materials science, including advanced high-temperature ceramics, plastics, and metals.

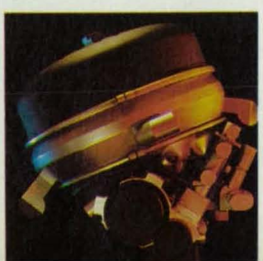

Technology 2000 will spotlight an array of NASA spinoffs, such as an automobile engine that runs on virtually any fuel—including alcohol, methane, and butane.

Power And Energy

- The Free-Piston Stirling Engine: From Space Technology To Terrestrial Applications
- Solar-Powered Stirling Cycle Electricity Generator
- Bi-Polar Batteries For Electric-Powered Vehicles

Manufacturing/Fabrication Technology

- Robotics In Space-Age Manufacturing
- Variable-Polarity Plasma Arc Welding
- Waterjet Cutting Without Thermal Distortion

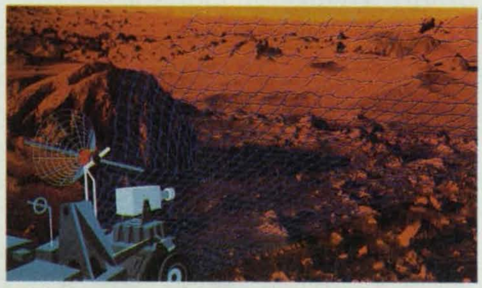

NASA experts will describe how autonomous vision systems and other technologies being developed for future space missions could be reapplied by U.S. industry.

Materials Science

- Dual-Beam Process Diamondlike Films For Industrial Applications
- Flexible Fluoropolymer-Filled Protective Coatings
- Silicon Carbide, An Emerging High-Temperature Semiconductor
- High-Performance Polymer Development
- Rapid Induction Bonding Of Composites, Plastics, And Metals

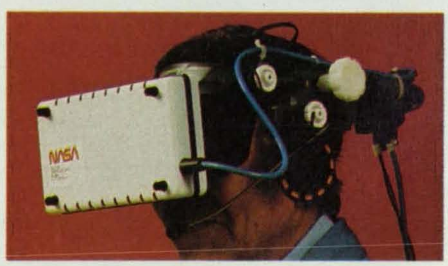

See cutting-edge inventions like the Virtual Workstation, a computer system that creates an "artificial reality."

Robotics

- Telerobotic System Technologies
- Intelligent Vision System For Autonomous Vehicle Operations
- Robotic Inspection/Verification
- Development of ROBOISM Simulation Software For Industry

Discover the latest advances in telerobotics.

Sensor Technology

- Technologies For Mission To Planet Earth
- Electron Tunnel Sensor Technology
- The "Smart" Hydrogen Sensor
- Application Of Resistance-Type Strain Gages On High-Temperature Composites

The above list represents only a sample of the research innovations NASA and its contractors will share with **TECHNOLOGY 2000** attendees. A full list of topics, speakers, and session times will accompany registration confirmations; registrants may then choose the sessions they wish to attend.

TECHNOLOGY 2000 EXHIBITORS

Here is a partial list of the high-tech firms and research labs exhibiting at TECHNOLOGY 2000:

Ames Research Center
Allied Signal
AMP
Aerospatiale
Astro-Med
Carnegie Mellon Robotics Institute
Corning
COSMIC
Datatape Inc.
Deltek Systems
Design And Evaluation
Dimension Technologies
Dolphin Scientific
E-Systems
Exos Inc.
General Dynamics
General Electric
Goddard Space Flight Center
Grumman Space Systems
Hewlett Packard
High Tech Services
Hi-Techniques
Hughes Aircraft
Hyperception
Ideas Inc.
Information Development Inc.
Information Handling Services
Instrument Technology
Jet Propulsion Laboratory
Johnson Space Center
JP Technologies
JR3 Inc.
Kennedy Space Center
Langley Research Center
Lewis Research Center
Lockheed
Lucas Datalab
Marshall Space Flight Center
Martin Marietta
Mechanical Technology Inc.
Micro Industries
Mikron Instruments
Motorola Govt. Electronics
NASA Industrial Applications Centers
NERAC
NIAC/Applied Research
Nicolet Instruments
Novespace
Numerical Algorithms Group
OCA Applied Optics
Optical Coating Lab
Pacific Precision Labs
Pantech Inc.
PMS Electro-Optics
Ramtek
Raytheon
RGB Spectrum
RG Hansen & Assoc.
Ribbon Technology
Rocketdyne
Rockwell Intl.
Rotating Memory Services
Scientific And Technical Information Facility
SCO Inc.
Silicon Graphics
STAC
Stennis Space Center
Stephens Analytical
Structural Research And Analysis
Technology Transfer Society
Tennessee Technology Foundation
Texas Innovative Info Network
Textron Specialty Materials
Tiodize
TRW Space And Technology
Turbomixer Corp.
United Technologies
University Of Florida
Valcor Engineering
Vermont Research
Vetronix Research Corp.
W.L. Gore
Wolfram Research
Zitel

These leading-edge companies and research centers will be displaying a wide array of inventions and products available for license or sale, including 3D computer monitors, CD-ROM databases, scientific and engineering software, desktop signal processors, high-resolution recorders, remote vision instruments, real-time video systems, dexterous robot controllers, fluid control components, cryogenic systems, high-strength composites, film deposition techniques, advanced engine concepts, high-temperature lubricants, HeNe lasers, digital signal processing hardware and software, digital storage oscilloscopes, and much, much more!

WHO SHOULD ATTEND TECHNOLOGY 2000

If you are a research director, project leader, design engineer, scientist, technology transfer agent, or small business owner/president, you cannot afford to miss **TECHNOLOGY 2000**. Top researchers and technology managers have already registered from the aerospace, electronics, computer, industrial equipment, defense, communications, bio-medical, materials, power, transportation, and chemical industries.

SHOW HOURS

Concurrent symposia sessions are scheduled for the 8:30 to 11:00 a.m. and 2:30 to 5:30 p.m. time slots on both Tuesday and Wednesday, November 27 and 28. Exhibits will be open from 11:00 a.m. to 5:00 p.m. both days.

THE LOCATION

All sessions will be held at the Washington Hilton Hotel and Towers, 1919 Connecticut Ave., NW, Washington, DC 20036. The hotel is conveniently located near the DuPont Circle stop on the Metro Red Line, and offers plenty of indoor parking.

REGISTRATION FEES

The full registration fee is $150 and includes symposia and exhibits for both days. For those wishing to attend for only one day, registration for technical sessions and exhibits is $100. Attendees may visit the exhibit area only at a cost of $20/day.

Clip the coupon below and return with your payment to: Technology Utilization Foundation, 41 East 42nd St., Suite 921, New York, NY 10017

HOTEL ACCOMMODATIONS

Reservations must be made directly with the Washington Hilton, Reservations Dept., 1919 Connecticut Ave., NW, Washington, DC 20036 (202) 483-3000.

THE SPONSORS

TECHNOLOGY 2000 is sponsored by NASA, NASA Tech Briefs magazine, and the Technology Utilization Foundation, a not-for-profit organization dedicated to technology transfer. For further information call (212) 490-3999.

SPACE AT TECHNOLOGY 2000 IS LIMITED; RESERVE YOUR PLACE TODAY.

The Washington Hilton • Washington, D.C. • November 27-28, 1990

REGISTRATION FORM

DEADLINE FOR RECEIPT: NOVEMBER 9, 1990
Please use separate form for each registrant. Type or print clearly.

Name ______________________________

Title ____________________ Phone ______________

Company ______________________________

Address ______________________________

City/State/Zip ______________________________

Which of the following best describes your industry or service?

A___Aerospace	G___Government	S___Computers
D___Defense	E___Electronics	Q___Industrial Eqpt.
X___Communications	R___Research Lab.	C___Chemicals
Y___Consumer gds.	M___Materials	U___Education
P___Power/Energy	K___Consultant	B___Bio-Medical
L___Library	T___Transportation	Z___Other__________

Your major responsibility is: (Check one)
1___ Management other than engineering
2___ Engineering management
3___ Engineering
4___ Research
5___ Other (specify)______________

Your principal job function is: (Check one)
1___ General & Corporate Management
2___ Design & Development Engineering
3___ Engineering Service-Tests/Quality
4___ Basic Research
5___ Manufacturing & Production
6___ Purchasing & Procurement
8___ Other (specify)______________

Your engineering responsibility is:
A___ Manage Engineering Dept.
B___ Manage a Project Team
C___ Manage a Project
D___ Member of Project Team
E___ Other (specify)______________

REGISTRATION FEES

Full registration $150	$________
One day $100/day (Circle day: Tues. Wed.)	$________
Exhibits only $20/day (Circle day: Tues. Wed.)	$________
Total amount due:	$________

Return with your payment to: Technology Utilization Foundation, 41 East 42nd St., Suite 921, New York, NY 10017

Physical Sciences

Hardware, Techniques, and Processes

Heat-Flux-Measuring Facility

An apparatus simulates conditions in turbine engines.

Lewis Research Center, Cleveland, Ohio

An automated facility generates and measures transient and steady-state heat fluxes at flux densities from 0.3 to 6 MW/m^2 and temperatures from 100 to 1,200 K. The facility is used to develop heat-flux gauges for turbine blades and to test materials for durability under rapidly changing temperatures.

The facility includes a commercial arc-lamp system, a heat exchanger, and a high-speed three-axis positioning system. Microcomputers in the lamp system and the positioning system control their functions. The main computer commands the microcomputers and controls the overall testing and acquisition of data. The lamp system focuses thermal radiation from an arc onto a 1-by-4-cm test area about 4 cm away. The heat exchanger cools the water circulated through the lamp. The positioning system is programmed to immerse a heat-flux gauge in liquid nitrogen at the start of a test, then place the gauge in the test area where the lamp heats it (see figure), and finally return the gauge to the liquid nitrogen.

Throughout the test, a main computer gathers data from the gauge under test, from thermocouples on the gauge, and from a current sensor in the lamp system. In a representative test, the lamp current is initially 30 A. When the test gauge has been in position in the test area for 0.3 s, the current is suddenly increased to 400 A. The increase in radiant heat increases the heat-flux density to about 5.2 MW/m^2, 0.4 s later. This corresponds to a transient heating rate of 12.6 MW/m^{2}s, typical of rates that can occur in some kinds of turbomachinery.

Two types of heat-flux gauges were used to evaluate the facility. Commercial water-cooled Gardon gauges yielded highly correlated data, suggesting that the instrument makes repeatable measurements as the current in the arc lamp is increased from 30 to 400 A. Gardon gauges are limited to temperatures between 280 and 360 K.

For use over the full temperature range of the facility, durable miniature plug-type gauges were fabricated from a nickel-base alloy. Data from the new gauges generally agree with those from the Gardon gauges during the initial transient and into the steady-state period of heating until about 2.6 s into the test. After that, the data from the two types differ by more than 20 percent, probably because of heat leaks and because data on the temperature-dependent specific heat and thermal conductivity of the nickel alloy are inaccurate.

This work was done by Curt H. Liebert and Donald H. Weikle of **Lewis Research Center**. *Further information may be found in NASA TM-101428 [N89-14418], "Heat Flux Measurements."*

Copies may be purchased [prepayment required] from the National Technical Information Service, Springfield, Virginia 22161, Telephone No. (703) 487-4650. Rush orders may be placed for an extra fee by calling (800) 336-4700.

LEW-14917

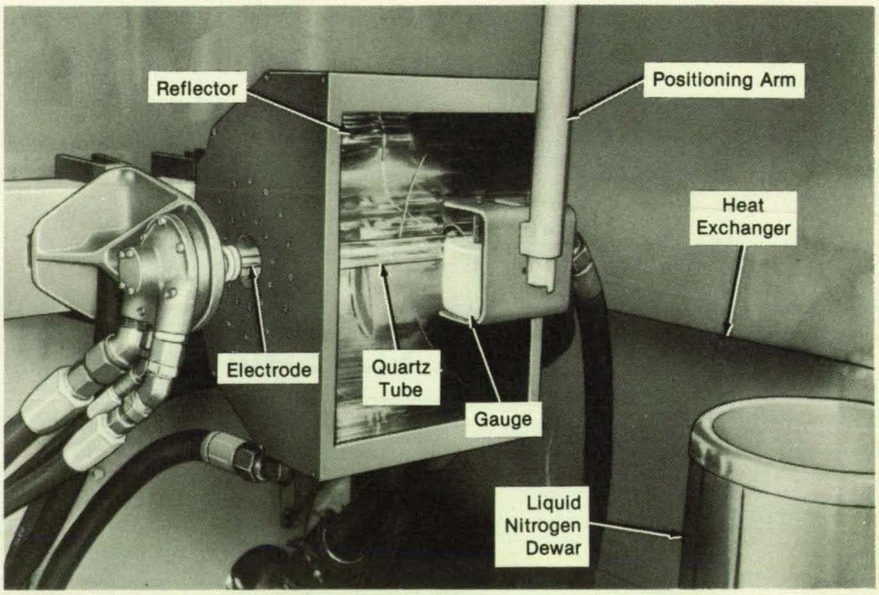

The **Positioning Arm Holds** the heat-flux gauge at the focal point of the arc lamp. The arm has previously chilled the gauge in liquid nitrogen in the Dewar flask at right. Cooling water flows through the lamp to the heat exchanger.

Measuring Irradiance Over Large Areas

The map of temperature on a thin reradiating sheet yields data on the thermal irradiance.

NASA's Jet Propulsion Laboratory, Pasadena, California

A relatively simple experimental technique yields data that can be processed, via a straightforward mathematical model, into a map of the thermal irradiance over a large area. The technique can be used to obtain rapid measurements of the incident-flux distribution over a broad spectral range at specific locations relative to such heat sources as infrared heat lamps or lasers. The technique was originally developed to verify efficiently the uniformity of irradiance that would be produced by a complex array of quartz-tube heat lamps and reflector elements over a large spacecraft solar panel during thermal vacuum-chamber tests.

A thin, opaque sheet of material having known solar absorptance and emittance is placed at the distance and orientation relative to the heat sources where the irradiance is to be evaluated. The heat sources are turned on, and the sheet is allowed to come to thermal equilibrium with the environment (which could be a suitable laboratory room or an evacuated chamber). An imaging infrared radiometer is used to map the temperature distribution on the sheet (see figure).

The sheet is extremely thin and has a very low thermal conductivity, so that the lateral diffusion of heat within it is negligible. The steady-state energy balance at any point on the sheet can therefore be described by a mathematical model that includes only the radiative and convective heat losses, plus absorbed irradiance. Only such parameters as the solar absorptance and emittance of the sheet, the temperatures of the sheet and the environment, and the convective film coefficients (if air is present) are required for a complete solution. The equation can be manipulated to solve directly for the local irradiance as a function of the local measured sheet temperature and the other parameters.

The equation is valid provided that the following additional conditions are satisfied:

1. The sheet is opaque and diffuse and has high emittance over a broad spectral range.
2. The heat sources are far enough away from the sheet that they do not significantly block the total view to the surroundings.
3. In air, the test should be conducted under conditions that permit reliable calculation of convective film coefficients.
4. Local variations in convective film coefficients are small.
5. Local variations in radiative properties of the sheet (solar absorptance, emittance, diffuseness, and the like) are negligible.
6. The facility in which the test is performed is large with respect to the sheet.
7. The chamber in which the test is performed is at a known, uniform temperature. In air, it is convenient (but not necessary) to assume the chamber is at the ambient air temperature.

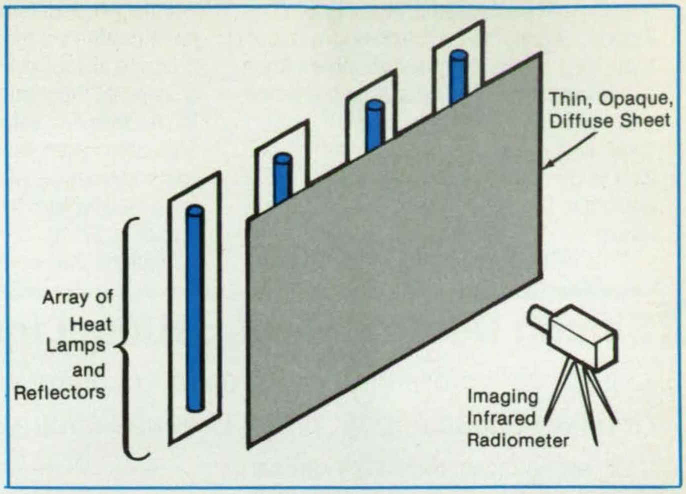

The **Imaging Infrared Radiometer** makes a temperature map of the sheet. The irradiance distribution at the sheet location is then deduced from the temperature map.

The mathematical model and radiometric flux-density mapping technique have been validated by comparison with calorimetrically obtained irradiance measurements for a complex heat-source geometry. The flux level was predicted with an accuracy of 15 percent or better, and the shape of the two-dimensional irradiance distribution matched the measured profile very closely. Modern commercial imaging infrared radiometers detect temperature differences sufficiently small to resolve irradiance differences of less than 1 percent, using this method. The technique can provide useful data on irradiance distribution at levels up to approximately 6 kW/m^2 in near real time over very large areas. It is especially useful in cases where accurate mathematical modeling is not practical because of the geometric complexity of the heat sources or of the targets, or where heat-source power outputs are not accurately known, or vary with time. The quick response also facilitates rapid adjustments to the heat-source geometry to obtain desired flux patterns.

This work was done by Stuart D. Glazer and Georg Siebes of Caltech for **NASA's Jet Propulsion Laboratory**. *For further information, Circle 140 on the TSP Request Card.*

NPO-17810

Improved Multiple-Species Cyclotron Ion Source

$^{86}Kr^{+17}$ is used instead of $^{80}Kr^{+16}$.

NASA's Jet Propulsion Laboratory, Pasadena, California

The use of the pure isotope ^{86}Kr instead of natural krypton in a multiple-species ion source enables the source to produce krypton ions that can be separated from argon ions by tuning a cyclotron with which the source is used. The modified source is used with the 88-in. Cyclotron at the University of California at Berkeley to simulate heavy-ion cosmic rays in studies of the effects of these rays on solid-state electronic circuits. The addition of the capability to produce and separate krypton ions at kinetic energies of 150 to 400 MeV is necessary for simulation of the worst-case ions that occur in outer space.

An electron cyclotron resonance (ECR) source can be tuned to emit a beam containing ions of several different species simultaneously, provided that each species has a similar ratio of atomic mass (A) to charge (Q). However, the A/Q ratios of the species must differ sufficiently to enable the separation of the species by use of the slight differences between their cyclotron frequencies. The advantage of such a multiple-species ion source is that it takes only a few minutes to retune the cyclotron from one species to another.

Previously, The ERC source had been used to provide $^{40}Ar^{+8}$, $^{20}Ne^{+4}$, and $^{15}N^{+3}$. The A/Q ratios of these ions differ enough that they can be separated by tuning (see table). Heretofore, it has not

Ion	Energy (MeV)	A/Q	Cyclotron Frequency of This Ion Minus Cyclotron Frequency of $^{40}Ar^{+8}$
Original Ions			
$^{15}N^{+3}$	62.5	5.00	– 13.416
$^{20}Ne^{+4}$	80.7	5.00	– 7.962
$^{40}Ar^{+8}$	156	5.00	0.0
Additional Ion			
$^{86}Kr^{+17}$	316	5.06	– 163.250
Contaminant Ion			
$^{80}Kr^{+16}$	291	5.00	1.486

The **Cyclotron Parameters** for the principal species of ions include the cyclotron frequency, which is tuned to select the desired species.

been practical to include natural krypton in the source because when the cyclotron is tuned to argon, the cyclotron beam is contaminated by the naturally abundant krypton isotope $^{80}Kr^{+16}$. The reason is that the resonant frequency for $^{80}Kr^{+16}$ is only 1.486 kHz away from that of $^{40}Ar^{+8}$, and well within the resonance width of the cyclotron (3 kHz, full width at half maximum).

This difficulty is surmounted by use of the single ion isotope $^{86}Kr^{+17}$, the tuning point of which differs by 163.250 kHz. Tests have confirmed that the ECR source can produce all four ion species simultaneously when its magnetic field is tuned to an intermediate A/Q value of 5.025. The source has performed flawlessly with the new four-ion mixture, with changeovers to and from the krypton ion in minutes. There was found to be no detectable krypton contamination that would affect the results of experiments with ions of lower atomic numbers and lower degrees of ionization. This new beam capability saves many hours of expensive tuning time and greatly facilitates the scheduling and use of the ion source.

This work was done by George A. Soli and Donald K. Nichols of Caltech for **NASA's Jet Propulsion Laboratory**. *For further information, Circle 28 on the TSP Request Card.* *NPO-17766*

Silicon Detectors for Helium Liquid and Vapor

Liquid cools more than vapor does, resulting in greater electrical resistance.

Goddard Space Flight Center, Greenbelt, Maryland

Simple electrical-resistance devices made of silicon indicate whether helium liquid or helium vapor is present. Although the devices were designed primarily for use in outer space, they have been tested and found to operate in normal Earth gravity. Such helium-liquid/vapor detectors can be incorporated into ducts or containers of laboratory equipment, for example, and used to infer locations of liquid/vapor interfaces in order to measure quantities of liquid and vapor or to control refill operations.

The devices are 0.25-mm cubes of silicon doped with antimony and boron. Ohmic contacts are formed on opposite faces by implantation of arsenic at 150 keV and coating with gold. One gold face of each cube is soldered or bonded with silver epoxy to a gold-plated, 0.05-mm-diameter 304 stainless-steel wire that serves as a support and as a common electrical conductor for all the devices in a string of them (see figure). The other face of each cube is soldered or silver epoxied to a 0.05-mm-diameter manganin wire. The cubes, wires, and solder or epoxy lumps are made small to make their heat capacities low to promote rapid thermal response.

The electrical resistance of each device depends strongly on its temperature. A small, fixed electrical current is passed through each device, heating it above the temperature of the surrounding helium and decreasing its resistance. Because the liquid helium cools the device more than does helium vapor at the same temperature, the device has a higher resistance in liquid than in vapor. Therefore, the voltage across the device is higher in the presence of liquid, and this voltage is measured to determine whether liquid or vapor is present.

The level of doping is selected so that the "liquid" reading is ≳2 V and the "vapor" reading is <0.5 V over a wide range of current. Each device is operated at a power (typically ≳0.3 mW) sufficient to boil away any liquid-helium film that remains on the device when it is immersed in vapor, but not so large a power as to cause boiling when the device is immersed in the bulk liquid. The doping level can be optimized for operation at a specified temperature. However, the operating characteristics of a typical device are nearly independent of its operating temperature over a relatively wide (for cryogenic practice) temperature range, e.g., <1.4 K to >4.2 K.

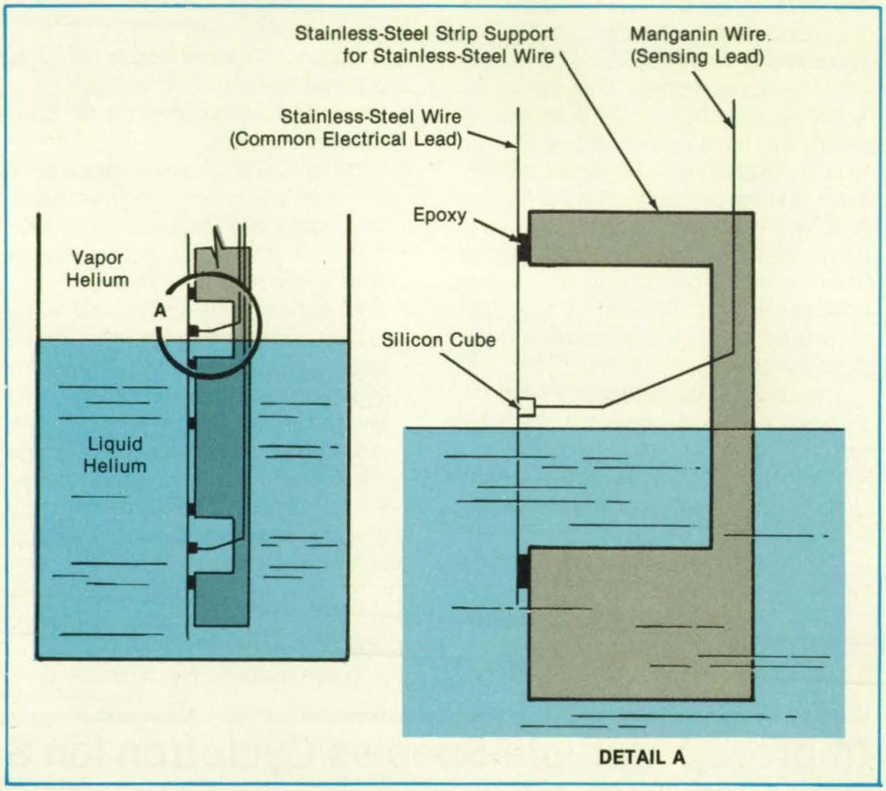

Silicon Cubes are supported by stainless-steel wires and strips. The voltage across each cube at a fixed current indicates whether it is immersed in helium liquid or vapor.

The detectors respond rapidly to changes in the surrounding medium. For example, in one set of tests in which thick superfluid helium films were boiled off the detectors, the transitions from "liquid" signals (~1.8 V) to "vapor" signals (~ 0.3 V) upon completion of boiloff took ≳ 5 ms.

This work was done by M. J. Di Pirro and A. T. Serlemitsos of **Goddard Space Flight Center**. *For further information, Circle 142 on the TSP Request Card.* *GSC-13281*

Isothermal Calorimeter

A pressure-feedback signal indicates the rate of heating.

NASA's Jet Propulsion Laboratory, Pasadena, California

An improved isothermal calorimeter measures the rate of heating in an object under test. It is called "isothermal" because the chamber that holds the object and its environment are maintained at or near a constant temperature to minimize spurious transfers of heat that would introduce errors into the measurements. Unlike in other types of calorimeters, the rate of heating is, therefore, not measured in terms of the rate of increase of temperature. Instead, it is measured in terms of the rate of boiling of a liquid.

As shown schematically in the figure, the calorimeter includes an insulated inner test chamber and an outer chamber, both partially filled with the liquid, which is usually trichloromonofluoromethane (CCl_3F). The object is immersed in the liquid in the inner chamber. A small hole in the bottom of the inner chamber allows the liquid to flow between the two chambers. The liquid in both chambers is kept at a low boil by heaters so that both liquids remain at or near the boiling temperature, and the space above the liquid in both chambers is filled with vapor. A condenser limits the height of the vapor space in the outer chamber.

A differential-pressure gauge at the top of the inner chamber measures the difference between the vapor pressures in the two chambers. A control circuit responds to the differential-pressure signal by applying a control voltage to a servovalve at the top of the inner chamber near the gauge. The control circuit adjusts the opening of the valve to maintain the vapor pressure in the inner chamber 0.1 psi (0.7 kPa) above that in the outer chamber.

When the item under test generates heat, the rate of boiling and the pressure in the inner chamber increase. The servovalve has to open wider to maintain the preset differential pressure. Thus, the valve-control voltage can be used as measure of the rate of heating.

In calibration tests, it was found that the valve-control voltage responds to a change in the rate of heating within about 1 second. At a rate of 20 W, the isothermal calorimeter measures the rate to within 0.3 percent.

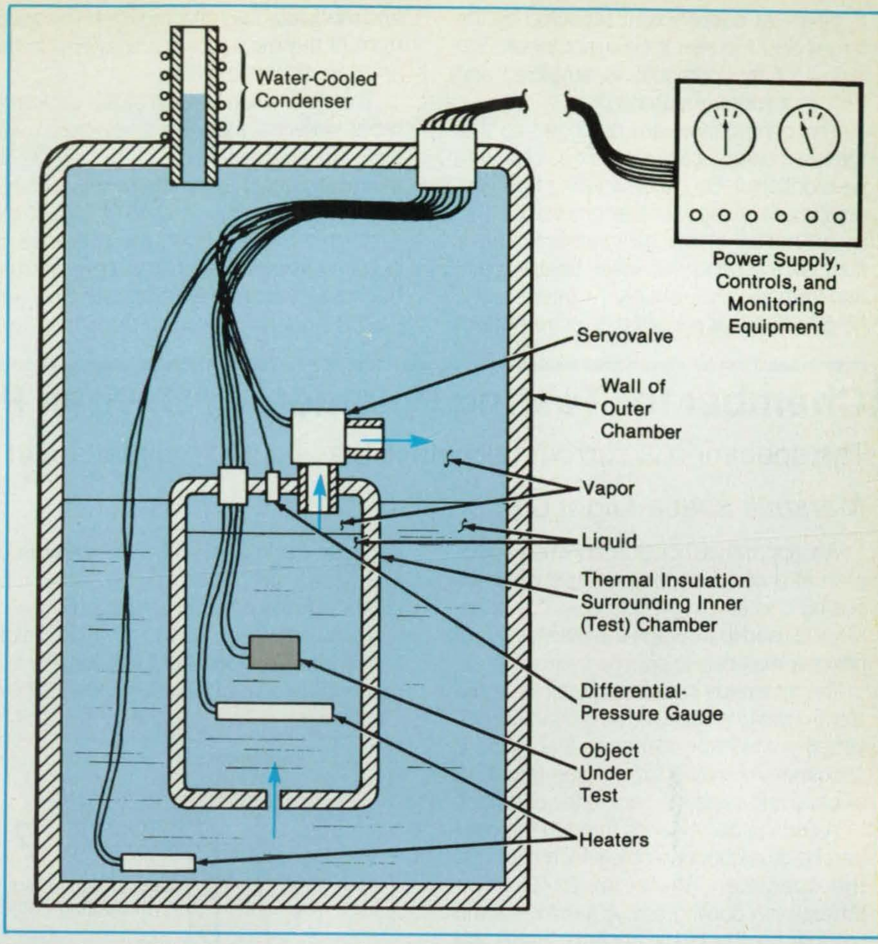

The **Isothermal Calorimeter** is shown here in simplified schematic form to illustrate the principle of operation. The rate of heating in the object under test is indicated by the control voltage applied to the servovalve to maintain a constant differential vapor pressure between the inner and outer chambers.

This work was done by John J. Rowlette of Caltech for **NASA's Jet Propulsion Laboratory**. *For further information, Circle 145 on the TSP Request Card.*
NPO-17419

Laser Schlieren System Detects Sounds of Leaks

Hostile environments can be monitored safely and noninvasively.

NASA's Jet Propulsion Laboratory, Pasadena, California

A modified laser schlieren system acts as a microphone to detect the sounds of leaks remotely. The system is sensitive to acoustical frequencies above the audible range and is especially suited for monitoring leaks of high-pressure steam from boilers or chemical vapors from processing equipment. The system does not require the placement of delicate equipment in the harsh environment to be monitored, and there need be no contact with the boiler or other unit being monitored.

In the latest (dual-beam) version of the system (see figure), light from a helium/neon laser is split into two beams that are aimed at a point on a retroreflective target. The angle between the beams is set so that the spatial period of the interference fringes formed by the intersecting beams equals the pitch of a moire pattern printed on the target. A Fresnel lens 5 in. (12.7 cm)

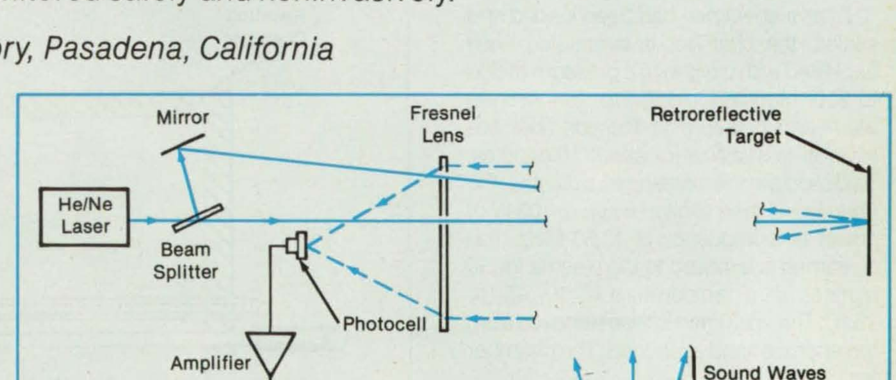

The **Laser Schlieren Microphone** detects sound waves via the variation of the index of refraction of air at the acoustical frequencies. This system can be used to monitor sound frequencies beyond the range of human hearing.

in diameter collects light reflected by the target and focuses it on a photocell. The output of the photocell is amplified and sent to a spectrum analyzer.

The components are arranged so that the laser beams pass by the equipment to be monitored. Sound emanating from this equipment causes fluctuations in the index of refraction of the atmosphere. These fluctuations bend the laser beams back and forth slightly, causing the interference fringes to move across the moire pattern and modulate the reflected light. The spectrum of the modulation is analyzed in the effort to diagnose a leak.

The dual-beam version of the system is more sensitive than the single-beam version. The single-beam version operates on a similar principle, but the target is illuminated by only a single spot of light. If the system is to be used in the presence of soot, an infrared laser may be preferred because of its greater penetrating power.

This work was done by Parthasarathy P. Shakkottai and A. Vijayaragavan Alwar of Caltech for **NASA's Jet Propulsion Laboratory**. *For further information, Circle 13 on the TSP Request Card.*

This is the invention of a NASA employee, and a patent application has been filed. Inquiries concerning license for its commercial development may be addressed to the inventor, Mr. Parthasarathy P. Shakkottai, 2622 Gardi Street, Duarte, CA 91010 [see page 16]. Refer to NPO-17009

Chamber for Testing Polymers in Oxygen Plasma

The specimen is surrounded with a plasma and maintained at a constant temperature.

Marshall Space Flight Center, Alabama

An apparatus holds a polymer specimen at a constant temperature while exposing it to an oxygen plasma. The apparatus is used to evaluate the resistances of polymer materials to plasma environments.

The apparatus includes a Pyrex (or equivalent) glass chamber with a removable poly(methyl methacryate) door that holds a specimen-mounting fixture (see figure). A silicone ring seals the door to the chamber.

A cooling coil extends through the door and holds a copper block, which supports the specimen. Water at 23 °C flows through the cooling coil. A thermoelectric module on the block cools or heats the specimen. A glass plate on the specimen holds it firmly against a thermocouple and the thermoelectric module. A hole in the plate exposes the specimen to the plasma.

The thermocouple, spring-loaded so that it presses against the specimen, monitors its temperature. The thermocouple is connected through the door to an external control circuit that adjusts the electric current in the thermoelectric module to maintain the specimen at a steady temperature.

After a specimen has been loaded and sealed, the chamber is evacuated, then backfilled with oxygen to a pressure of 600 to 900 mtorr (80 to 120 Pa). The temperature and pressure in the chamber are allowed to stabilize for about 15 minutes. To dissociate the oxygen into a plasma, the chamber is then excited by up to 100 W of power at a frequency of 13.56 MHz. The specimen is exposed to the plasma for 30 minutes at a temperature of 10, 45, or 75 °C. The specimen is then removed from the chamber and examined. The chamber can also be instrumented for analysis of the gases produced by the attack of plasma on the polymer specimen.

This work was done by Ann F. Whitaker of **Marshall Space Flight Center**. *For further information, Circle 132 on the TSP Request Card.*

Inquiries concerning rights for the commercial use of this invention should be addressed to the Patent Counsel, Marshall Space Flight Center [see page 16]. Refer to MFS-28368

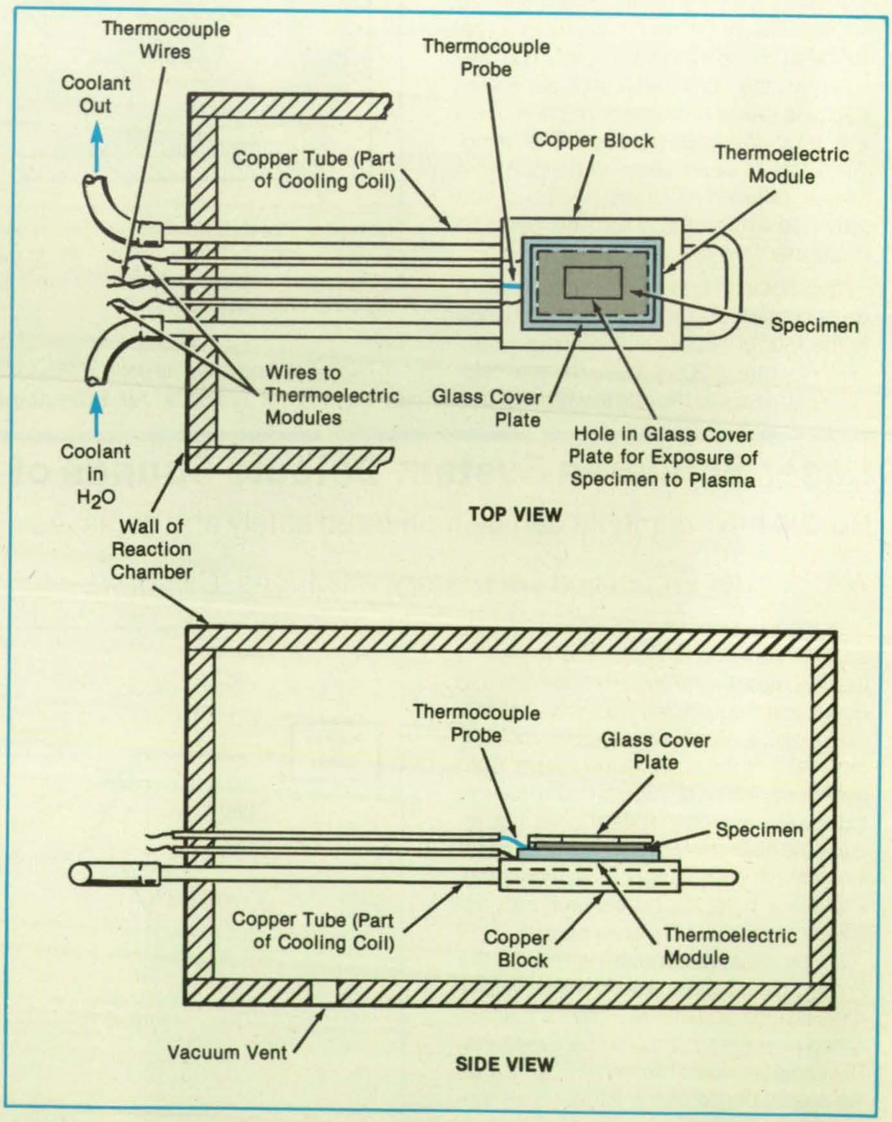

The **Copper Tube** (part of the cooling coil) extends into the plasma chamber, supporting the copper block and the thermoelectric module on which the specimen is mounted. The copper block is made small — 4.4 by 3.8 by 1.6 cm — so that it has little effect on the plasma.

Materials

Hardware, Techniques, and Processes

Low-Noise, Long-Life, High-Gain Microchannel-Plate Glass

Dark noise is reduced substantially without degrading other properties.

Langley Research Center, Hampton, Virginia

A glass suitable for use as the active material for microchannel plates (MCP's) is free of constituents that include significant amounts of radioactive isotopes. Background noise, or "dark noise," in well-outgassed MCP's that are free of hotspots is due largely to β radiation emitted by isotopes of constituents of glass. Although considerable research has been performed during the last several years and improved MCP's have been produced, background noise is still present, even in the best commercially available MCP's. Consequently, work was undertaken to produce a glass that has minimal intrinsic radioactivity and can be used to manufacture MCP's with electron gain, strip current, lifetime, and operating characteristics equivalent to those of the best commercially available MCP's.

This objective was accomplished by the formulation of glasses that have the following range of compositions, in weight percent:

SiO_2	30 to 35
PbO	50 to 57
Cs_2O	2 to 10
$\Sigma[MgO + CaO + SrO + BaO]$	0 to 5
$\Sigma[Al_2O_3 + ZrO_2 + TiO_2 + Nb_2O_5]$	0.1 to 1

where the mole ratio of SiO_2 to PbO is 2.0 to 2.4.

The ranges of proportions of SiO_2, PbO, and Cs_2O were chosen on the basis of estimates of the influences of these components on the properties of glasses. These ranges provide desired levels of glass-transition temperature, coefficient of thermal expansion, durability in acid, surface resistivity, softening point, and glass conductivity. These properties influence such factors as dimensional control and acceptable stress levels during production of the MCP, and attainment of appropriately high and stable strip currents for proper operation of the MCP. Alkaline earth elements, in the form of MgO and CaO, are incorporated to control forming viscosities and chemical durability. Al_2O_3, ZrO_2, TiO_2, and Nb_2O_5 are specifically incorporated to improve chemical durability.

Measurements of dark noise on a chevron pair of sample MCP's at ambient temperature (23 °C) have given a figure of 0.08 counts/(cm^2•s), one-eighth that of standard MCP's and one-third that of the quietest prior-art MCP's. However, this figure may also include residual radioactivity from non-MCP components in the test detector. Replacement of ceramic hardware, which is known to contain radioisotopes, is currently underway. Thus, the ultimate dark-noise figure of the MCP could be even lower.

This work was done by W. Bruce Feller and Lee M. Cook of Galileo Electro-Optics Corp. for **Langley Research Center**. *No further documentation is available.*

In accordance with Public Law 96-517, the contractor has elected to retain title to this invention. Inquiries concerning rights for its commercial use should be addressed to

Paul L. White
Galileo Electro-Optics Corp.
Galileo Park
P.O. Box 550
Sturbridge, MA. 01566

Refer to LAR-14010, volume and number of this NASA Tech Briefs *issue, and the page number.*

Rewaterproofing Chemical for Use With Silicones

An agent restores impermeability without degrading silicone adhesives and substructures.

Lyndon B. Johnson Space Center, Houston, Texas

Dimethylethoxysilane (DMES) has been found to rewaterproof tiles and composite panels internally without harming the materials that underlie them. DMES replaces hexamethyldisilazane (HMDS) as the postmission rewaterproofing agent for the tiles of the thermal-protection system on the Space Shuttle. Much of the original waterproofing is lost during the rigors of launch and reentry. Potential terrestrial application may include composite materials in such structures as bridges and submarines.

Although HMDS rewaterproofed effectively, it released reaction products that turned the silicone substrate into a soft, gummy layer. Like HMDS, DMES is an internal agent, injected into the tiles. Internal agents are more reliable than are external waterproof coatings, which form only surface barriers that water can breach if the coverage is not complete or the force driving the water is great enough.

DMES was selected from among 45 silicon-based candidate materials from 3 manufacturers. The materials were rated on how well they rewaterproofed tiles and on their chemical compatibility with the materials under the tiles. Two candidates showed the greatest promise: DMES and isobutyltriethoxysilane (IBTES). DMES was chosen for further tests because it is more readily available. DMES was then tested for its ability to rewaterproof adequately without adversely affecting the substrate materials. Its performance with thermal blankets as well as with tiles was studied. It was also subjected to environmental tests (humidity, rain, and wind, and heating in a vacuum).

DMES does not attack substrate materials as HMDS does because it does not give off harmful vapors as it cures. HMDS reacts with moisture in the tile to produce ammonia, which breaks up supporting polymers in the substrate. The broken molecules become end-capped with trimethylsiloxy groups that prevent them from rejoining. Moreover, HMDS vapor causes the polymers to swell and release their tin-based catalyst, which in turn breaks up and caps polymers in the silicone adhesive.

DMES, on the other hand, reacts to produce ethanol, hydrogen gas, and tetramethylsiloxane, none of which attacks the substrate materials. The hydrogen gas is in low concentrations and quickly dissipates and thus does not create a stress-corrosion problem for the titanium structure under the substrate.

This work was done by William L. Hill, Shirley M. Mitchell, and Howard S. Massey of Rockwell International Corp. for **Johnson Space Center**. *For further information, Circle 48 on the TSP Request Card. MSC-21569*

Polyimidazoles via Aromatic Nucleophilic Displacement

These polymers are suitable for use as films, moldings, and adhesives.

Langley Research Center, Hampton, Virginia

Experiments have shown that a variety of polyimidazoles can be prepared by aromatic nucleophilic displacement, from the reactions of bisphenol imidazoles with activated difluoro compounds. These polyimidazoles have good mechanical properties that make them suitable for use as films, moldings, and adhesives.

In each of the experiments a polyimidazole was prepared from the reaction of stoichiometric quantities of 4,5-bis(4-hydroxyphenyl)-2-phenylimidazole and an activated aromatic difluoro compound in the presence of potassium carbonate in N,N-dimethylacetamide (DMAc) (see figure) at a solids content of 15 to 20 percent. Toluene was used as an azeotroping agent to remove the water formed in the reaction, and the mixture was stirred at a temperature of ~ 155 °C overnight under a nitrogen atmosphere. The resulting viscous solution was diluted with DMAc and precipitated into water containing acetic acid, to obtain the polymer at a yield of more than 95 percent.

DMAc solutions of the experimental polyimidazoles were cast onto glass and dried to make film specimens. Powders of the polymers were compression-molded and cut to make tension and fracture-toughness specimens. One of the polymers was processed into an adhesive-tape specimen by multiple steps of coating from DMAc solution followed by drying, and used to make tensile shear specimens.

The inherent viscosities of the experimental polyimidazoles ranged from 0.24 to 0.89 dL/g, and the glass-transition temperatures ranged from 230 to 318 °C. The polyimidazoles were amorphous, as evidenced by differential scanning calorimetry and wide-angle x-ray diffraction analysis. Thermogravimetric analysis showed no loss of weight below a temperature of 300 °C in air or nitrogen, and a loss of 5 percent of weight at a temperature of ~ 400 °C in air and ~ 495 °C in nitrogen. The melt viscosities of the new compounds were found to be comparable to those of poly(arylene ethers) of similar molecular weights. The tensile strengths and tensile moduli of thin-film specimens at 25 °C ranged from 12.0 to 14.2 ksi (82.7 to 97.9 MPa) and from 362 to 407 ksi (2.50 to 2.81 GPa), respectively. The specimens retained large fractions of these strengths and moduli at 177 °C.

The polyimidazole prepared from 1,4-bis(4-fluorobenzoyl)benzene and the bisphenol imidazole was found to have a desirable combination of properties and to be readily processable. Neat resin moldings fabricated at 300 °C under 200 psi (1.38 MPa) exhibited a fracture toughness of ~ 3,000 psi in.$^{1/2}$ (3.3 MPa•m$^{1/2}$). The texture of the fracture surface was rough and slightly crazed. Such phenomena are often seen in tough thermoplastics. Preliminary adhesive-bonding work indicated that relatively mild pressures of 100 to 200 psi (0.7 to 1.4 MPa) gave better strengths than

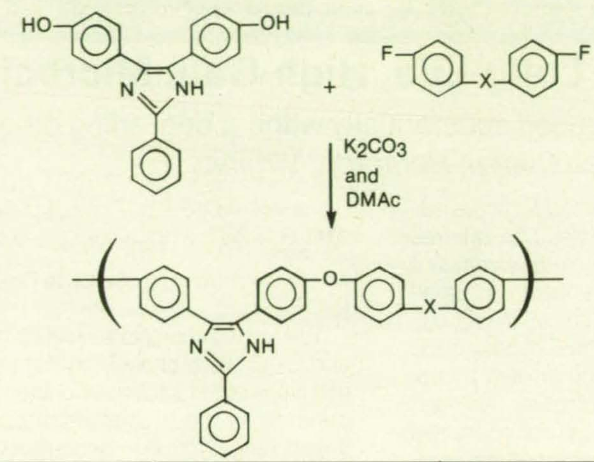

Polymer	X	Inherent Viscosity, dL/g	Glass-Transition Temperature, °C
P1	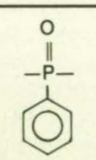	0.24	318
P2	SO_2	0.41	277
P3	CO	0.61	259
P4	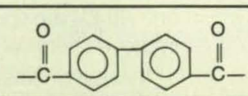	0.53	258
P5	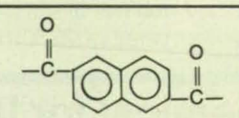	0.40	248
P6	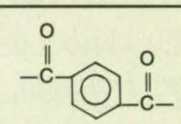	0.89	248
P7	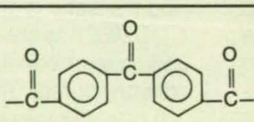	0.49	239
P8	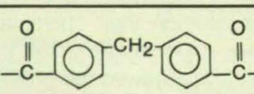	0.58	231
P9	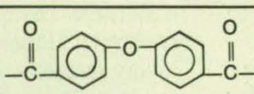	0.64	230
P10	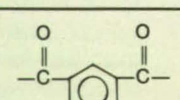	0.55	230

Ten **Different Polyimidazoles** were synthesized by this general chemical reaction, with X as shown in the table.

higher pressures did. Titanium-to-titanium adhesive specimens bonded at 300 °C under 200 psi (1.4 MPa) gave lap shear strengths at 25, 177, and 200 °C of 4,800, 3,700, and 3,000 psi (33, 26, and 21 MPa), respectively.

This work was done by John W. Connell and Paul M. Hergenrother of **Langley Research Center**. *For further information, Circle 4 on the TSP Request Card.*

This invention is owned by NASA, and a patent application has been filed. Inquiries concerning nonexclusive or exclusive license for its commercial development should be addressed to the Patent Counsel, Langley Research Center [see page 16]. Refer to LAR-14145.

Additives Lower Dielectric Constants of Polyimides

Dielectric constants as low as 2.43 make polyimides more attractive for electronic applications.

Langley Research Center, Hampton, Virginia

Linear aromatic condensation polyimides are being used increasingly as high-performance film and coating materials by the electronic-circuit industry. A new process makes aromatic condensation polyimide films and coatings with dielectric constants that have been lowered by the incorporation of diamic acid additives.

Polyimides are being exploited for four primary applications in microelectronics: (1) as fabrication aids, including photoresists, planarization layers, and ion-implant masks; (2) as passivant overcoats and interlevel insulators; (3) as adhesives; and (4) as substrate components. To be useful, particularly as a passivant or protective overcoat, the material must be an excellent insulator. The dielectric constants of conventional polyimides currently used as state-of-the-art materials for passivants and interlevel dielectrics range from approximately 3 to 4.0. Recent studies at NASA Langley Research Center have produced polyimides with dielectric constants in the range of 2.4 to 2.8.

In the new process, the additives are incorporated into low-dielectric-constant polyimides to lower the dielectric constants further. The preparation of a polyimide film or coating involves the room-temperature reaction of an aromatic diamine in a solvent with an aromatic dianhydride to yield a polyamic acid. This polymer resin is then cast as a film and thermally cured at 250 to 300 °C to obtain a polyimide film. To make a low-dielectric-constant film or coating, one incorporates 3 to 15 weight percent of low-molecular-weight amic acid additives in the polyamic acid resin before thermal imidization of the film.

Additive	Concentration of Additive, Weight Percent	Dielectric Constant at 10 GHZ
6FDA/4-BDAF Base Polymer (No additive)	—	2.53
6FDA-An	3	2.56
	5	2.56
	10	2.43
3,3′-DDSO$_2$-PA	3	2.50
	5	2.49
	10	2.56
ODPA-An	5	2.48
4-BDAF-PA	5	2.48
3-BDAF-PA	5	2.56
3,3′-ODA-PA	10	2.45

Selected Additives Lower the Dielectric Constant of the polymer 6FDA/4-BDAF.

The monomers chosen for the synthesis of these additives offer means of physically incorporating bulky $-CF_3$ groups and of introducing meta-isomerism in the diamine monomers. Studies of the relationship between structures and properties have shown that these are effective means of lowering the dielectric constants of polyimides.

In experiments, the additives were incorporated into two polymers, BDSDA/4-BDAF and 6FDA/4-BDAF. As shown in the table, the 6FDA-An additive lowered the dielectric constant of 6FDA/4-BDAF from 2.53 to 2.43. Other additives that lowered the dielectric constant, though not as effectively, included ODPA-An, 4-BDAF-PA, and 3,3′-ODA-PA. The 4-BDAF-PA additive was the most effective of those screened in the BDSDA/4-BDAF system (not shown in table), providing a decrease from 2.84 to 2.59.

The new materials provide better electrical insulation without sacrificing the temperature stability of the polyimide binders. This temperature stability enables the materials to serve as superior fabrication aids; for example, photoresists, planarization layers, and passivants. The process should be applicable whenever high temperature, low absorption of moisture, and high electrical-insulation properties are needed. Specific applications include semiconductors and printed-circuit boards for the computer industry and possibly the automotive industry.

This work was done by Diane M. Stoakely, Anne K. St. Clair, Burt R. Emerson, Jr., and Kenneth M. Proctor of **Langley Research Center**. *For further information, Circle 58 on the TSP Request Card.*

This invention is owned by NASA, and a patent application has been filed. Inquiries concerning nonexclusive or exclusive license for its commercial development should be addressed to the Patent Counsel, Langley Research Center [see page 16]. Refer to LAR-13902

Computer Programs

COSMIC: Transferring NASA Software

COSMIC, NASA's Computer Software Management and information Center, distributes software developed with NASA funding to industry, other government agencies and academia.

COSMIC's inventory is updated regularly; new programs are reported in *Tech Briefs*. For additional information on any of the programs described here, circle the appropriate TSP number.

If you don't find a program in this issue that meets your needs, call COSMIC directly for a free review of programs in your area of interest. You can also purchase the annual *COSMIC Software Catalog*, containing descriptions and ordering information for available software.

COSMIC is part of NASA's Technology Utilization Network

COSMIC® — *John A. Gibson, Director,*
(404) 542-3265
The University of Georgia, 382 East Broad Street, Athens, Georgia 30602

Computer Programs

These programs may be obtained at a very reasonable cost from COSMIC, a facility sponsored by NASA to make computer programs available to the public. For information on program price, size, and availability, circle the reference number on the TSP and COSMIC Request Card in this issue.

Electronic Systems

Program Aids Simulation of Neural Networks

The user can design patterns of connections between layers in neural networks.

The computer program NETS — A Tool for the Development and Evaluation of Neural Networks — provides a simulation of neural-network algorithms plus a software environment for the development of such algorithms. Neural networks are a class of systems modeled after the human brain. Artificial neural networks are fomed from hundreds or thousands of simulated neurons, connected to each other in a manner similar to that of neurons in the brain. Problems that involve the matching of patterns readily fit the class of problems that NETS is designed to solve.

NETS uses the back-propagation method of learning for all of the networks that it creates. Typically, the nodes of a network are grouped together into clumps called "layers." Generally, a network has an input layer through which the various environmental stimuli are presented to the network, and an output layer for determining the response of the network. The number of nodes in these two layers is usually tied to some features of the problem being solved. Other layers, which form intermediate stops between the input and output layers, are called "hidden layers." NETS enables the user to customize the patterns of connections between layers of a network. NETS also provides features for saving the weight values of a network, thereby providing for more precise control over the learning process.

NETS is an interpreter. Its method of execution is the familiar "read–evaluate–print" loop found in such interpreted languages as BASIC and LISP. The user is presented with a prompt, which is the simulator's way of asking for input. After a command is issued, NETS attempts to evaluate the command. The attempt may produce more prompts that request specific information or may produce an error signal if the command is not understood. The typical process involved when using NETS consists of translating the problem into a format that uses input/output pairs, designing a network configuration for the problem, and finally training the network with input/output pairs until an acceptable error is reached.

NETS is written in C and can be executed on a variety of machines with no code changes. To date, NETS has been implemented on IBM personal computers and on Apple Macintosh, VAX, SUN, and HP 9000 computers. The memory requirements for NETS are 4 bytes per node and 4 bytes per connection. NETS was released in 1989.

This program was written by Paul T. Baffes for **Johnson Space Flight Center**. *For further information, Circle 81 on the TSP Request Card.*
MSC-21588

Mathematics and Information Sciences

Displaying TeX Files on Graphics Terminals

Previewing of printouts saves time and paper.

TeX is a public-domain typesetting program developed by Donald Knuth of Stanford University. It produces output in a device-independent form called DVI, which is then run through a device driver to obtain a printed copy. Often, it requires many iterations to change a TeX document into the desired version. Printing each version on a hard-copy device, such as a laser printer, to provide the feedback correction for the next iteration wastes time and paper. The DVIVIEW program previews output from TeX on graphics terminals. It enables the user to specify a range of pages to be viewed, to change the magnification of the document, and to view each page in seven different modes that affect the size and orientation of each page.

DVIVIEW uses vector-specified fonts speed-loaded into memory by use of a VMS system call. The fonts can then be used at a variety of magnifications. The fonts were originally drawn from the Hershey character set, and were heavily modified. The fonts most closely resembling the TeX fonts have been used. For some TeX fonts, a few esoteric characters are absent because they were not represented in the Hershey set and have not yet been designed. The terminals supported include VT100 and VT220 with Selanar boards installed; VT240, Tektronices 4010/4014, MacIntosh and Pericom; and Grinnell and Ramtek raster-frame-buffer display devices.

The DVIVIEW program is written in Pascal, FORTRAN, C, and Assembler. It has been implemented on a DEC VAX series computer under VMS. DVIVIEW was developed in 1985, and Version 2.04 was released in 1986.

This program was written by Peter J. Scott and David B. Coons of Caltech for **NASA's Jet Propulsion Laboratory**. *For further information, Circle 122 on the TSP Request Card.*
NPO-17296

Collection of Software for Computer Graphics

ARCGRAPH provides assistance in the generation, manipulation, and display of graphical data.

Ames Research Graphics System (ARCGRAPH) is a collection of software libraries and software utilities that assist researchers in generating, manipulating, and visualizing graphical data. In addition, ARCGRAPH defines a metafile format that contains device-independent graphical data. This file format is used with various computer-graphics-manipulation and -animation software packages at Ames, including SURF (COSMIC Program ARC-12381) and GAS (COSMIC Program ARC-12379).

In its full configuration, the ARCGRAPH Software System consists of a two-stage "pipeline" that can be used to put out graphical primitives. Stage one is associated with the graphical primitives (i.e., moves, draws, color, and the like) along with the creation and manipulation of the metafiles. Five distinct data filters make up stage one. They are as follows: (1) PLO, which handles all two-dimensional vector primitives, (2) POL, which handles all three-dimensional polygonal primitives, (3) RAS, which handles all two-dimensional raster primitives, (4) VEC, which handles all three-dimensional raster primitives, and (5) PO2, which handles all two-dimensional polygonal primitives.

Stage two is associated with the process of displaying graphical primitives on a device. To generate the various graphical primitives, create and reprocess ARCGRAPH metafiles, and obtain access to the device drivers in the VDI (Virtual Device Interface) software library, users link their application programs to GRAFIX library routines in ARCGRAPH. Both FORTRAN- and C-language versions of the GRAFIX and VDI libraries exist for enhanced portability within these respective programming environments.

The ARCGRAPH libraries were developed on a VAX computer running VMS. Minor documented modification of various routines, however, enables the system to run on the following computers: Cray X-

MP running COS (no C version), Cray 2 running UNICOS, DEC VAX running BSD 4.3 UNIX or Ultrix, SGI IRIS Turbo running GL2-W3.5 and GL2-W3.6, Convex C1 running UNIX, Amhdahl 5840 running UTS, Alliant FX8 running UNIX, Sun 3/160 running UNIX (no native device driver), Stellar GS1000 running Stellex (no native device driver), and an SGI IRIS 4D running IRIX (no native device driver). Currently with version 7.0 of ARCGRAPH, the VDI library supports the following output devices: VT100 terminal with RETRO-GRAPHICS board installed, VT240 using the Tektronix 4010 emulation capability, SGI IRIS Turbo using the native GL2 library, Tektronix 4010, Tektronix 4105, and Tektronix 4014. ARCGRAPH can be purchased separately or in a package (COSMIC Program COS-10020) containing GAS, ARCGRAPH, and SURF. ARCGRAPH version 7.0 was developed in 1988.

This program was written by Eric A. Hibbard of **Ames Research Center** *and George Makatura of Sterling Software. For further information, Circle 56 on the TSP Request Card.*
ARC-12350

Least-Squares Curve-Fitting Program

The user can specify the error of fit or the degree of the fitting polynomial.

The Least Squares Curve Fitting program, AKLSQF, easily and efficiently computes the polynomial that provides the least-squares best fit to uniformly spaced data. The program enables the user to specify the tolerable least-squares error in the fit or the degree of the polynomial. In both cases, AKLSQF returns the polynomial and the actual least-squares-fit error incurred in the operation. The data can be supplied to the routine either by direct keyboard entry or via a file.

AKLSQF produces the least-squares polynomial in two steps. First, the data points are least-squares fitted by use of the orthogonal factorial polynomials. The result is then reduced to a regular polynomial by use of Sterling numbers of the first kind. If an error tolerance is specified, the program starts with a polynomial of degree 1 and computes the least-squares-fit error. The degree of the polynomial used for fitting is then increased successively until the error criterion specified by the user is met. At every step, the polynomial as well as the least-squares-fit error is printed to the screen.

In general, the program can produce a curve fitting up to a 100-degree polynomial. All computations in the program are carried out under double-precision format for real numbers and under long-integer format for integers to provide the maximum accuracy possible.

AKLSQF was written for an IBM PC X/AT or compatible using Microsoft's Quick Basic compiler. It has been implemented under DOS 3.2.1 using 23K of RAM. AKLSQF was developed in 1989.

This program was written by Anil V. Kantak of Caltech for **NASA's Jet Propulsion Laboratory**. *For further information, Circle 112 on the TSP Request Card.*
NPO-17819

Newton/Poisson-Distribution Program

Newton's method is used to extract the Poisson parameter.

NEWTPOIS is one of two computer programs that make calculations involving cumulative Poisson distributions. Both programs, NEWTPOIS (NPO-17715) and CUMPOIS (NPO-17714), can be used independently of one another. NEWTPOIS determines the Poisson parameter for a given cumulative probability, from which one can also obtain percentiles for Γ distributions with integer shape parameters and percentiles for χ^2 distributions with even degrees of freedom. It can be used by statisticians and others concerned with probabilities of independent events that occur over specific units of time, area, or volume.

NEWTPOIS determines the Poisson parameter (λ); that is, the mean (or expected) number of events occurring in a given unit of time, area, or space. Direct calculation of the Poisson parameter becomes difficult for small positive values of the number of occurrences (n) and unmanageable for large values. NEWTPOIS uses Newton's iteration method to extract λ, taking successive estimations until some error term (ε) specified by the user is reached.

The NEWTPOIS program is written in C. It was developed on an IBM AT computer with a numeric coprocessor using Microsoft C 5.0. Because the source code is written using standard C structures and functions, it should compile correctly on most C compilers. The program format is interactive, accepting ε, n, and the cumulative probability of the occurrence of n as inputs. It has been implemented under DOS 3.2 and has a memory requirement of 30K. NEWTPOIS was developed in 1988.

This program was written by Paul N. Bowerman and Ernest M. Scheuer of Caltech for **NASA's Jet Propulsion Laboratory**. *For further information, Circle 147 on the TSP Request Card.*
NPO-17715

Flow-Control Unit for Nitrogen and Hydrogen Gases

A replaceable unit connects to a single manifold plate for ease of service.

Ames Research Center, Moffett Field, California

A gas-flow-control unit (see figure) that can be installed and removed as one piece replaces a system that included nine separately serviced components. The unit controls and monitors the flows of nitrogen and hydrogen gases. The unit is designed for connection via a fluid-interface manifold plate, reducing the number of mechanical fluid-interface connections from 18 to 1, and reducing the time required for maintenance.

Compared to the original system, the unit provides the following:

- A reduction in mass of 78 percent, from 29.8 to 6.5 lb (13.5 to 2.9 kg);
- A reduction in volume of 77 percent, from 440 to 100 in.^{3} (7,210 to 1,640 cm^3); and
- A reduction in power consumption of 91 percent, from 21 to 2 W.

This redesign is an engineering case study in techniques for increasing reliability, safety, and ease of maintenance, and for reducing weight, volume, and power consumption.

The unit performs valving, restriction of flow, and sensing of pressure during steady-state operation and intermode transitions. It controls reference and purge flows of nitrogen, production flow of nitrogen, vacuum, and vent flows. Operating gas pressures range up to 300 psia (2 MPa); the proof pressure is 750 psia (5 MPa).

The unit includes six two-state (open or closed) valves. Two motor-driven rotary camshafts operate the valves and provide the 14 desired combinations of valve states (out of the 64 possible combinations). Valve transitions take approximately 2 s. Positive-action valve lifters are used instead of return springs. Both visual and electronic valve-position indicators are provided. The valve-position indicator potentiometers are driven by gears to eliminate exposed electrical contacts.

A computerized process controller controls all functions. A manual override and a redundant battery power supply enable actuation of the valves when primary power is lost.

In 30 days of cyclic testing, which included 2,244 operating cycles and tank-filling sequences, the unit demonstrated consistent and accurate valve positioning, exhibited no forward valve leakage at operating pressures, and demonstrated the sensitivity, accuracy, and reliability of sensors of pressure and flow.

This work was done by B. J. Chang and D. W. Novak of Life Systems, Inc., for **Ames Research Center**. *For further information, Circle 149 on the TSP Request Card.*

Inquiries concerning rights for the commercial use of this invention should be addressed to the Patent Counsel, Ames Research Center [see page 16]. Refer to ARC-11772.

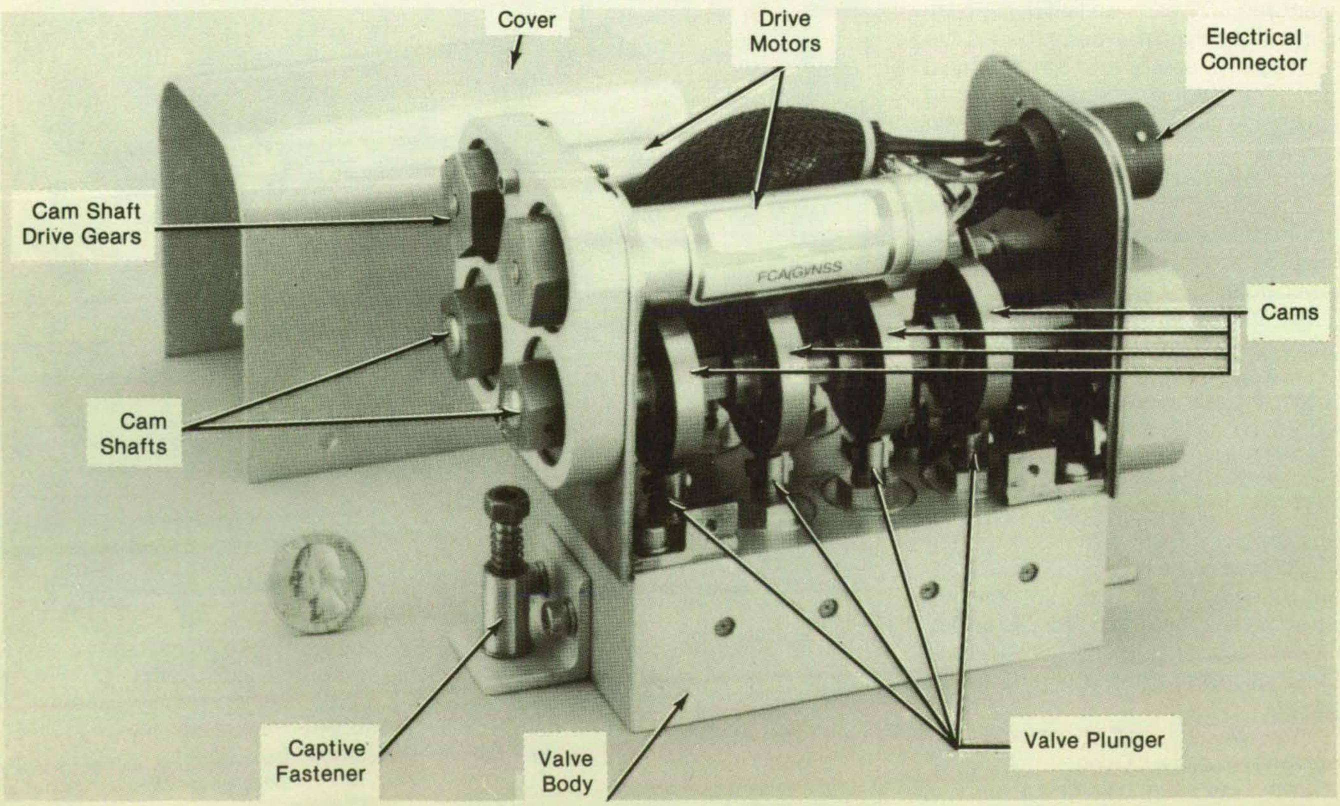

A **Gas-Flow-Control Unit** replaces a system that had nine separately serviced components.

Four-Wheel Vehicle Suspension System

Levers reduce tilt and provide three-point suspension of the chassis.

NASA's Jet Propulsion Laboratory, Pasadena, California

A four-wheel suspension system (see figure) uses a simple system of levers with no compliant components to provide three-point suspension of the chassis of a vehicle while maintaining four-point contact with uneven terrain. The system provides the stability against tipping of a four-point rectangular base, without the rocking contact to which a rigid four-wheel frame is susceptible. The new four-wheel suspension system is similar to the six-wheel suspension system described in "Articulated Suspension Without Springs" (NPO-17354), *NASA Tech Briefs* Vol. 14, No. 1, p. 60.

The elevation of each of the three body points from which the chassis is suspended is determined by the average of the elevations of two of the wheels. Thus, the suspension averages over the roughness of the terrain to some degree, and provides a smoother ride than would be obtained if the body were directly supported on three wheels located at the suspension points.

The four-wheel suspension provides a greater moment arm to resist overturning than does a three-wheel suspension of the same overall length and width. If a wheel sinks into a low spot in the terrain, the corresponding corner of the chassis sinks by a lesser amount. Thus, the tilt angle (and the attendant shift of weight that aggravates the situation) is less than occurs with a rigid four-wheeled frame that rocks at the same low spot.

This work was done by Donald B. Bickler of Caltech for **NASA's Jet Propulsion Laboratory**. *For further information, Circle 102 on the TSP Request Card.*
NPO-17407

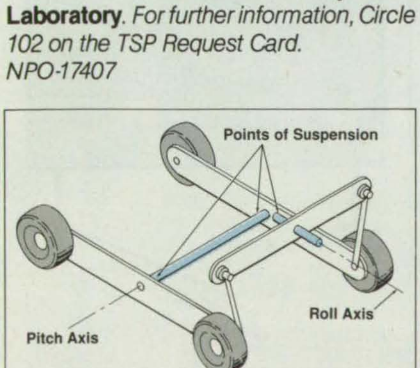

The **Four-Wheel Suspension System** uses levers to provide three-point suspension of the chassis (which is not shown) without the use of compliant members.

Reducing Aerodynamic Drag of Bluff Bodies

The simple addition of two panels eliminates as much as 80 percent of drag.

Langley Research Center, Hampton, Virginia

A new method has been found to reduce the aerodynamic drag of noncircular bluff bodies like road-transport vehicles. The drag on such bodies consists mainly of pressure drag. The flow fields are usually characterized by large wakes and periodic vortex shedding. Substantial amounts of energy can be required to overcome the high drag forces associated with such flow patterns.

The Reynolds number associated with small- and medium-size road vehicles usually falls in the subcritical (1.0 to 2.0×10^6) range. A popular conventional method of reducing the aerodynamic drag of noncircular bluff bodies at subcritical Reynolds numbers is the rounding of sharp corners, which can reduce drag by as much as about 50 percent. The new method consists of the installation of thin, flat panels on the forward side of the body, facing the airstream (see figure). This concept was developed using two-dimensional wind- and water-tunnel tests on a typical noncircular cylinder.

Panels of various sizes were employed, and their locations on the windward side were varied systematically. Detailed pressure measurements with Reynolds numbers in the subcritical range were performed in a low-speed, open-circuit wind tunnel having a maximum velocity of 115 ft/s (35 m/s). Measured surface pressures were integrated to obtain drag coefficients, and the test results were corrected for blockage effects. Systematic water-tunnel flow-visualization tests (Reynolds number = 6,000) were also carried out. Both the height and the locations of the panels have a strong influence on the drag coefficient. The maximum reduction of drag obtained in this investigation was 81.5 percent.

The panels produce a streamlining effect over the body. The width of the wake is reduced, and vortex shedding is greatly suppressed, as evidenced by flow-visualization photographs. This effect is caused by the transition in the flow consequent to separation at the panels and subsequent smooth reattachment to the body. The reattached flow continues along the surface but eventually separates. This type of flow pattern is typical of flow around bluff bodies at supercritical Reynolds numbers, and the associated drag coefficient is well

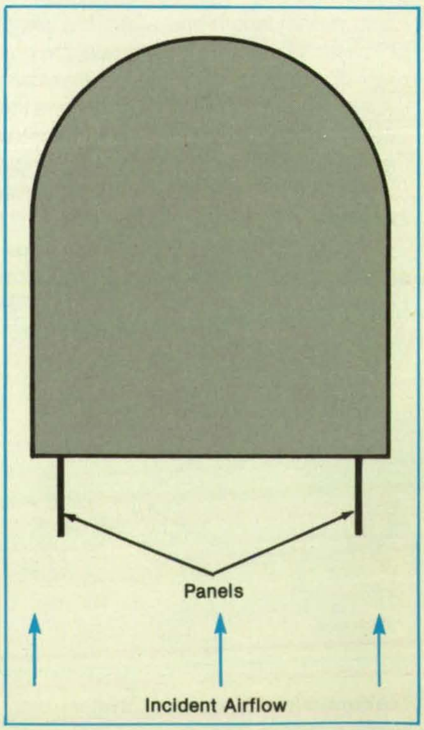

Thin, Flat Panels on the Front of a bluff body produce a streamlining effect over the body.

below the subcritical value. Thus, the panels have made supercritical flow possible at subcritical Reynolds numbers.

A novel feature of this technique is the generation of significant suction over the windward face. With panels on the windward face, the positive pressures are confined to the region bounded by the panels. Between the panels and the windward corners, high suction is produced by the sharp turning of the flow. These negative pressures contribute significantly to the reduction of drag and are responsible for the drastic fall in the drag coefficient.

The installation of flat panels is quite simple and should not require a major modification of the shape and size of the body to which they are attached. This technique could have significant potential for trucks, buses, automobiles, trains, surface ships, and submarines.

This work was done by Lawrence W. Taylor, Jr., of **Langley Research Center** *and Bandu N. Pamadi of Vigyan Research Associates. For further information, Circle 152 on the TSP Request Card.*

This invention is owned by NASA, and a patent application has been filed. Inquiries concerning nonexclusive or exclusive license for its commercial development should be addressed to the Patent Counsel, Langley Research Center [see page 16]. Refer to LAR-13768.

Ultrasonic Monitor To Determine Crack-Opening Load

Harmonics of acoustical signals are generated by cracks.

Langley Research Center, Hampton, Virginia

A new ultrasonic monitor to determine the crack-opening load in a compact tension specimen uses transducers to pass an acoustic wave across the crack region. Previous methods to determine the condition of full crack opening when the specimen is placed under load suffer from limitations imposed by the equipment used. For example, in the commonly used load-reduced-displacement and load-slope-change methods, an extensiometer is placed at a notch in a compact tension specimen. The extensiometer measures the opening of

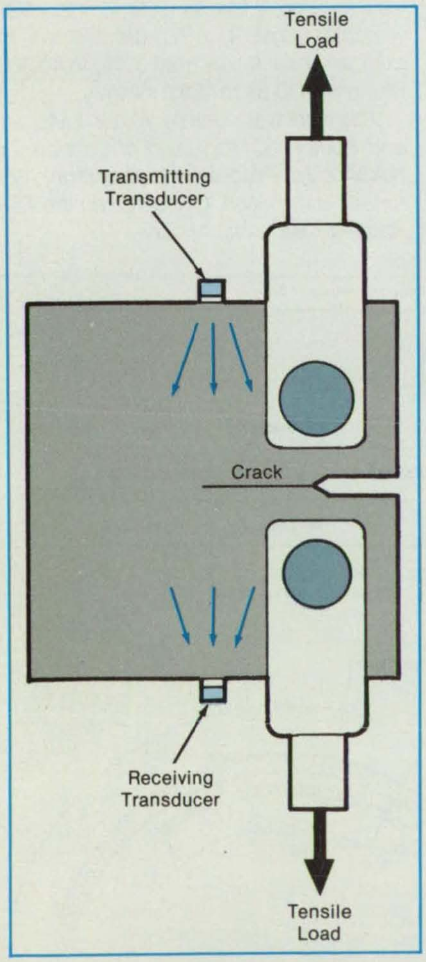

An **Acoustic Signal** is transmitted across the crack and partially mechanically "rectified" as the crack opens.

the notch and, hence, of the crack. By plotting the load against the reduced displacement or against the increase in slope, the load at which the crack is really open can be determined. One of the main disadvantages of these methods is that the signals from strain sensors, such as extensiometers, are noisy. Because of this, there is uncertainty in the determination of the crack-opening load.

The figure shows a compact tension specimen with a transmitting and a receiving transducer mounted so that the acoustic signal passes through the cracked region. A signal generator sends out a burst of a specific frequency. This signal is amplified and sent to the transmitting transducer, where it excites acoustic waves in the specimen. These waves propagate toward the cracked region. When the crack is closed, the acoustic signal is transmitted across the cracked region by the portions of the two surfaces that are in intimate contact. As the surfaces of the crack begin to separate, the signal propagates only during a portion of the cycle, giving rise to a mechanical "rectification" of the acoustic signal. The action of a barely opened crack is to enrich the relative proportion of the second harmonic of the signal.

The acoustic signal, as altered by the crack, travels to the receiving transducer, the output of which is processed by a receiver. The frequency is selected by tuning the receiver. The output of the receiver is monitored by an oscilloscope. The process is repeated at different loads while holding the received fundamental-frequency output fixed. The harmonic output is measured and plotted as a function of load.

One advantage of this technique is a definite improvement in signal-to-noise ratio. The process also possesses substantial immunity from the noise that is caused by the operation of the load frame and its associated parts. In addition to applications for the aerospace community, this monitor and concept clearly have general utility in the testing of materials and potentially in nondestructive evaluation of solid parts.

This work was done by William T. Yost of **Langley Research Center**. *For further information, Circle 150 on the TSP Request Card.*

This invention has been patented by NASA (U.S. Patent No. 4,823,609). Inquiries concerning nonexclusive or exclusive license for its commercial development should be addressed to the Patent Counsel, Langley Research Center [see page 16]. Refer to LAR-13889.

Probe Measures Fouling as in Heat Exchangers

Combustion deposits reduce the transfer of heat.

NASA's Jet Propulsion Laboratory, Pasadena, California

An instrument measures fouling like that on the gas side of a heat exchanger in a direct-fired boiler or heat-recovery system. Users can determine when fouling is approaching unacceptable levels so that they can schedule cleaning and avoid the decreased transfer of heat and increased drop in pressure that fouling causes. At the same time, users can avoid the cost of premature, unnecessary maintenance.

The probe is inserted through a port directly into the combustion gas stream. The instrument includes a conventional calorimeter apparatus and a heat-flux meter in a cylindrical probe (see figure). The calorimeter yields data on the average fouling in the system, and the heat-flux meter yields data on the fouling at its location. Both parts measure, in real time, the flow of heat through the wall of the probe; when the flow falls below a predetermined level, fouling has become excessive.

Products of combustion include, in addition to noncondensing gases, a variety of impurities — particles, drops of liquid, and condensible gases. As hot combustion products cool in a heat exchanger, some of the impurities deposit on the heat-transfer surface. The deposits — fouling — gradually accumulate and eventually seriously impair the transfer of heat. Users of fossil fuels have long recognized a need for a standardized gas-side fouling measuring device like that embodied in the new instrument.

The heat-flux meter is electron-beam-welded in a window cut into the probe and is in direct contact with the stream of gas. It consists of a sandwich of Chromel layers on an alloy, with electrical leads insulated with alumina tubes and sleeves of woven ceramic fiber. The electrical output of this thermopile represents the rate of flow of heat through the meter.

The calorimeter includes an inner air-feeding tube within the hollow cylindrical probe. Cool air enters through the inner tube and flows out through the annular gap between the inner tube and inner wall of the outer probe tube, absorbing heat from the wall as it does. A control system varies the rate of flow of air to maintain the inside temperature of the probe wall at a constant value. The average heat flux is calculated from the temperatures of the air at the inlet and outlet and the mass-flow rate of air.

Made of 304 stainless steel for strength and resistance to corrosion, the probe tube withstands severe thermal-shock and wide-ranging temperature cycles. In tests, the instrument operated over a wide range of conditions, including gas temperatures from 745 to 2,214 °F (396 to 1,212 °C), velocities from 9.91 to 27.7 ft/s (3.02 to 8.44 m/s), and heat fluxes from 3,440 to 40,800 Btu/(h•ft^2) (10.84 to 128.6 kW/m^2).

This work was done by Wilbur J. Marner and Kenton S. MacDavid of Caltech for **NASA's Jet Propulsion Laboratory**. *For further information, Circle 103 on the TSP Request Card. NPO-17322*

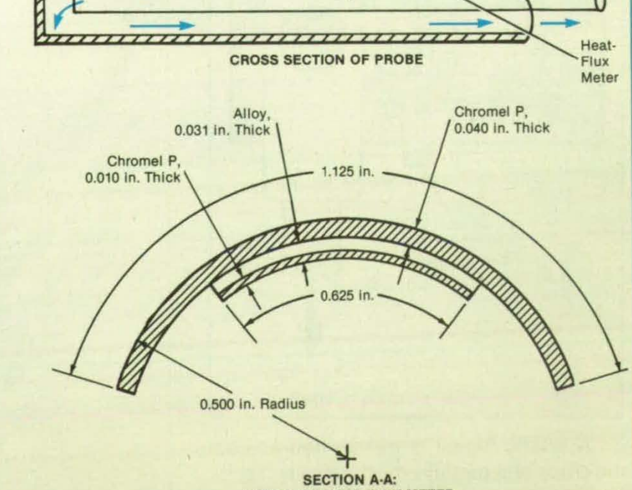

The **Heat-Flux Probe** includes a tube with an embedded meter in the outer shell. Combustion gases flow over the probe, and fouling accumulates on it, just as fouling would on a heat exchanger. The embedded heat-flow meter is a sandwich structure in which thin Chromel layers and a middle alloy form a thermopile.

Machinery

Hardware, Techniques, and Processes

Books and Reports

Piezoelectric Pushers Suppress Vibrations

Actuators are small, lightweight, and rugged.

Lewis Research Center, Cleveland, Ohio

Vibration-suppressing control systems that include piezoelectric actuators are undergoing development. These systems are intended primarily to enhance safety and prevent damage in rotating machinery by sensing and counteracting vibrations. The new systems should be particularly useful in suppressing unpredictable vibrations caused by changes in loads, losses of rotating components (e.g., turbine blades) and the consequent imbalances in rotors, and the ingestion of foreign objects into turbines.

The new systems offer several advantages over other active and passive vibration-suppressing systems. The piezoelectric actuators are compact, light in weight, and capable of operation at temperatures from cryogenic to above ambient. Unlike squeeze-film dampers, they do not require heavy, bulky lubrication systems. In contrast with active magnetic suspension systems, the piezoelectric systems require much simpler electronic control subsystems and do not require large electromagnet coils. Also unlike magnetic systems, piezoelectric systems continue to provide support and some passive damping even when electronic control subsystems or power supplies fail.

In a representative system (see Figure 1), the housing of a ball bearing that supports one end of a rotor shaft is supported by horizontal and vertical piezoelectric actuators. Eddy-current probes, which operate even when submerged in oil or cryogenic liquids, are used to sense the horizontal and vertical vibrations of the bearing and shaft. The outputs of the probes are sent to a relatively simple electronic control subsystem that includes only differentiators, filters, and amplifiers. The output of the control subsystem is fed to amplifiers that drive the piezoelectric actuators. If the control subsystem is designed properly with respect to electronic and mechanical stability and the vibrational modes and damping of the rotor, actuators, and supports, then the amplitudes and phases of the signals applied to the actuators should be such as to oppose the vibrations.

Figure 2 shows the results of an experiment in which one end of a rotor was suspended by a system like that of Figure 1. The rotor was deliberately unbalanced and operated at various speeds, including the critical speeds for the onset of instability caused by resonant coupling between rotations and vibrations. The plots show that with sufficient feedback gain, the amplitudes of vibrations at the critical frequency are reduced by factors of about 5. The plots also show that the increase in feedback gain increases the critical frequencies for instability. This suggests that one might vary the feedback gain during runup or coastdown to avoid instability as the speed passes through the critical range.

This work was done by Albert F. Kascak of **Lewis Research Center**. *For further information, Circle 146 on the TSP Request Card.* LEW-14927

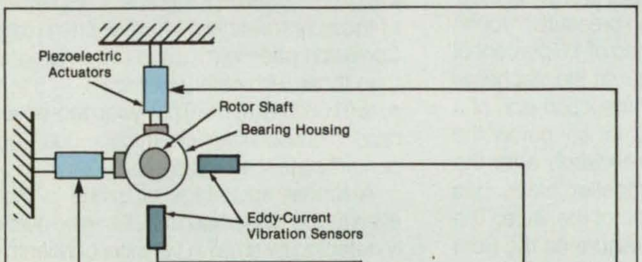

Figure 1. **Piezoelectric Actuators** driven by relatively simple feedback circuits suppress the vibrations of a rotating shaft..

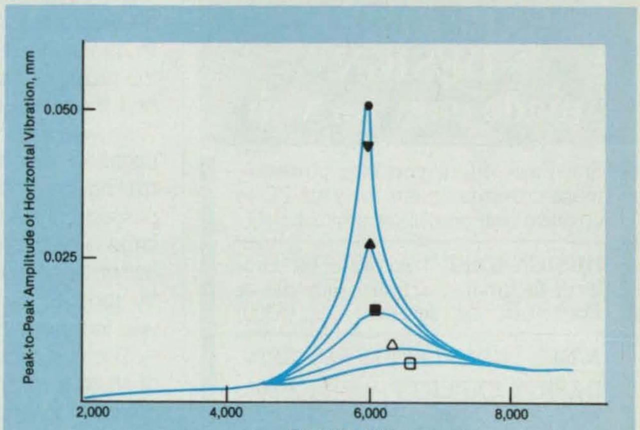

Figure 2. The **Vibrations of a Rotor** suspended as shown schematically in Figure 1 decrease as the feedback gain is increased. The peak near 6,000 rpm is caused by resonant coupling between rotations and vibrations.

Books and Reports

These reports, studies, handbooks are available from NASA as Technical Support Packages (TSP's) when a Request Card number is cited; otherwise they are available from the National Technical Information Service.

Rotor/Stator Interaction in a Diffuser Pump

Measurements of steady and fluctuating pressures are reported.

A report describes experiments designed to investigate interactions between blades of the impeller and both a vaned and vaneless diffuser (stator) in a diffuser pump. Although the pump was designed to handle oxygen at high pressure, water was used in the tests. Measurements of both steady and fluctuating pressures were taken at various locations on the diffuser vanes of the vaned diffuser and on the shroud walls of both the vaned and vaneless diffusers. The measurements were taken at various flow coefficients, shaft speeds, and radial gaps between the blades and vanes.

The fluctuations in pressure were found to be larger on the suction side than on the pressure side of a vane. The maximum fluctuations occurred in the vicinity of the leading edge and were of the order of magnitude of the total rise in pressure through the pump. For a radial gap of 1.5 percent of the radius of the impeller at the discharge end, the pressure on the suction side of a vane was found to fall locally below the upstream pressure immediately after the trailing edge of an impeller blade has passed the leading edge of the vane. The large fluctuations in pressure on the front half of the suction side of a vane decreased by about 50 percent when the radial gap was increased from 1.5 to 4.5 percent.

The steady and unsteady components of lift on a vane were computed from the pressure measurements at its mid height. The magnitude of the fluctuating component was found to be greater than that of the steady component, indicating that the vane is subject to a large periodic load. The magnitude of the fluctuating component and the ratio of magnitude of the fluctuating component to that of the steady component were found to decrease strongly when the gap was increased from 1.5 to 4.5 percent.

The fluctuations in pressure near the hub were found to be considerably larger than were those near the shroud. The fluctuations in pressure on the front of the shroud on the vaned diffuser were found to be considerably larger than were those on the vaneless diffuser. This indicated that close spacing of the impeller and the diffuser increased the unsteadiness of the flow.

This work was done by A. J. Acosta, C. E. Brennen, and of T. K. Caughey of Caltech for **Marshall Space Flight Center**. *To obtain a copy of the report, "Rotor-Stator Interaction in a Diffuser Pump." Circle 120 on the TSP Request Card.*

Inquiries concerning rights for the commercial use of this invention should be addressed to the Patent Counsel, Marshall Space Flight Center [see page 16]. Refer to MFS-26092

Ozone Treatment for Cooling Towers

Bacteria and scale are reduced without pollution and at low cost.

A report presents the results of a study of a cooling tower in which the water was treated with ozone instead of the usual chemical agents. Ozone is at least as effective as other chemicals in controlling the growth of microbiota in the tower and in the recirculation system and in inhibiting the deposition of scale in heat-exchanger tubes and water boxes.

Operating and maintenance costs with the ozone treatment are about 30 percent of those of treatment by other chemicals. Corrosion rates with ozone are no greater than those with other chemicals — 3 to 5 mils (0.08 to 0.13 mm) per year. Moreover, ozone, unlike other chemicals, does not contaminate the environment.

A further advantage of ozone is that, even though it is poisonous, it can be quickly detected by smell in very low concentrations. The U.S. Government has set a maximum-continuous-exposure level of 0.1 ppm, but ozone has a perceptible odor at 0.01 to 0.02 ppm. Coughing and eye-watering occur long before dangerous concentrations are reached.

The ozone treatment was tested in a tower that had a recirculating flow of 1,700 gal/min (107 L/s) and a total volume of 6,000 gal (22,700 L). An ozone generator produced 4.75 lb/d or 90 g/h. The ozone was introduced into the circulating water by an in-line contactor. Air was prepared for the generator by an oilless compressor and a dual heatless air dryer. The dryer reduced the dewpoint of the air to −60 °F (−51 °C) at a pressure of 15 psi (0.1 MPa). A previous study had shown that dry air was necessary for the efficient production of ozone; as the moisture in the source air increases, the concentration of N_2O_5 increases, and that of ozone decreases.

Before the ozone treatment, the average bacteria count on the cooling tower was 3×10^6. Within 3 weeks of the start of ozone treatment, the count had dropped to 200 to 300. The bacterial growth and scale on the slats of the tower became soft and loose, and much of it fell off. Furthermore, the treatment removed scale and prevented further deposition by reversing the calcium carbonate equilibrium toward the bicarbonate salt; by precipitating calcium ions and other metal ions as a fine, sandy deposit in the tower basin; or by a combination of these two effects.

This work was done by Rick Blackwelder of **Kennedy Space Center** *and Leroy V. Baldwin and Ellen S. Feeney of EG&G, Inc. To obtain a copy of the report, "The Investigation and Application of Ozone for Cooling Water Treatment," Circle 153 on the TSP Request Card.*
KSC-11384

Shock-Absorbing, Retractable Docking Mechanism

The new version would save considerable weight.

A brief report contains a description and drawings of a conceptual docking mechanism that would join the Space Shuttle orbiter with the proposed Space Station. The new mechanism would weigh about 1,500 lb (680 kg) less than the previous version.

According to the previous concept, the docking mechanism and the associated pressure-vessel docking module were to be carried aloft by the Space Shuttle on every trip to the Space Station. In the new conceptual system, the docking module would be left on the Space Station after assembly, and only the docking mechanism would be carried aboard the Space Shuttle.

The docking mechanism would include eight actuator/attenuators — legs equipped with shock absorbers and motor-driven ball screws. The actuator/attenuators would extend or retract to deploy or store a docking structure containing a docking ring, guides, latches, and a bulkhead adapter. The attenuators would reduce the loads of the docking impact by absorbing an approach stroke of 33 in. (0.83 m). The docking module on the Space Station would include a mating ring-and-guide structure and trunnions for the final tie.

This work was done by Jon B. Kahn of **Johnson Space Center**. *To obtain a copy of the report, "Actuator/Attenuator Docking Mechanism," Circle 10 on the TSP Request Card.*

This invention is owned by NASA, and a patent application has been filed. Inquiries concerning nonexclusive or exclusive license for its commercial development should be addressed to the Patent Counsel, Johnson Space Center [see page 16]. Refer to MSC-21327

Fabrication Technology

Hardware, Techniques, and Processes

Combined Borescope and Flushing Wand

This dual-purpose tool eliminates trial and error in removal of contamination.

Marshall Space Flight Center, Alabama

A proposed combination borescope/flushing wand would let an operator locate contaminant particles in narrow, intricate internal passages and simultaneously remove them. The tool would eliminate a repetitious trial-and-error procedure in which the operator first inserts a borescope into a passage, then, when contamination is found, removes the borescope and inserts a flushing wand, positioning its tip at the estimated location of the contamination. The operator must reinsert the borescope to check whether the contamination has been dislodged by a jet of water from the wand. If not, the operator must repeat the flushing operation.

With the new tool, the operator would observe the contamination continuously and would know the position of the tip of the flushing wand. The operator would see the contamination being flushed away.

The tool would include a tube containing pressurized flushing water from a pump, a tube containing filtered shop air, optical fibers from a source of light to illuminate the contamination, and optical fibers to a video camera and monitor to display the contamination and the flushing operation (see figure). The operator would apply the shop air to a passage immediately after flushing it; the jet of air would dry the passage so that residual flushing water could not obscure the view.

This work was done by Mike J. Trost of Rockwell International Corp. for **Marshall Space Flight Center**. *No further documentation is available.*
MFS-29581

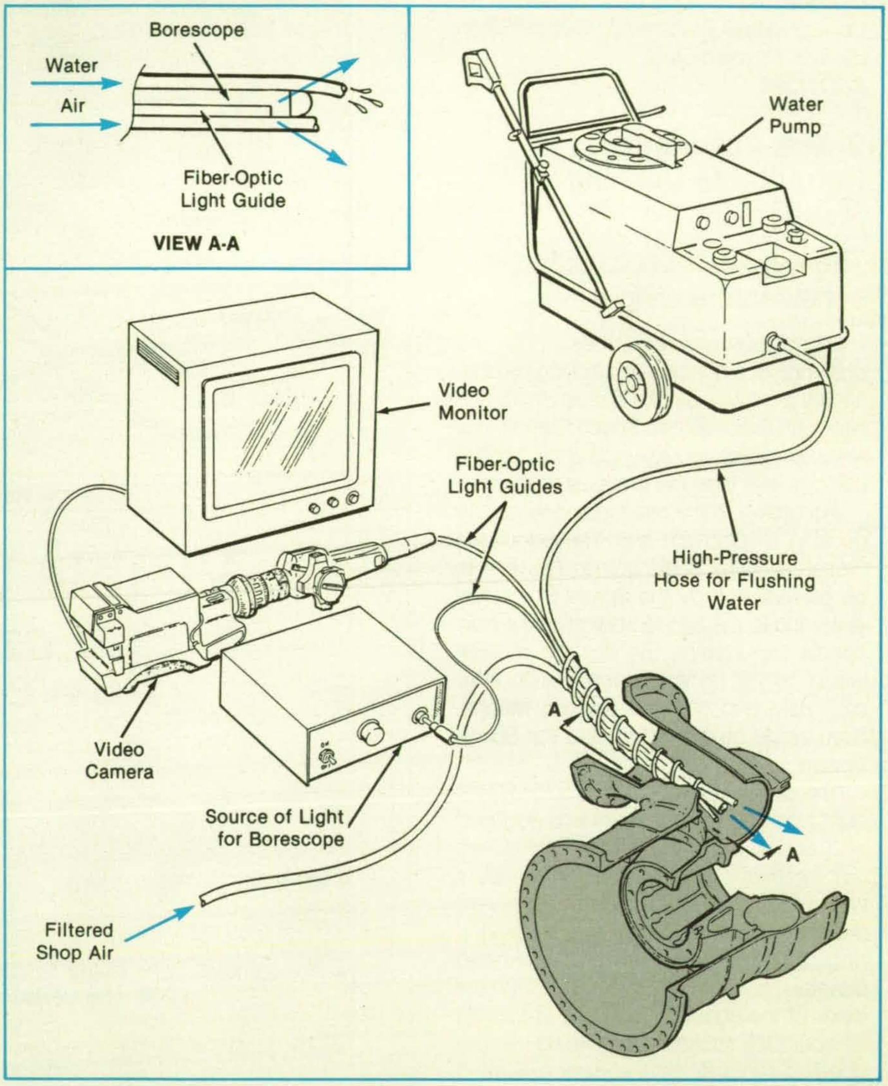

A Video Monitor Would Display a view of contamination in an internal passage, while it is being flushed away. The operator would see immediately whether the contamination has been removed. A plastic isolator would protect the borescope. For further protection and for reduction of blurring, the borescope would be slightly recessed from the tip of the wand.

Grinding Away Microfissures

Any of a variety of abrasive tips is attached to a small motor.

Marshall Space Flight Center, Alabama

A treatment similar to dental polishing can be used to remove microfissures from metal parts without reworking adjacent surfaces. The treatment was devised to eliminate spurious marks on welded parts. Such marks could give rise to false indications of cracks during penetrant-dye inspections. In some cases, the marks can be caused by the spurs of rotary files used to remove excess material.

As shown in the figure, an abrasive tip on a dental drill or other small rotary power tool is applied to the spot to be treated. When treating an inaccessible area or a surface of complicated shape, the tip should be a dental rubber abrasive-holding cup filled with a polishing compound or other abrasive that is compatible with the workpiece. The rubber cup conforms to the surface of the workpiece. When the spot to be treated is more accessible, the tip could be a grinding stone, wire brush, rubber/abrasive composite, or Scotch Brite (or equivalent).

This work was done by Gary N. Booth and R. Michael Malinzak of Rockwell International Corp. for **Marshall Space Flight Center**. *No further documentation is available.* *MFS-29566*

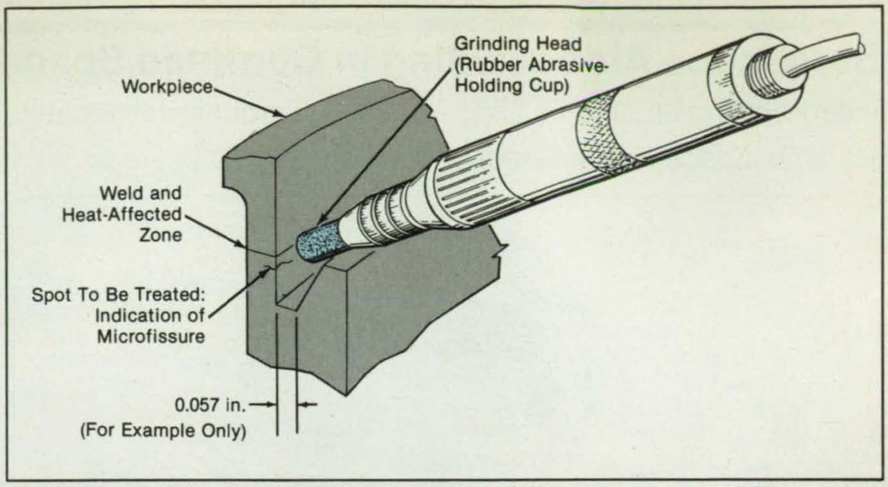

An **Abrasive Tip Driven by a Small Motor** is used to grind the spot to be treated. The configuration of the grinding head must be compatible with the configurations of the motor and workpiece.

Positioning X-Ray Film by Balloon

Film is placed securely against a wall, without wrinkles.

Marshall Space Flight Center, Alabama

An inflated balloon holds x-ray film against the inside wall of a duct for radiographic inspection. The balloon ensures that the film is positioned in contact with a welded joint far along the duct from the opening through which it is inserted, so that a clear x-ray image of the joint can be obtained.

Heretofore, films with magnets inside ducts were maneuvered into position by use of magnets outside the ducts. This method is tedious and time-consuming and positions the film only approximately. Moreover, the film can easily become wrinkled and disoriented.

In the new method, the film is rolled around the deflated balloon before being inserted in the duct (see figure). The film is clamped at the end of a segmented flexible cable and fed with the balloon into the duct to the predetermined point at which the inspection will be made, as indicated by the length of cable paid out. The balloon is inflated through a long tube from the outside, pressing the film against the wall. The film is also maintained in the same orientation with which it is inserted in the duct.

This work was done by Frederich Windbiel and Kamal Guirguis of Rockwell International Corp. for **Marshall Space Flight Center**. *No further documentation is available.*

Inquiries concerning rights for the commercial use of this invention should be addressed to the Patent Counsel, Marshall Space Flight Center [see page 16]. Refer to MFS-29588

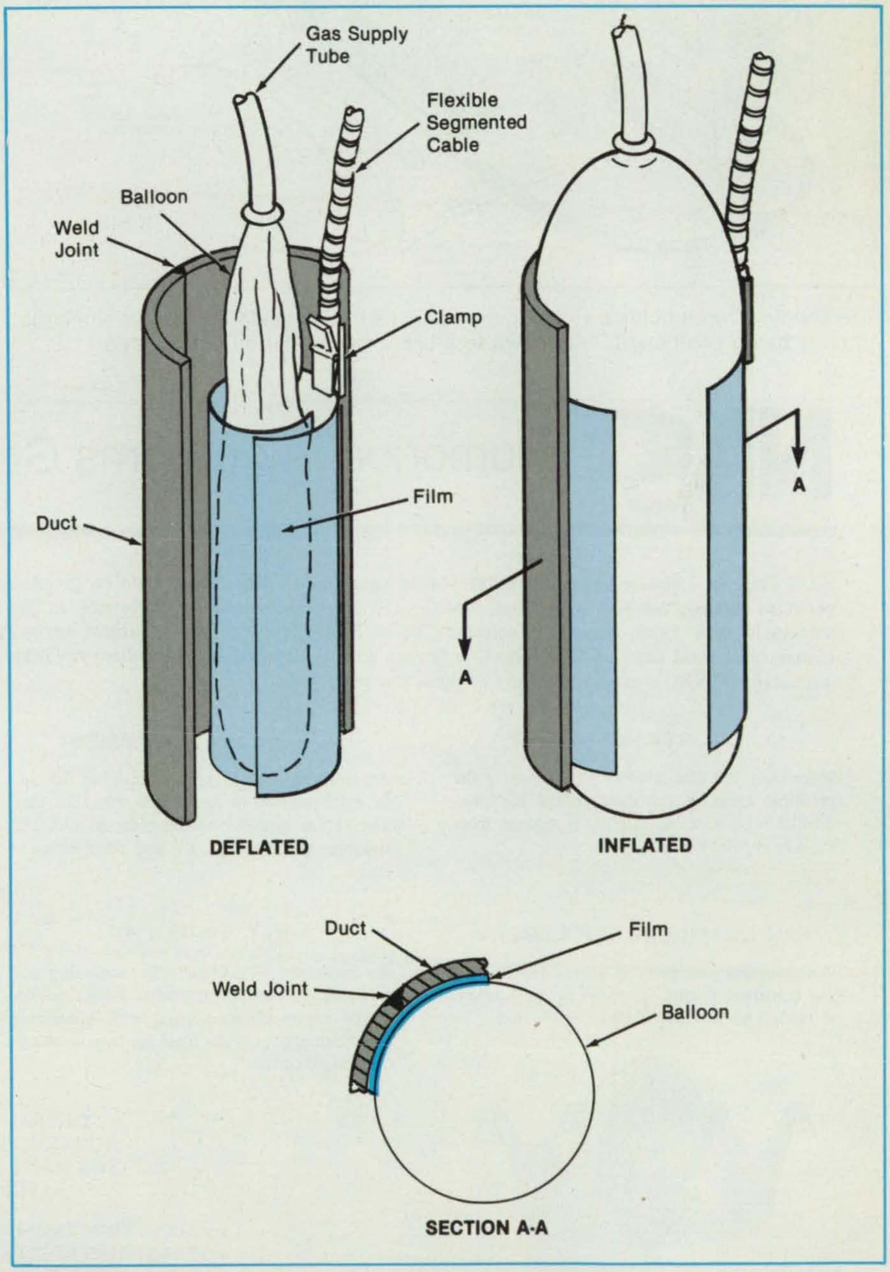

The **Deflated Balloon Easily Passes** with rolled film to the inspection site in duct. When inflated, the balloon secures the film against the inner wall of the duct, where it is exposed to x-rays generated outside the duct.

Borescope Aids Welding in Confined Spaces

Video viewing eliminates blind welding in inaccessible locations.

Marshall Space Flight Center, Alabama

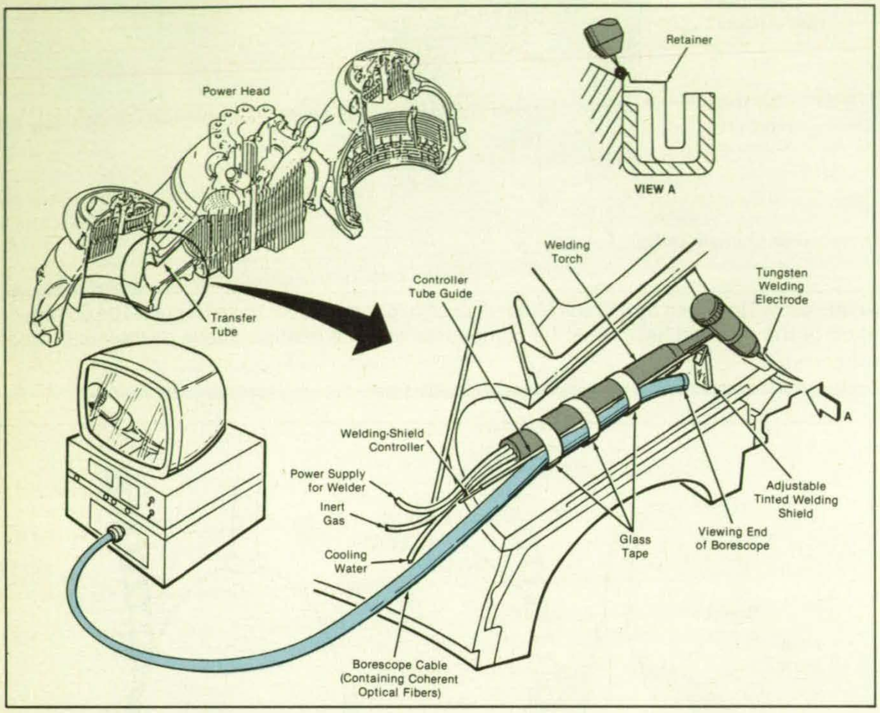

The **Welding Torch** holds a video borescope. The tinted shield is tilted up while the torch is being positioned, then down to block excess light during welding.

A welding torch holds a video borescope to give its human operator a view of a workpiece in an enclosed space. The operator sees a clear, magnified image on a video monitor and can manipulate the torch accordingly, despite the visual obstruction presented by the enclosure.

The video torch was developed for welding a retainer to a support in the main injector of the Space Shuttle main engine. Previously, the operator could not see the rings and had to weld them blindly.

The video borescope is attached to the body of the tungsten arc-welding torch with glass tape (see figure). The operator grasps the torch and places it in the enclosed space near the joint to be welded. When the tip of the torch is in position, as seen on the video display, the operator flips a small tinted shield in front of the video borescope and strikes the arc. The shield protects the video borescope from the excessive glare of the arc so that the operator can continue to observe the weld. The use of the video system reduces welding time by 50 percent. It also increases the quality of the weld substantially.

This work was done by Eddie Carrasco and Ronald A. Acuna of Rockwell International Corp. for **Marshall Space Flight Center**. *No further documentation is available.* *MFS-29635*

Balancing Loads Among Parallel Data Processors

A heuristic algorithm minimizes the amount of memory used by a multiprocessor system.

Lyndon B. Johnson Space Center, Houston, Texas

Algorithms may distribute the load of many identical, short computations among multiple parallel digital data processors, each of which has its own (local) memory. Each processor operates on a distinct and independent set of data in a larger shared memory. As an integral part of the load-balancing scheme, the total amount of space used in the shared memory is minimized. Possible applications include artificial neural networks or image processors for which the "pipeline" and vector methods of load balancing may be inappropriate.

TERMS: A **process** is a computation and/or other operation upon **total memory**, which is the sum of all shared memory, both source (read but not changed) and **target** [changed by some process(es)]. A memory **partition** is a disjoint subset of either source or target memory (but not both) sharing no members with any other subset. A **partition threshold** is some number of partitions that represent the current maximum memory size allowed for a **processing set**, or collection of processes. **Load** is a number proportional to the time it takes to complete the process. The desired load is the **balance load**, equal to the sum of all loads divided by the number of processing units.

The first half of the algorithm (see figure) collects processes into processing sets. First, a two-dimensional array or "grid" of the shared memory is created, with source memory on one axis and target memory on the other. Next, values are placed at each intersection of source/target-memory pairs to represent the load (or section of load) of the process that operates upon that source/target pair. Then source and target memories are divided on the grid, creating rectangular regions with one source and one target partition, so that no process is spread across two regions. Regions are then sorted in terms of the sum of the loads included within their bounds. Any regions exceeding the balance load are split into equal parts, each with the same source/target-partition pair and no more than the desired balance load.

The second half of the algorithm performs mergers of processing sets by combining one processing set at a time with another set that can take on some or all of the load. This is repeated until the total number of sets equals the number of processing units. First, the smallest processing set, **S**, is chosen. "Merge candidates" are found among all other processing sets that have loads smaller than the balance load. Any merge that would exceed the partition threshold is discarded. Of the remaining candidates, the one that has the most partitions in common with **S** is chosen as the target for merge.

Execution of the algorithm is very quick when a small number of partitions is used (the first half of the algorithm runs in linear time; the second half runs in constant time). Thus the second half of the process can be repeated several times, each with a different starting partition threshold, and the "best" (or lowest threshold) solution chosen. Because the algorithm uses such a simple merging heuristic, it is not possible to generalize an ideal starting partition threshold. Making multiple runs of the algorithm is the only way to obtain the best result.

This work was done by Paul Thomas Baffes of **Johnson Space Center**. *For further information, Circle 55 on the TSP Request Card.*

This invention is owned by NASA, and a patent application has been filed. Inquiries concerning nonexclusive or exclusive license for its commercial development should be addressed to the Patent Counsel, Johnson Space Center [see page 16]. Refer to MSC-21348.

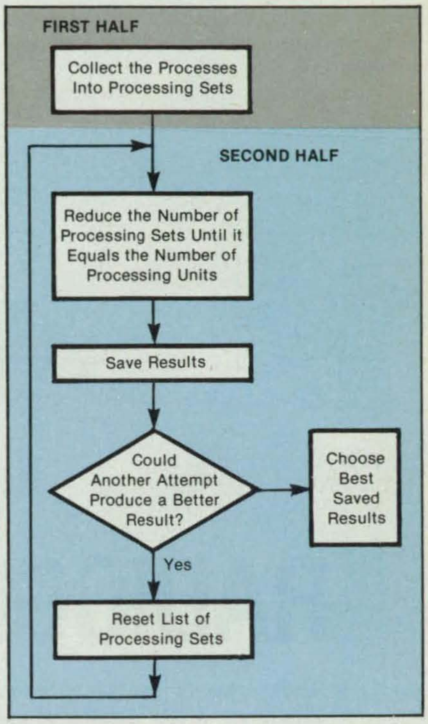

The **Main Steps of the Algorithm** can be considered to be divided into a first half and an iterative second half. The result of the iteration is a balancing of computational load (including memory) among the processors of a parallel multiprocessor system.

Spectral Analysis of Linear, Shift-Invariant Interpolants

A method provides quantitative evaluation of interpolation techniques.

Langley Research Center, Hampton, Virginia

A method of analysis provides a quantitative measure of the reconstruction and interpolation performances of linear, shift-invariant interpolants. The criterion of performance is based upon the mean-square error of the difference between the sampled and reconstructed functions. The analysis is applicable to reconstruction algorithms used in the processing of signals and images and to many of the types of interpolants used in numerical analysis, computer-aided design, and computer graphics. When formulated in the frequency domain, the mean-square error clearly separates the contribution of the interpolation method from that of the sampled data and provides a rational basis for selecting an "optimal" interpolant; i.e., one that will minimize the mean-square error.

The method has been applied to a selection of frequently used interpolants: parametric cubic and quintic Hermite splines, exponential and ν splines (including the special case of the cubic spline), parametric cubic convolution (PCC), Keys fourth-order cubic, and a cubic with a discontinuous first derivative. The method is applicable to band-limited data sampled at fixed intervals in which the sampling rate exceeds the Nyquist frequency and the reconstruction is linearly dependent on the sample values. The performances of these techniques have been analyzed for the case in which no a priori knowledge of the frequency spectrum of the sampled function is assumed other than that of band-limited sufficient sampling.

It was found that with proper identification of parameters, interpolation with parametric cubic Hermite splines (developed for computer graphics and curve fitting) is identical to reconstruction with parametric cubic convolution (a family of algorithms for the reconstruction of signals and images). Of all the interpolants investigated, the cubic spline provides the best performance. In general, the addition of tension to a cubic spline, in the form of either an exponential or ν spline, increases the mean-square error. Fifth-degree Hermite splines showed no advantage over third-degree Hermite splines. However, a parametric quintic spline possesses two parameters that might be selected to tailor an optimal interpolant for a specific application. Of the reconstruction algorithms studied, Keys cubic exhibited the best performance, as expected, followed by the very similar cubic Hermite/PCC with $\alpha = -1/2$, and a cubic with a discontinuous first derivative.

This work was done by Donald L. Lansing and Stephen K. Park of **Langley Research Center**. *For further information, Circle 59 on the TSP Request Card. LAR-13751*

Truncation of Images for Correlation

Correlation could be performed on a relatively small computer.

NASA's Jet Propulsion Laboratory, Pasadena, California

As part of a proposed method for processing video images in slowly changing scenes, renditions of complicated objects

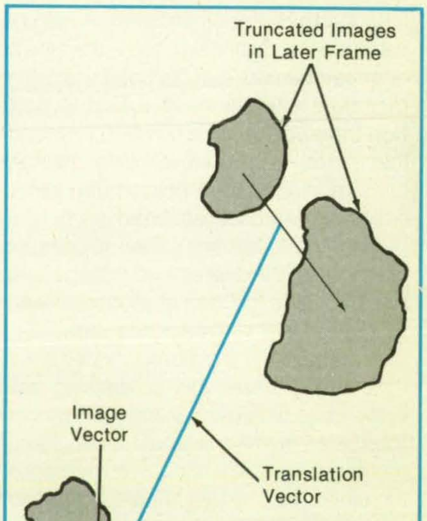

Figure 1. A **Vector Between Contours** in a truncated image translates to a new position in a subsequent frame. The translation vector is proportional to the velocity of the object(s) represented by the contours.

would be truncated to points, lines, polygons, or other simplified geometrical objects. The truncated images would be processed by image-correlating algorithms to extract information; for example, to recognize features and to track the displacements of features in subsequent image frames to determine velocities. The principal advantage of the truncated images is that they would entail the correlation of far fewer data than the original images would. Thus, correlations could be performed on relatively small computers or, alternatively, much more rapidly on larger computers.

The image recorded on a charge-coupled-device or other suitable camera during a frame period would first be subjected to a thresholding operation so that up to three salient features could be selected for further processing. The selected features would then be turned into contours when the surviving picture elements form an assembly of closed lines, or else would be represented by straight lines connecting pairs of end picture elements when the surviving picture elements do not form closed lines. Next, the positions of the centroids of the areas enclosed by the contours and/or the midpoints of the straight lines would be calculated and recorded. Computations for further truncation and use of the already truncated images would then begin.

Figure 1 illustrates an example of such further processing of a truncated image that consists of contours of two objects. First, a straight line would be constructed between the centroids enclosed by the two contours. This line would be a vector of known length and direction. The translation and rotation of the vector to new positions and orientations in subsequent image frames could be used to compute the velocity of relative motion between the camera and the two objects represented by the contours.

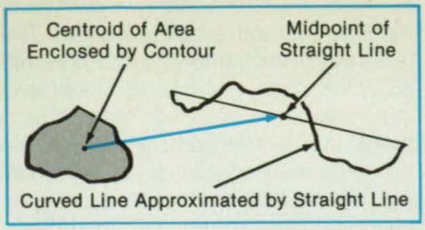

Figure 2. A **Curved Line Is Represented by a Straight Line**, and its position is represented by the midpoint of the straight line.

Figure 2 illustrates an example in which an open line is represented by a straight line between its end points and a closed contour is also present. In this case, the vector used to detect motion would be drawn from the centroid of the area enclosed by the contour to the midpoint of the straight line.

This work was done by Katsunori Shimada of Caltech for **NASA's Jet Propulsion Laboratory**. *For further information, Circle 124 on the TSP Request Card.*

Inquiries concerning rights for the commercial use of this invention should be addressed to the Patent Counsel, NASA Resident Office-JPL [see page 16]. Refer to NPO-17847.

Laws for Stable Control of Orientation

Tradeoffs can be made among complexity, performance, and information available for mathematical models.

NASA's Jet Propulsion Laboratory, Pasadena, California

A class of globally stable laws for control of the orientation of a rigid body has been established. This development has significance for the reorientation, pointing, and slewing of airplanes, helicopters, spacecraft, and rigid objects held by single or multiple robot arms.

In most approaches that have prevailed heretofore, attitude dynamics are linearized, and a three-parameter local representation of orientations is used. However, because there are no globally nonsingular three-parameter representations of orientation, planning of paths becomes complicated, and admissible attitudes can be seriously constrained. This undesirably limits the allowable motions for purely mathematical reasons that have nothing to do with what is physically possible. In contrast, the new approach involves the use of the globally nonsingular four-parameter unit-quaternion (Euler-parameter) representation. The attitude dynamics are described by the nonlinear Euler equation together with the nonlinear kinematic equations, which relate a representation of attitude to the angular velocity of the body.

A second unique feature of the new approach is the use of a suitable energy-motivated Lyapunov function to analyze stability. In the case of nonadaptive tracking control, the candidate Lyapunov functions consist of three basic terms: the kinetic energy of the error (the kinetic energy with the angular-velocity error substituted for the angular velocity), the desired potential energy, and a product term of angular momentum and some measure of the position error. An analysis based on the use of this Lyapunov function results in global convergence of the error to zero. The product term is chosen small enough that the Lyapunov function is positive definite. The sole purpose of this term is to establish local *exponential* convergence of the error to zero and facilitate generalizations to adaptive control. Without the product term, global stability can still be deduced, through one then needs to use the invariance principle, and neither the local exponential rate of convergence nor the generalization to adaptive control is possible.

This theoretical framework opens the gateway to analysis of robustness with respect to errors in parameters of mathematical models, noise in signals, and such external disturbances as friction. It also makes possible the enhancement of robustness by use of a sliding-mode type of modification and adaptive control. The generality of this framework is demonstrated by the range of stabilizing control laws that have been obtained, ranging from model-independent, proportional/derivative (PD) tracking control, to model-dependent tracking control, and finally to adaptive control. The tradeoff among these control laws with respect to complexity of the controllers, achievable performances, and required a priori information for mathematical models can be quantified rigorously.

This work was done by Kenneth K. Kreutz of Caltech and John Ting-Yung Wen of Rensselaer Polytechnic Institute for **NASA's Jet Propulsion Laboratory**. *For further information, Circle 108 on the TSP Request Card. NPO-17790*

Averaging Sampled Sensor Outputs To Detect Failures

Fluctuating signals are smoothed by taking consecutive averages.

Marshall Space Flight Center, Alabama

A sampling-and-averaging technique processes noisy or otherwise erratic signals from a number of sensors to obtain indications of failures in a complicated system that contains the sensors. Though the technique was devised to detect faults in the Space Shuttle main engine, the underlying concept could prove useful in monitoring automotive engines, chemical-processing plants, powerplants, and other systems in which the outputs of sensors contain noise or other fluctuations in the measured quantities.

The output of each sensor is sampled periodically (e.g., every few milliseconds), and an average is computed from samples taken during an averaging period of, say, 80 to 100 ms. This sampling-and-averaging procedure is repeated during subsequent sampling periods, providing a sequence of averages. One can also multiply each average by the averaging period to obtain the integral average, which is an approximation of the integral of the signal during the averaging period. In the average or integral average, noise and other short-term fluctuations are suppressed more than are the more-smoothly-varying components of the signal. In effect, the sequence of averages or integral averages is a sequence of samples of a smoothed or low-pass-filtered version of the signal.

The sequence of averages or integral averages is recorded. The standard deviation of all the averages or integral averages in the sequence from the beginning of operation up to the present moment is computed. At the beginning of a nominally-steady-state operating condition, "a safety band" of three standard deviations computed from past measurements is placed around the average of the averages in the sequence from past measurements. This precomputed "safety band" is used for a specified period (e.g., 2 seconds). Thereafter, the integral average is updated every averaging period to incorporate the latest average or integral average. If the most recent average or integral average(s) from a given sensor falls outside its most-recently-computed safety band during a specified number of consecutive averaging periods (or if this occurs for all sensors in a specified group during one or more consecutive averaging periods), then an alarm can be given.

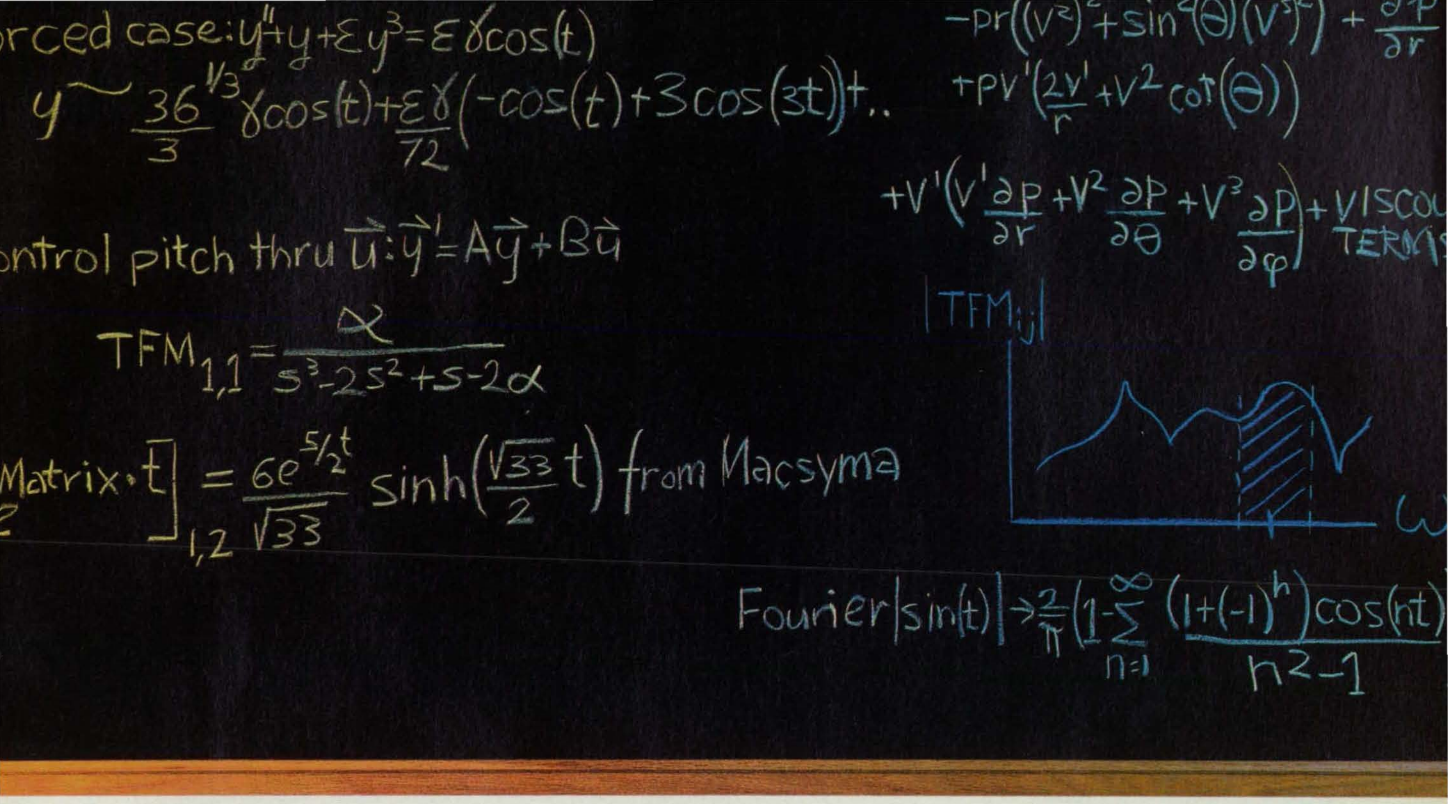

Macsyma®...

the most powerful math software in the world of workstations, mainframes, *and* PCs*

Now available on SPARC-stations

When it comes to solving complex symbolic and numerical math problems, there's no substitute for power. Other math packages claim they have it, but when it comes to the crunching they can't do much more than pretty graphics.

MACSYMA has the power you need.

With MACSYMA, you can easily tackle math modeling problems that other packages just sit and stare at. You can perform complex symbolic, numerical, and graphical calculations automatically — in applications ranging from plasma physics to aeronautics, from economics to fluid mechanics and more — right at your desk. Calculations such as differential and integral equations, Laplace and Fourier transforms, vector and tensor calculus...with greater depth and accuracy than any other software.

And MACSYMA is getting more powerful all the time, with dozens of new features to simplify even the most complex math.

But there's one thing about MACSYMA that isn't complex — using it. You can get right to work using our On-line Help and Quick Reference Card — without even opening a book.

Call 1-800-622-7962 (in Massachusetts, 617-221-1250.)

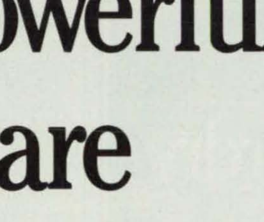

Circle Reader Action No. 524

symbolics Inc.

Macsyma Division

8 New England Executive Park East
Burlington, MA 01803 USA

*including Sun-4, Sun-3, Symbolics and Apollo workstations, VAXes and 100% IBM-compatible 386/DOS-based PCs.

This sampling-and-averaging technique can be used under both transient and steady-state conditions. In contrast, prior sampling-and-averaging techniques could not handle transients. An additional advantage of the new technique is that a continuous increase or decrease in a sequence of averages or integral averages indicates a trend that could lead to a failure. Such a trend is less sensitive to fluctuations in the signal than are the averages themselves.

This work was done by Hagop V. Panossian of Rockwell International Corp. for **Marshall Space Flight Center**. *No further documentation is available.*
MFS-29719

Books and Reports

These reports, studies, handbooks are available from NASA as Technical Support Packages (TSP's) when a Request Card number is cited; otherwise they are available from the National Technical Information Service.

Organizing Performance Requirements for Dynamical Systems

A top-down analysis facilitates possible engineering compromises.

A paper describes a methodology for establishing performance requirements for complicated dynamical systems. The methodology uses a top-down approach. In a series of steps, it makes connections between the high-level mission requirements and the lower-level functional performance requirements. The steps include the following:

1. Identification of system activities,
2. Identification of the activity-derived state-vector elements associated with each activity,
3. Definition of state-maintenance functions, and
4. Affirmation of the need for performance requirements for each state-vector-maintenance action.

Because the methodology follows a top-down structure in a sequence of branch points — that is, a tree — traceability is a built-in feature. Connections between components and mission requirements are established in the process of laying out requirements. For a given system, a preliminary layout of performance requirements could be established in a set of data. Automation would then enable a computer to scan the data and answer questions about which component will limit the performance of the system or which mission activity will impose the most-difficult design requirements on a given component.

The top-down structure provides for a systematic delineation of elements that might accommodate design compromises. Trades at the component level can be identified by systematic pairings of components. Generally, a potential trade will exist between hardware and software components within a subsystem function. At the subsystem-function level, trades can be made among the requirements for each function. Trades also exist between levels, between components and subsystems, and between subsystems and missions.

The methodology aids the evolution of a system design. After the first complete set of requirements has been established, design-trade studies can be done, and components can be specified. The specified system can then be mapped upward by simulation from components to the performance of the mission, in a process that is essentially a mirror image of the decomposition of the complete system requirements.

This work was done by Harvey L. Malchow and Steven R. Croopnick of The Charles Stark Draper Laboratory, Inc., for **Johnson Space Center**. *To obtain a copy of the report, "A Methodology for Organizing Performance Requirements for Complex Dynamical Systems," Circle 109 on the TSP Request Card.*
MSC-21235

Mathematical Model of Nerve/Muscle Interaction

The model is coarsely homeomorphic to a biological system.

NASA's Jet Propulsion Laboratory, Pasadena, California

The Phasic Excitation/Activation (PEA) mathematical model simulates the short-term nonlinear dynamics of the activation and control of a muscle by a nerve. The model, which includes electronic and mechanical elements, is based on published experimental studies of nerve/muscle interactions. It is homeomorphic at the level of its three major building blocks, which represent the motoneuron, the dynamics of activation of muscle, and the mechanics of the muscle, respectively.

The motoneuron block is a highly simplified submodel that reproduces the important short-term dynamical phenomena. This block consists of a transresistance amplifier, high-pass filter, and voltage-to-frequency converter (see figure). Its output is a series of unit-value action-potential impulses that exhibit a decline in firing rate (adaptation) with constant-current input.

The activation-dynamics block, which is not homeomorphic in its details, includes a pulse-frequency-to-voltage converter, a unit that implements a piecewise-linear gain-versus-voltage function, a nonlinear resistor-and-capacitor low-pass filter, and a multiplier. This block multiplies the effects of the action-potential impulses to produce an increase, dependent upon the intervals between the impulses, in the force produced by the muscle in response to each impulse in the sequence. This interval-dependent enhancement of force is known to workers in the field as the "catch-like effect."

The muscle-mechanics block represents a second-order nonlinear model of a single muscle removed from a sixth-order nonlinear model of a joint movement. This block contains a subblock that represents a first-order model of activation and deactivation. The output of the subblock represents a tension proportional to a low-pass-filtered version of the input. The muscle force is coupled to the load through a series elastic element, represented by a spring, which may be nonlinear. The internal viscosity of the muscle, which diminishes the force it can apply, is represented by a nonlinear dashpot.

The PEA model was developed to extend a previously successful modeling strategy to "early" dynamics; that is, those involving times less than one-hundred milliseconds. The addition of the motoneuron and "catch-effect" blocks is intended to help develop an understanding of the control of the fastest voluntary movements.

This work was done by Blake Hannaford of Caltech for **NASA's Jet Propulsion Laboratory**. *For further information, Circle 5 on the TSP Request Card.*
NPO-17816

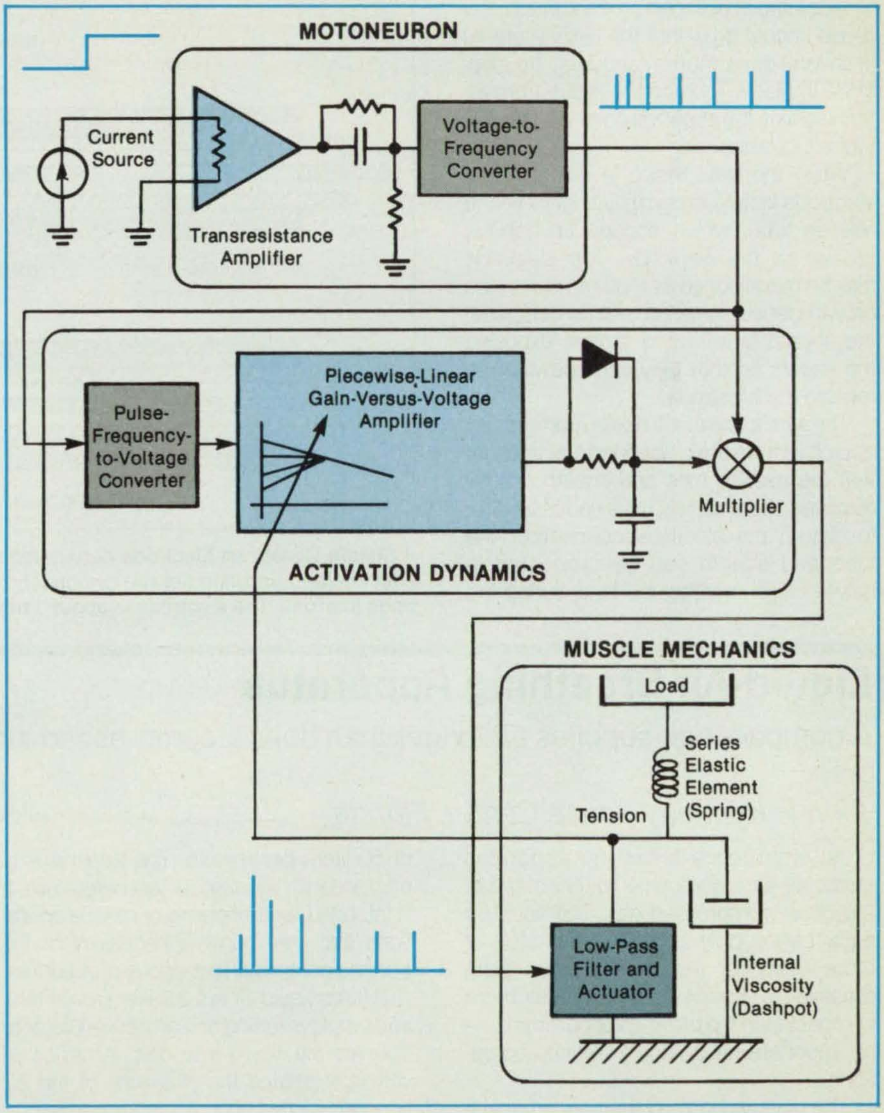

The **Phasic Excitation/Activation** model consists of three blocks, the outputs of which approximate aspects of the control of a muscle by a motoneuron.

Implantable Electrode for Critical Locations

Tissue should grow readily around a fuzzy covering.

NASA's Jet Propulsion Laboratory, Pasadena, California

An implantable electrode is expected to hold itself in place until body tissue grows around it and retains it. The electrode is intended to provide electrical stimuli to muscles that have become inactive through accident or disease. The stimuli can help paraplegics and others to exercise voluntary control over arms and legs.

The electrode is covered with fuzzy material like Velcro (or equivalent) loops of plastic thread. For insertion, the electrode is housed in a sheath. A release tube within the sheath surrounds the electrode wire. Once the electrode is inserted, its position can be finely adjusted to produce maximum muscle response.

After the electrode has been finely positioned in the tissue, the sheath is retracted to expose the fuzzy surface. Encouraged by a coating of collagen on the surface, the tissue should grow into the fuzzy material in several days, thereby securing the electrode in place. To keep the tissue from attaching to it, the sheath is covered with polytetrafluoroethylene.

While the new tissue is growing, the electrode is held in place by fingers on the release tube, which engage an annular groove on the electrode. The electrode may be repositioned as required during the growth period. When growth is complete, the sheath is retracted farther, exposing the fingers so that they spring away and release the electrode.

The wire to the electrode is momentarily detached from the embedded electrode so that the release tube and sheath can be removed. Alternatively, if it is necessary not to disturb the electrical connection, the tube and sheath can be fabricated in halves. Held together by tape during the growth of the tissue, the halves would be separated from around the wire after withdrawal from the body.

This work was done by Earl R. Collins, Jr., of Caltech for **NASA's Jet Propulsion Laboratory**. *For further information, Circle 155 on the TSP Request Card.*

In accordance with Public Law 96-517, the contractor has elected to retain title to this invention. Inquiries concerning rights for its commercial use should be addressed to

Edward Ansell
Director of Patents and Licensing
Mail Stop 305-6
California Institute of Technology
1201 East California Boulevard
Pasadena, CA 91125

Refer to NPO-17264, volume and number of this NASA Tech Briefs *issue, and the page number.*

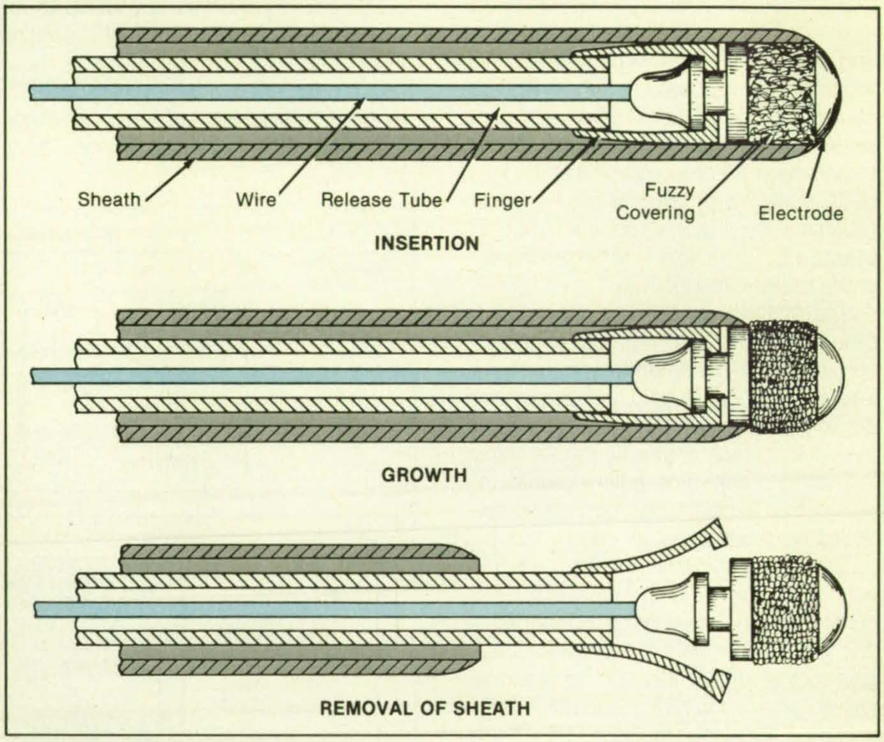

A Sheath Covers an Electrode during implantation (top). The sheath is partially retracted after implantation (middle) and completely retracted after the growth of tissue onto the electrode (bottom). The electrode is about 1 mm in diameter and 2 mm long.

Liquid-Air Breathing Apparatus

A compact unit supplies air longer than does a compressed-air unit.

John F. Kennedy Space Center, Florida

An emergency breathing apparatus stores air as a cryogenic liquid instead of the usual compressed gas. The liquid-air pack can supply air for 60 minutes or more — longer than the previous compressed-air version does. It is also more compact than the previous apparatus is — an important advantage in rescue operations.

The pack is worn on the user's back. It weighs approximately 28 lb (12.7 kg) when full and 22 lb (10 kg) when empty. It supplies gaseous air at regulated pressure at a rate of 50 liters per minute. The apparatus is charged with liquefied air just before use. It is intended for firefighting or rescue operations that may become necessary during planned potentially hazardous procedures.

It holds liquid air in a 3.5-liter Dewar tank and employs tubing and an accumulator to convert the liquid into gas. A series of valves regulates the pressure of the air supplied to the user. A backup pressure-control system is included.

After 2 years of testing, no malfunctions have occurred in the liquid-air pack. The only major disadvantage is that the unit is not designed to work for long intervals while the user is lying down.

This work was done by Robert D. Mills of EG&G Florida, Inc., for **Kennedy Space Center**. *For further information, Circle 33 on the TSP Request Card.*

Inquiries concerning rights for the commercial use of this invention should be addressed to the Patent Counsel, Kennedy Space Center [see page 16]. Refer to KSC-11431

New on the Market

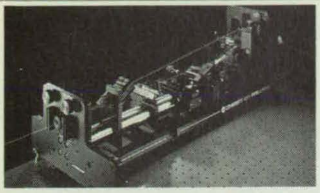

Coherent's Model 899 Ti:Dye™ CW **tunable laser** features interchangeable titanium:sapphire and dye modules and is tunable from approximately 370 to 1100 nm. When equipped with the Model 7500 frequency doubling option, the laser's tuning range can be extended down to 217 nm. The Model 899 can accommodate pump lasers from 4 to 20 watts by simply exchanging pump focusing optics and ouput couplers.
Circle Reader Action Number 768.

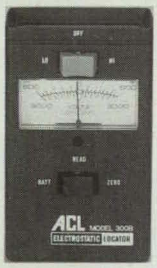

The Model 300B **electrostatic locator** from ACL Inc., Elk Grove Village, IL, measures static charges from 0 to 30,000 volts and is designed for close-in repetitive readings. Application areas include electronic component production, assembly areas, clean rooms, printing presses, packaging, production lines, and computer, medical, and R&D laboratories.
Circle Reader Action Number 766.

The Dimensional Inspector, a portable noncontact **thickness measurement system** from Ultrasonic Arrays Inc., Woodinville, WA, features automatic recalibration for continuous measurement accuracy of +/-.001". The system offers a sample rate of up to 58 measurements per second and is accurate within 24 inches of the target. A sequential menu guides the operator through the programming of measurement and communication parameters.
Circle Reader Action Number 784.

Designed to simplify environmental product testing, the Host **software package** from Thermotron Industries, Holland, MI, networks up to 30 environmental testing chambers; centralizes creation, storage, and modification of test parameters; and provides independent control of each chamber. Test parameters can be displayed in real time on a computer monitor, logged in system data files, printed, or transmitted to another computer for data analysis and report generation. Programmed temperature profile and actual temperature acquired during operation can be monitored and displayed graphically. The software runs under MS-DOS on any IBM PS2 or compatible.
Circle Reader Action Number 772.

The H20 **pocket humidity computer** from Thunder Scientific Corp., Albuquerque, NM, is easily configured for complex humidity conversions and performs psychrometer, two pressure humidity generator, two temperature humidity generator calculations. The only required inputs are temperature, pressure, gas type, and one humidity parameter, such as frost point, dew point, or vapor pressure.
Circle Reader Action Number 774.

The CC143 **VMEbus graphics board** from Compcontrol, Eindhoven, Holland, offers up to 4 Mbytes of multi-port video RAM and connects to virtually any resolution RGB monitor. The board incorporates an Inmos IMS G300 color video controller and displays 256 colors from a palette of 16 million. Optional video RAMs enable the board to perform fast bit manipulation; a block write operation can write 16 bytes/cycle for clearing windows and copying patterns.
Circle Reader Action Number 770.

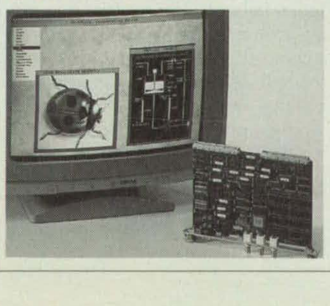

The Model 750SCK noncontact **superconductor screening system kit** from Lake Shore Cryotronics Inc., Westerville, OH, is easily adapted to closed-cycle refrigerator systems, liquid cryogen dewar systems. Its noncontact measurement technique is based on the frequency change in an RF oscillator circuit resulting from the change in conductivity of the sample. This provides an accurate analysis of sample superconducting properties often masked in contact-based techniques by single superconducting paths in the sample. The kit consists of a temperature controller, eddy current electronics option card, oscillator circuit, excitation/sensing coil assembly, system operating software, interconnecting cables, and instructions.
Circle Reader Action Number 782.

3M's Scotch™ Brand **Electrical Tape** #1182 features a copper foil base with electrically-conductive adhesive on both sides for reliable point-to-point grounding. The UL-recognized tape has a dynamic range over a frequency of 1 MHz to 1 GHz, and provides an excellent heat conductive path to protect sensitive areas from excessive thermal exposure — Class 155° C continuous operating temperature. Applications include shielding of PC boards, microwave antennas, and display boards; grounding; and static charge draining.
Circle Reader Action Number 780.

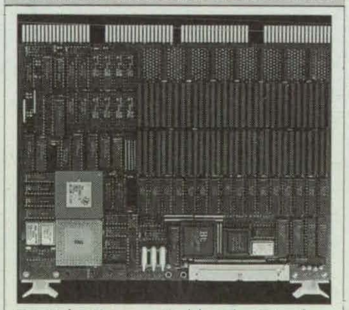

Peritek Corp., Oakland, CA, has announced the first 24-bit **color graphics controller** with 32-bit CPU for Q-bus DEC computers. Dubbed the VCT-Q, the quad-height board runs in true or pseudo color modes and supports a 1024 x 1024 x 24 bits/pixel graphics display with a 1024 x 1024 x 4 bits/pixel graphics overlay. Its BT473 24-bit color map controller provides 16.7 million colors.
Circle Reader Action Number 776.

Used singly or in an array for multiple-temperature-point measurements, the Pyrosor® **infrared thermometer** from Heimann Systems, Iselin, NJ, is suited for applications such as non-transparent plastics, construction materials, and coated surfaces. The compact surface sensor offers a choice of three optical systems including one capable of viewing a 0.11" spot diameter at 1.5" distance. Other features include: 8 to 14 micron spectral response; a choice of eight temperature ranges; and a temperature-stabilized, optically-chopped detector.
Circle Reader Action Number 778.

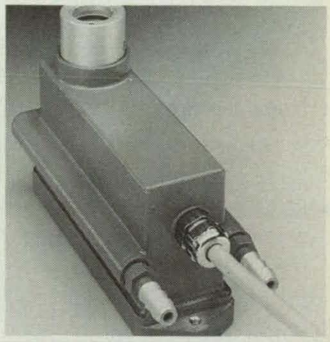

Designed for portable and semi-permanent applications, the MPM-4000 **datalogger** from Solomat Instrumentation, Stamford, CT, can measure, monitor, and control up to 32 channels. Operational modes include simple digital display with unit symbols; average, minimum, and maximum display; automatic datalogging on intervals from 0.1 seconds to 24 hours; manual "snapshot" datalogging including site code; real-time communication to a computer; high/low setpoint alarm; and datalogging on alarm. The MPM-4000's software package allows measurements to be transferred to a PC file.
Circle Reader Action Number 788.

Laserdyne's Model 890 Beam-Director™ **laser machining system** enables high-speed cutting, trimming, drilling, and welding of formed parts up to 8 feet wide and 3 feet high by virtually unlimited length. The system consists of a 5-axis moving beam workstation, a Laserdyne System 84 CNC, and either a CO2 or Nd:YAG laser. Its linear motion system uses brushless DC servomotors and precision ground leadscrews with linear glass scale and encoder feedback for high accuracy and reliability.
Circle Reader Action Number 786.

New on the Market

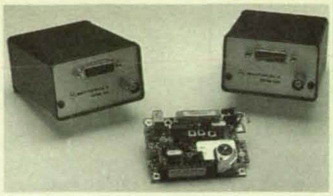

The RNet 150 and 450 Series **telemetry radios** from Motorola Inc., Schaumburg, IL, offer two-channel UHF and VHF operation with low current drain, voice and data transmission capability, and variable power levels. They measure 3.3" x 1.52" x 2.70" and weigh only 10.2 ounces.
Circle Reader Action Number 796.

A portable **UV inspection probe** from Spectronics Corp., Westbury, NY, illuminates tight, hard-to-reach locations such as turbine engines and small diameter pipes. The 1-inch diameter, 6-1/2-inch-long probe offers typical peak 365 nm UV intensity of 5000 μW/cm²at the light source and over 1200μW/cm² at 1 inch. The probe comes with eight alkaline batteries, a 10-foot power cord, 10-foot extension cord, an adjustable mirror, and a spare 4-watt tube.
Circle Reader Action Number 800.

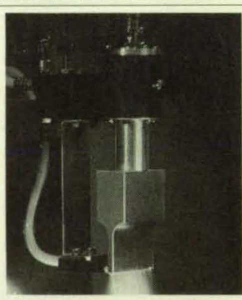

The Ultra-Spray™ **coating system** from Ultrasonic Systems Engineering Inc., Kingston, NY, delivers a uniform atomized spray in a rectangular pattern. The system features an external liquid applicator and operates multiple spray heads from a single power supply for precision coating with minimal overspray. Applications include: solder flux, conformal, and flat glass coatings; coating of plastic, paper, and fabric webs; aseptic packaging; and chemical additives.
Circle Reader Action Number 798.

Cadis-FASTENERS™, the first in a series of **Engineering Standards and Specifications (ESAS) packages** from CAD Information Systems Inc., Englewood, CO, enables mechanical engineers and designers to incorporate standards, specifications, and manufacturers' parts data directly into their CAD designs. The new package contains over 150,000 component graphic files, text files, page images, and product grids covering government and industry standards and specifications for the most commonly used mechanical fasteners — including bolts, nuts, screws, and rivets. Updated quarterly on CD-ROMs, Cadis-FASTENERS operates on PCs running AutoCAD; UNIX-based Sun workstations; and DEC VAX/VMX systems.
Circle Reader Action Number 790.

A **fiber optic installer's kit** featuring the essential tools to terminate and test ST, SMA, FC, and Biconic connectors is offered by Radiant Communications Corp., South Plainfield, NJ. The kit includes an 850 nm wavelength test set; a test set operating at 850 and 1300 nm is available for single-mode work.
Circle Reader Action Number 794.

A new 1000-watt **Nd:YAG laser** from the Lumonics Corp., Livonia, MI, welds steels at speeds up to 120 inches per minute, and to depths of 7 mm. It can produce up to 500 spot welds per second. The laser's high-average-power output enables deep-penetration welds in exotic alloys that previously required electron-beam processing, and allows for easy processing of materials highly reflective to laser energy, including various precious metals, aluminum, and copper.
Circle Reader Action Number792.

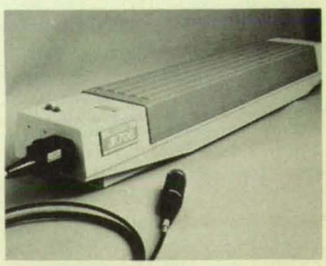

Cut out this ad. And cut yourself some slack.

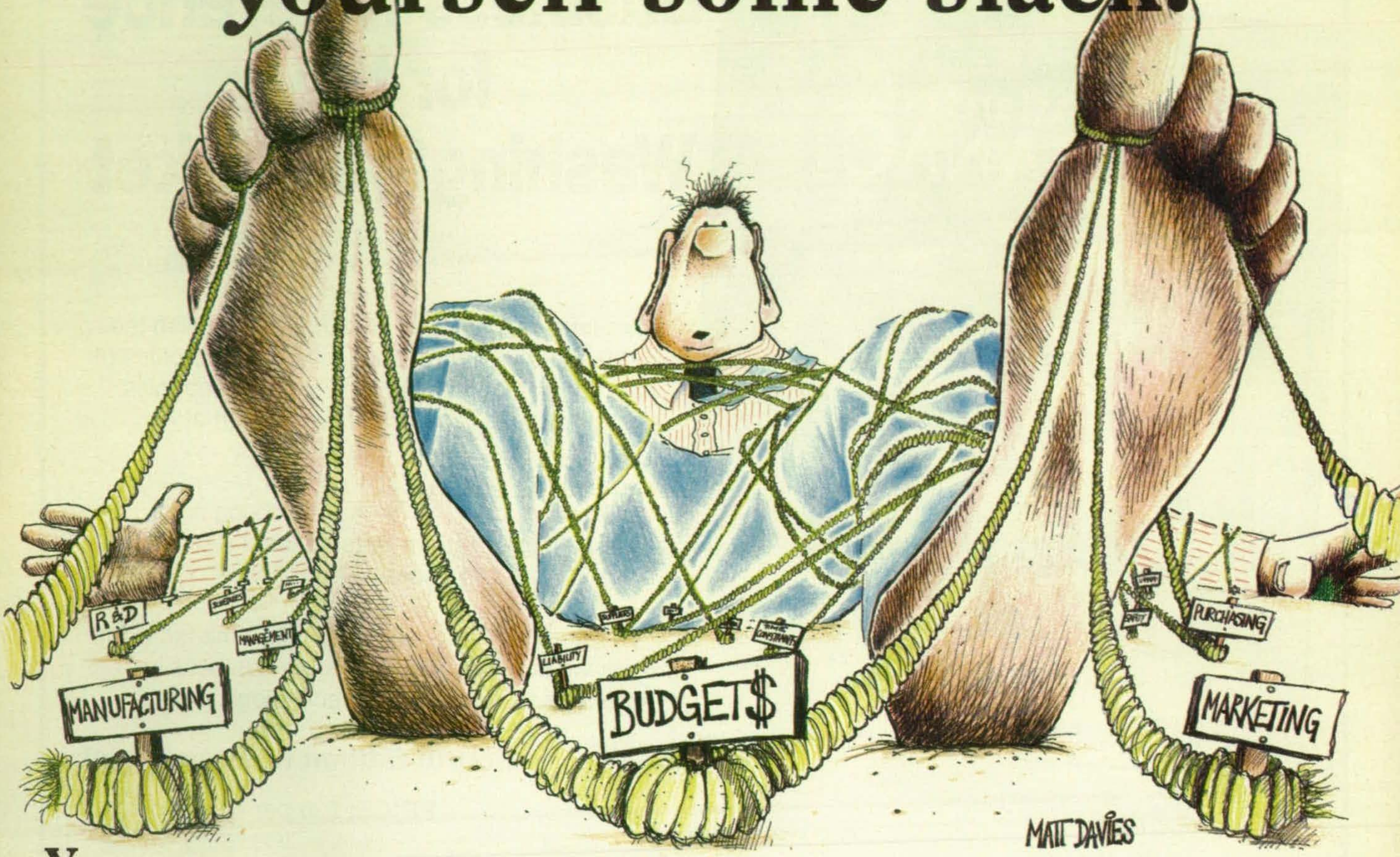

Your workload can be a struggle. As deadlines loom over you, you're tied down by budget constraints. You're no Houdini. But somehow you must design marketing's requirements to meet manufacturing's capabilities.

To meet these challenges it's vital that you stay on top of technology. But there never seems to be time.

Escape to Design/West

Meet with over 275 leading manufacturers. Materials. CAD. Mechanical, electrical and electronic components. Fluid power. Joining systems. Power transmission. Castings. Coatings. Design management services.

In one convenient location you can quickly find all the products, systems and services you need to move your projects from the drawing board to production!

Design/West is your best opportunity to:

- Get new ideas. See the latest products up-close in working demonstrations.
- Solve your design problems. Bring your project specs. Technical experts will be on hand to answer your questions.
- Stop by our special pavilions. One features computers and software for engineering, the other showcases the latest in advanced materials and composites.
- Update your knowledge. Sign up for a session in our ASME-sponsored Conference Program. (For more information call 1-800-255-7798, 9am-5pm EST)
- Have some fun and win prizes. Participate in the Design/West Autocross sponsored by Willow Springs International Drivers School or our "Build a Better Mousetrap" contest.

Cut yourself loose from the ties that bind. Cut out to Design/West. And save $25 when you cut out this ad. Just give it to the attendee typist at the Show for free Show admission.

Design Engineering Show & Conference™/West

September 17-19, 1990
Anaheim Convention Center
Anaheim, California

California's OEM EVENT

XY

Free admission with this ad
Circle Reader Action No. 441

New Literature

"Six Sigma", a new concept in **zero-defect manufacturing,** is described in a six-page brochure from Thermotron Industries, Holland, MI. Six Sigma provides a means of establishing and adhering to performance benchmarks throughout the manufacturing process. Designed as a resource for reliability engineers, the brochure explains how this concept is replacing old industry standards and provides basic guidelines for implementation.
Circle Reader Action Number 716.

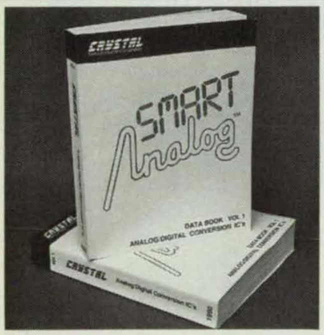

An 848-page data acquisition book from Crystal Semiconductor Corp., Austin, TX, spotlights the company's full range of SMART Analog™ **data acquisition integrated circuits.** The publication is divided into six categories: Analog-to-digital converters, digital-to-analog converters, sample and hold amplifiers, filters, voltage references, and power monitors. Product information includes specifications, block diagrams, operation theories, application notes, schematics, and packaging data.
Circle Reader Action Number 714.

A new catalog from Oriel Corp., Stratford, CT, spotlights the company's complete line of **optical components and filters**. Product categories include: lenses; filters; polarization optics; windows and substrates; mirrors; prisms; beam splitters; fiber optics; and coatings. Optical and physical properties and transmittance and reflectance curves are included for all materials.
Circle Reader Action Number 712.

A 56-page **switching power supply** catalog from Kepco Inc., Flushing, NY, features the company's RAX, RBX, and ERD heavy-duty industrial-grade switchers; OEM, open-frame AC-DC power supplies in single- and multi-output forms; and rack-style power assemblies.
Circle Reader Action Number 708.

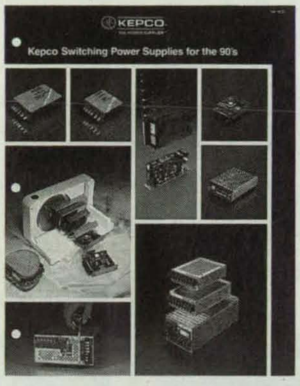

A new catalog from Philips Components, Riviera Beach, FL, features sections on **ferrite materials**; pot, square, and toroid cores; E,U, and I cores; EC, ETD, and EP cores; and shielding beads, chokes, rods, and tubes. The publication contains a wire table for design calculations; a list of publications on soft ferrites; and a glossary.
Circle Reader Action Number 718.

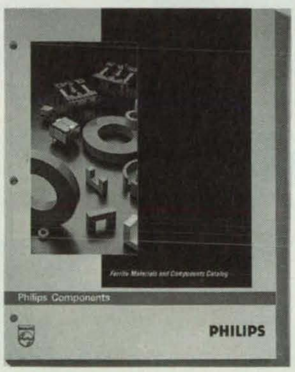

Precision Nesting Systems Inc., Cresskill, NJ, has announced a new brochure detailing the company's **plasma and oxyfuel PINS system.** Highlighted in the brochure is a new capability called "Complex Beveling" that allows profiling and beveling operations to be processed in one step. Traditionally, parts cut from heavy plate are moved from the flamecutting table to another location where secondary processes are used to cut the bevel. By combining these two processes, Precision's software eliminates the secondary step, saving processing time, peripheral equipment costs, and associated labor costs.
Circle Reader Action Number 726.

A free catalog from PERX, San Mateo, CA, features a broad range of **data acquisition and control, test and measurement, and design automation software products** from such industry leaders as Data Translation, Metrabyte, Analog Devices, Strawberry Tree, National Instruments, Fluke, Wavetek, and OrCAD. The publication includes graphics and data analysis software, signal analysis and processing software, data communication boards, image and voice digitizing boards, and PC enhancement products such as AT expansion chassis that take 8- and 16-bit cards.
Circle Reader Action Number 722.

A 30-page booklet on the benefits of using the **Ada programming language** is available free of charge from Alsys Inc., Burlington, MA. Designed for software engineers and program managers, the publication covers the purpose, history, and unique features of Ada, and illustrates how the language decreases the cost of developing, verifying, and maintaining large programs while increasing their reliability. It also explains the relationship between Ada and other technologies such as 4GLs, CASE products, secondary standards, and object-oriented design.
Circle Reader Action Number 706.

Voltek, Lawrence, MA, is offering several brochures containing colorful samples of its crosslinked **polyolefin foam products.** Included with the materials are specification sheets and a comparison chart listing sizes, densities, and strengths.
Circle Reader Action Number 702.

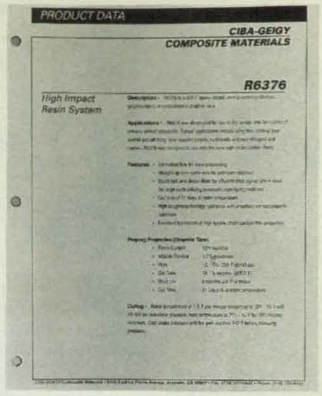

The new R6376 high-impact **resin system** is detailed in an eight-page data sheet from CIBA-GEIGY Composite Materials, Anaheim, CA. Developed for use in primary aircraft structures, the R6376 is a 177°C epoxy-based resin preimpregnated on graphite fabric or unidirectional graphite tape. In addition to its high toughness and damage tolerance, R6376 features controlled flow for easy processing, straight up cure cycle with no post cure required, good tack/drape for easy layout, and 21 day out time.
Circle Reader Action Number 724.

A new catalog from DCT Instruments, Columbus, OH, provides specifications for more than 100 **display and control instruments,** including the SCI series Model 11 with peak and hold capability. Input signals can range from 0.5 to 50 mV/V full scale with proportional analog output of 0 to 5 V. The catalog also features pressure transducers, pressure transmitters, and load cells.
Circle Reader Action Number 710.

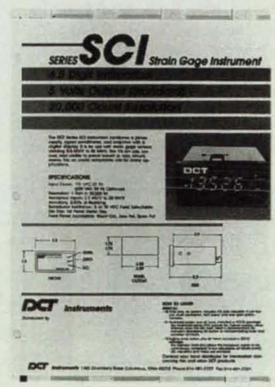

Micromint's new catalog of **single-board computers and industrial controllers** provides specifications and pricing for the company's RTC and BCC product families. Other product highlights include the Rover/PC, a system for transmitting black and white video to a remote monitoring location using standard telephone lines, and the ImageWise serial digital imaging system, which employs a high-speed flash A/D converter and 64K SRAM to capture images in 1/60 of a second.
Circle Reader Action Number 704.

DIAMOND

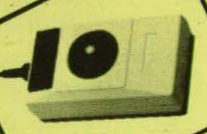

WORKSTATION TRACKBALL

- low cost, compact, all-in-one unit
- direct plug-in replacement for all popular "mice"
- RS232 serial trans/rec lines, selective baud rate, dynamic resolution
- direct replacement units for **SUN, DEC, MASS-COMP, CAL-COMP, PCs, ATs, XTs (IBM** or compatibles)

Evergreen
SYSTEMS INTERNATIONAL
31336 Via Colinas
Westlake Village, CA 91362
(818) 991-7835 • Fax: (818)991-4036

Circle Reader Action No. 573

Now, you can afford the high precision you really need.

With new YSI Precision Machine-Insertable Thermistors. Tape and reel packaging reduces manufacturing costs and YSI precision gives you the edge in circuit accuracy and reliability. Call 800 343-4357 for information. In Ohio, call 513 767-7241.

YSI Incorporated
Yellow Springs, Ohio 45387 USA

Circle Reader Action No. 596

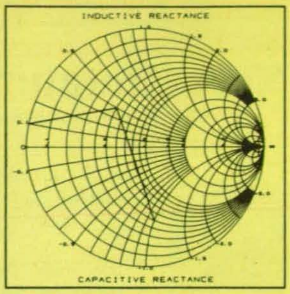

Great Graphics for Scientists and Engineers! FORTRAN, C, QuickBASIC, and Pascal.

Source code. No royalties.

$295.00

INGRAF 2.10 supports video, printers, and plotters

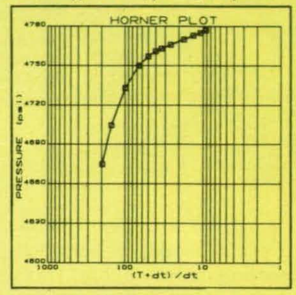

Over 100 routines give you complete control of axes, scaling, windows, and more

Sutrasoft
10506 Permian Dr.
Sugar Land, TX 77478
Info: (713) 491-2088
Orders: 1-800-888-8460

Circle Reader Action No. 450

FREE! 130 Page Catalog

"Optics for Industry"

Free 130 page product catalog from Rolyn, world's largest supplier of "Off-the-Shelf" optics. 24-hour delivery of simple or compound lenses, filters, prisms, mirrors, beamsplitters, reticles, objectives, eyepieces plus thousands of other stock items. Rolyn also supplies custom products and coatings in prototype or production quantities. **ROLYN OPTICS Co.,** 706 Arrowgrand Circle, Covina, CA 91722-2199, (818)915- 5707, FAX (818)915-1379

Circle Reader Action No. 551

IEEE-488

Complete Hardware and Software Solutions

Platforms: EISA, PC/XT/AT, PS/2, 386, Risk System/6000, Macintosh Plus/SE/II, Sun, DEC, Apollo, MASSCOMP, 382, Q-BUS, UNIBUS, VMEbus, MULTIBUS, STD Bus, S-100, and SBX Bus

Operating Systems: DOS, OS/2, XENIX, UNIX, 386/ix, Domain/OS, SunOS, AIX, RT, RSX, RSX, VMS, ULTRIX, VAXELN, PDOS, VERSAdos, RMX-86, Z-DOS, STO-DOS

Support Products: Extenders, Expanders, Converters, Controllers, Buffer, Analyzer

Call for *FREE* Catalog
(800) IEEE-488 • (512) 794-0100

NATIONAL INSTRUMENTS®
The Software is the Instrument™

Circle Reader Action No. 681

Schematic Capture on the PC Only $495

OrCAD, the world's largest supplier of electronic design automation tools, wants NASA Tech Briefs readers to examine OrCAD/SDT III schematic capture tools for themselves. Please call for a **FREE** evaluation kit including demonstration disk and documentation .

OrCAD®
(503) 690-9881 (sales)
(503) 690-9891 (fax)

Circle Reader Action No. 399

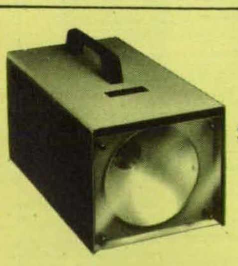

PIONEER
Model DS-312
Digital
STROBOSCOPE
used for
Accurate Motion
Analysis

Study machinery and equipment while in motion by "freezing" it as if it were not moving. A slight adjustment allows viewing slow motion action of interacting parts. Also used as a remote digital tachometer(RPM) without contact. Readout on 5 digit LED. Flashing rate in 2 overlapping ranges: 0-4,000 and 4,000-12,000 FPM

PIONEER ELECTRIC & RESEARCH CORPORATION
7333 W. Harrison • Forest Park, IL 60130
Phone: 708-771-8242

Circle Reader Action No. 561

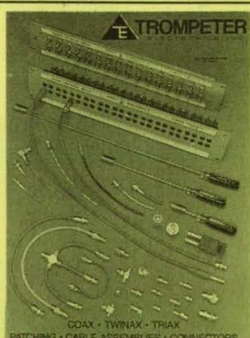

Interconnect Components & Accessories:

New T-17 catalog! Specifications and photos of quality lines of HF, RF and Patching connectors for coax/twinax/triax applications. Products include In-line and Bulkhead jacks and plugs, patch-panels, patch-cords, looping-plugs, adapters, cable assemblies and accessories. Extensive list of cable manufacturers and their parameters plus a "Technical Guide" for cable selection is included.

Trompeter Electronics, Inc.
31186 La Baya Drive
Westlake Village, CA 91362-4047
(818) 707-2020 FAX (818) 706-1040

Circle Reader Action No. 373

Free Standing Wire Grid Polarizers
For Spectroscopy at Millimeter and Sub-millimeter wavelength

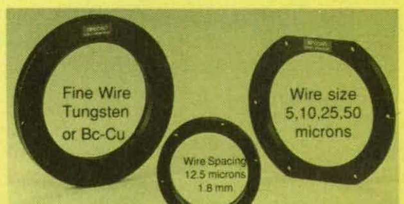

Applications
- **FAR-IR Wavelength Polarization**
- **Interferometer Beam Divider**
- **Variable Reflector**
- **Coupling Device for Long Wavelength Lasers**
- **Suitable for High Vacuum and Cryogenic Conditions**

Custom design available

Another quality product from SPECAC

SPECAC ANALYTICAL INC.
10 Higgins Drive Tel (203)878-7993
Milford, CT 06460, USA Fax (203)878-4085
A Cambridge Electronics Industries (CEI) Company

Circle Reader Action No. 388

MARKETPLACE

Subject Index

A

B

C

D

E

F

G

H

I

Advertiser's Index

*RAC stands for **Reader Action Card.** For further information on these advertisers, please circle the RAC number on the Reader Action Card elsewhere in this issue. This index has been compiled as a service to our readers and advertisers. Every precaution is taken to ensure its accuracy, but the publisher assumes no liability for errors or omissions.

Classifieds

Classified advertising rates and specifications are as follows:
Set in 8 point light typeface, with up to five words at beginning of copy in bold caps. Count box numbers as six words.

50 words or less $195
100 word $285

Check or money order must accompany order to: Classified Advertising Manager, NASA Tech Briefs, Suite 921, 41 East 42nd Street, New York, NY 10017-5391.

NASA Tech Briefs, ISSN 0145-319X, USPS 750-070, copyright © 1990 in U.S., is published monthly by Associated Business Publications Co., Ltd. 41 E. 42nd St., New York, NY 10017-5391. The copyrighted information does not include the individual Tech Briefs which are supplied by NASA. Editorial, sales, production and circulation offices at 41 E. 42nd Street, New York, NY 10017-5391. Subscriptions for non-qualified subscribers in the U.S., Panama Canal Zone, and Puerto Rico, $75.00 for 1 year; $125.00 for 2 years; $200 for 3 years. Single copies $10.00. Remit by check, draft, postal or express orders. Other remittances at sender's risk. Address all communications for subscriptions or circulation to NASA Tech Briefs, 41 E. 42nd Street, New York, NY 10017-5391. Second-class postage paid at New York, NY and additional mailing offices.

POSTMASTER: please send address changes to NASA Tech Briefs, 41 E. 42nd Street, Suite 921, New York, NY 10017-5391.